ESA Space Weather STUDY
Alcatel Consortium

SPACE Weather Parameters

WP 2100

Version V2.2

1 Aout 2001

C. Lathuillere, J. Lilensten, M. Menvielle

With the contributions of T. Amari, A. Aylward, D. Boscher, P. Cargill and S.M. Radicella

1 INTRODUCTION

Space weather can be considered from two different standpoints:

- the numerical modelling of the solar-terrestrial system, by means of models based upon the physical equations which govern its behaviour;
- the needs of the users, i.e. monitoring and forecasting the values of some specific quantities.

In both cases, observations are needed:

- specific observations, to check the numerical models. They depend on both the observational possibilities and modelling needs;
- accurate data series homogeneous over long time periods, to monitor the behaviour of the solar-terrestrial system.

In this workpackage, we present parameters and observations necessary to describe and monitor the solar-terrestrial system in the Space Weather context. We have deliberately chosen to start from the numerical modelling stand point. The identification of the Space Weather parameters from the user point of view is addressed in the workpackage WP1300.

This report is based on the document 'Modèles, paramètres clés, indices en météorologie de l'espace' that has been edited by C. Lathuillère et M. Menvielle after the French Grenoble Space Weather workshop of November 1999. It takes advantage of the discussions and assistance of our colleagues of the Alcatel Space Weather Programme Study Team.

The first part mainly deals with a presentation of the models that describe the different parts of the Sun-Earth system: the Sun, the interplanetary medium, the magnetosphere, and the ionosphere-thermosphere system, with an emphasis on the models developed by the European scientific community. Models dealing with space debris and meteoroids are also presented.

The Space Weather parameters are then presented, focusing on the needs for modelling each sub-system. For a given sub-system, the parameters may include quantities that are outputs of another subsystem: for example the EUV flux is a parameter needed to model the ionosphere-thermosphere system but is not a fundamental parameter for the magneto-hydro-dynamic modelling of the Sun.

The observed quantities are presented and discussed according to their sources. Special care is paid to indices, that are long term homogeneous series of summarised quantities routinely derived and circulated.

In this report on the space weather parameters, we have chosen to focus on the short term effects of the solar activity. However, in a last paragraph, we make a short point on the links between the solar activity and the long term variations of the climate : the climatology.

2 THE MODELS

Our understanding of the whole Sun-Earth system is still incomplete and the elucidation of the physical processes involved is an important key in any Space Weather program.

This entire system can be described as a succession of subsystem who exchange material and energy: the Sun atmosphere, the interplanetary medium, the magnetosphere, the ionosphere and finally the thermosphere. Research models are available for these sub-systems. However their maturity is very dependant on the complexity of physical phenomena and on the available observations. Operational models are also available for some sub-systems.

We have chosen to organise our presentation by classifying the models in two main classes:

- the empirical models which characterise the relations between relevant parameters from available observations,
- the physics-based models which describe a given sub-system.

Recently developed Space Weather models based upon artificial intelligence techniques like neural networks genetic algorithms and expert systems, are not presented here. Some of them, called hybrid models, combine empirical models and physics-based models. These models are described in workpackage WP 3200.

The presentation made in this section will be the starting point of the definition of the relevant parameters made in next part of the report.

2.1 THE SUN

Most of the structures and phenomena present in the solar atmosphere - in particular eruptive phenomena such as flares and coronal mass ejections (CME's), result from the presence of a dominant magnetic field. Eruptive events correspond to a liberation of magnetic energy stored in the solar corona. This energy is then converted into:

- heating of the environment associated to UV/EUV and X beams;
- particle accelerations (electrons and ions) associated to an X emission when those particle interact with the environment;
- movement of matter.

Solar non eruptive flares correspond to a more localised phenomena covering at most a few percent of the surface of the Sun, while CME's are larger scale phenomena that can involve a non negligible part of the Sun global configuration. Those may have different origins and associated events such as global magnetic non equilibrium or prominence disruption.

The global solar atmospheric models are mainly developed in the framework of Magnetohydrodynamics (MHD). The relevant set of equations describes the interaction of ionised coronal plasma with the coronal magnetic field in the presence of the plasma pressure and gravity forces. We present thereafter two main classes of complementary models used for different purpose. Those may be presented in the context of space weather, although they are still essentially used for theoretical purpose. The associated numerical codes are mostly research tools because of the actual state of art in solar MHD modelling. They can be divided in two categories, the *Static* models *for Equilibrium Reconstruction* of the solar coronal magnetic field and the *Dynamic* models to describe its *evolution*.

- The first class of models arises from the impossibility to measure the coronal magnetic field. The structure of the active regions should be estimated before an eruptive event in order to

determine the intrinsic properties of the magnetic configuration. One has thus to *reconstruct* the coronal magnetic field and therefore to solve the equations of the solar atmospheric physics when the boundary conditions are the values of the magnetic field measured in the colder photosphere by vector magnetographs such as THEMIS.

- The second class of models aims at studying the *dynamical evolution* of the active regions. The energy storage and energy release in these regions as well as their stability are described from the evolution of the magnetic configurations which are constrained by a driver whose origin may be sub-photospheric (emerging flux), photospheric (boundary motions) or coronal (interaction with other active regions). These models solve (to a certain extent) the full MHD equations.

Both classes of models are complemented by a whole set of boundary conditions which then defines a set of boundary value problems.

2.1.1 Reconstruction and study of the active region static structures

Equilibrium reconstruction of the coronal magnetic field above active regions using photospheric magnetic data has been the subject of numerous studies since the first attempts (Schmidt, 1964). Those may range from observational problems such as those related to the 180° ambiguity resolution which remains on the transverse component of the photospheric magnetic field, to crucial theoretical problems related to the nature and the determination of the correct type of boundary conditions that have to be used in order to avoid an ill-posed problem, such as what was the case for a long time. Details and numerous relevant aspects of these studies are discussed in Amari et al. (1992, 1997).

In an active region, prior to any eruptive event, typical time variations are so small that one can then solve the MHD equations under static hypothesis. The coronal magnetic pressure is much larger than the gas and gravity can be neglected outside prominences. This is the so-called force–free approximation. This is equivalent to assume that at any point the current density and the magnetic field are parallel. The proportionality factor $\alpha(\mathbf{r})$ and the magnetic field are determined by the boundary conditions defining the boundary value problem.

In the regions of higher density, the plasma pressure gradients and the gravity have been included. This can be done self consistently in full MHD methods or more qualitatively by seeking magnetohydrostatic solutions of the MHD equations.

2.1.1.1 Current free (Potential) Model

The simplest physical approximation is the so-called "current free" approximation ($\alpha=0$) which only requires the longitudinal photospheric component of the magnetic field as boundary condition. It was first considered by Schmidt (1964) and is currently routinely used in most of **t**he terrestrial solar physics centres on the basis of observations (Sakurai, 1989). It is also used as initial conditions for fundamental MHD studies dealing with synthetic problems. This kind of reconstruction is performed following a Green function approach or using a Laplace solver to compute potential scalar function and associated magnetic field.

2.1.1.2 Linear Force-Free Model

The zero-current approximation does not apply to many active regions, which have a magnetic energy above the minimum energy that corresponds to the current free field (for the same distribution of the vertical distribution of the photospheric normal magnetic field). The first step towards a more realistic modelling consists in considering a non zero but constant α, that allows to introduce coronal electric currents. There exist different methods that uses the longitudinal

component of the magnetic field. They are based on Green functions (Chiu, 1977) or Fourier transform (Alissandrakis, 1981), the latter being currently used (Demoulin et al 1997).

Following the general approach of Low (1992), this linear constant-alpha Fourier method has been extended to take into account gravity and pressure forces by Demoulin in a linear computational program and has been applied (Aulanier et al., 1998.).

Although they suffer from several limitations (see below) linear models can be used for some classes of problems (topology, prominence) in moderately sheared structures. Their main advantage remains the weak computational resources they need and their computational speed, as for the current free approximation, which explain why they could be used routinely in a space-weather program.

2.1.1.3 Non-linear Force-Free Model

As for the reconstruction without current, there exists several limitations to the use of the linear reconstruction model:

- the solutions correspond to a minimisation problem for the energy, constrained by the normal component of the magnetic field and by the total magnetic helicity, inducing a limited amount of available magnetic free energy;
- the electric currents cannot be locally intense, while the observations show very clearly important localised shear concentrated along the inversion line of the normal component of the photospheric magnetic field.

The only hope to incorporate large localised electric currents is to assume that the configuration is in a non linear force-free state, that is to say that α (which now depends on the position **r**) is also an unknown of the problem. Different types of boundary conditions define different boundary value problems and codes :

- *A first relatively natural method* consists in imposing the three component of the magnetic field **B** measured at the photospheric level. The problem amounts to *progressively extrapolate* the data step by step toward the corona. This is the vertical integration method introduced by Wu (1990). However, this method is based on a mathematical formulation associated to a ill posed boundary value problem. This lead to an exponential divergence which limits the reconstruction at low altitudes. Some method have been proposed in order to avoid this divergence (Cuperman, 1990, Cuperman et al 1991, Demoulin et al 1992)). Other attempts have been made to regularise the linear version of this method (Amari et al., 1998).
- *A second class of reconstruction methods* is based on a well-posed formulation, which corresponds to observed boundary conditions that imply :
  - the normal component of the photospheric magnetic field (in the local system of reference associated to the Sun),
  - α at the photospheric level when the sign of the normal component B_z of the measured magnetic field has a given a priori value: as an example, α is set in the areas where B_z is positive and then computed through transport along the magnetic field lines to the photospheric zones where B_z is negative.

  This kind of mathematical formulation was introduced by Grad-Rubin (1958) and consists in a decomposition of the non-linear problem in two sets of elliptical (for the magnetic field) and hyperbolic (for α) problems. It gives rise to two types of numerical codes, which correspond to the Lagrangian and Eulerian approaches :
  - Sakurai (1981) uses a Lagrangian approach for each field line. He injects progressively the photospheric electric current on each field line.

- Amari et al (1997) use a global approach in order to solve the elliptical and hyperbolic problems. The corresponding codes with their different versions constitute the EXTRAPOL code.

These two codes, localised in Japan and in France are used in order to reconstruct the configurations of the active regions coming from MITAKA data for the Japanese version and from Hawaii (HSP, IVM) and Boulder (ASP) for the French one. The local Lagrangian approach (Japan) seems to imply a more important limit for the reproducible maximum shearing than the Eulerian approach (France).

- *A third class of methods* is based on solving the MHD equations, injecting the vertical component of the electric current and imposing the normal component of the magnetic fields as photospheric boundary conditions. The system relaxes toward a state which corresponds to the observed values. This method is called the "**resistive-relaxation**" method. It was introduced by Mikic (1994) and also implemented in the French METEOSOL MHD-research code. Although the mathematical justification for this method is not yet clear, the corresponding codes have been used on real cases with a relatively good success.
- *An other method is still at a very experimental state of development.* It is the "**weighted residue method** " (Pridmore-Brown, 1981). This method minimises two residuals: one is associated to the magnetic force, and the second one to the difference between the directions of the photospheric transverse components of the computed and observed magnetic fields. This method has been used only in theoretical situations corresponding to fictive periodic data.
- *A method called* **"constraint and relaxation method"** consists in two repeated steps :
  - impose on the vector potential the minimisation of the difference between the computed and observed transverse components,
  - relax toward an equilibrium state, using a relaxation code which incompletely solves the MHD equations,
  - then, back to the first step (Roumeliotis, 1997).

  This method has been tested with encouraging results on a theoretical case as well as on observed active region.

It is worth noticing that a World Wide Web service tool is currently being developed under a convention between the Centre de Physique Théorique (CPhT, Ecole Polytechnique, Palaiseau, France) and the Département d'Astrophysique Solaire de l'Observatoire de Paris (DASOP, Meudon, France), named FROMAGE (FRench Online MAGnetic Extrapolations). FROMAGE will host several numerical reconstruction codes. This tool could be of valuable interest for space weather purpose.

2.1.2 Evolution of the magnetic configurations

As far as the evolution of the magnetic configurations is concerned, the MHD codes belong to the domain of research even more than for the reconstruction codes. It concerns the fundamental numerical research for the codes themselves (boundary conditions, geometry, temporal scheme, mesh definition, …) but also the fundamental solar physics. The objective is to elucidate the fundamental mechanisms that govern the eruptive phenomena (flux emergence, energy storage, influence of the photospheric movements such as differential rotations or magnetic reconnection …). The existing codes depend on the different classes of problems they address: there is no universal MHD code, in the same way as there is no universal telescope. However, one can foresee a – long – way to the use of the MHD codes for Space Weather purposes in order to test the stability of the magnetic configurations in active regions. These

regions may be first reconstructed by using an equilibrium reconstruction code. This is the approach followed by some groups.

The existing world-wide codes can be distinguished by the following characteristics:

- *dimension* : 2D, 2.5D where the vectors have 3 components but only depend on 2 space variables, 3D;
- *geometry* : spherical for the global models, Cartesian for the description of the active regions at local scales, cylindrical for more specific problems such as the stability of the coronal loops or of the coronal heating;
- *numerical scheme* and space discretisation: finite elements, finite volumes, spectral methods, collocation …
- *physical approach* : heating, resistivity, solar wind inclusion (facing the particularly important and difficult problem of brake down of MHD approximation)…

The table 1 only attempts to synthesise these different approaches, world-wide. We are aware that on-going work may give rise to new codes in a near future. We only show here the codes and the associated developing groups. The more numerous groups which only use the codes are excluded from the table.

Laboratories	**Characteristics**	**Aims**
San Diego (USA)	2.5D, 3D Finite differences **Semi**-implicit	coronal MHD
NRL et NASA (Wash. DC)	2.5D, 3D Spectral + finite volumes Explicit Boundary conditions (….)	Coronal and internal MHD
Japan NAO/Mikata	2.5D, 3D Explicit artificial viscosity η anomalous	Chromospheric and internal MHD
Observatoire de Meudon Ecole Polytechnique (France)	2.5D, 3D differences and finite volumes (**semi**) and implicit	coronal MHD
Strasbourg (France)	cylindrical Boundary conditions	coronal MHD stability
Pisa / Firenze (Italy)	cylindrical (3D) San Diego 2D reduced MHD	coronal MHD turbulence
Nice (France)	1D, 2D Finite differences, Spectral	Turbulence Intermittence
Argentina	Reduced MHD (2D+) Cartesian Spectral (Fourrier)	Turbulence « Flare »-heating
University of Michigan (USA)	2D, 2.5D, 3D (?) Roe scheme Finite volumes	Comets – wind astrophysics
NCSA (Illinois)	2.5D, (3D ?) « Finite volumes » Van Leer, PPM	Astrophysics laboratories
DAEC + DESPA (France)	cylindrical /(Spherical 2.5D) Z-periodic	Dynamo + wind laboratories

	Spectral – Finite differences	
Chicago (USA)	Spherical, cylindrical, Cartesian ASCII project	Astrophysics laboratories

Table 1 : *MHD codes for the Solar atmosphere*

2.2 THE INTERPLANETARY MEDIUM

The solar wind is a prominent part of the Sun-Earth system which is difficult to model because observations are difficult and often indirect. The solar wind corresponds to the outflow from the upward solar atmosphere of the coronal plasma (heated up to several millions K). Its speed ranges between 250 and 950 $km.s^{-1}$ at 1 AU. It is structured by the Sun magnetic field lines frozen in the flow. The solar wind interacts in the interplanetary medium with galactic cosmic rays. Because the solar wind expansion occurs not into a vacuum but into an interstellar space filled with neutral and ionised gases, galactic cosmic rays and galactic magnetic fields, the region where the solar wind dominates is limited by the heliospheric boundary – a region where the energy densities of the solar wind and the interstellar space are equal. This boundary is located between about 50 and 100 AU.

Averaged solar wind parameters in near Earth environment are about 400 $km.s^{-1}$ for the velocity, 5.5 cm^{-3} for the ion number density, 1.5 x 10^5 K for the proton temperature. The number density of He^{++} particles is in the order of 4 – 5 % of the proton number density. The number density of heavier positive ions (including their isotopes) does not exceed about 0.5 % of the proton number density.

Cosmic rays at Earth are high energy particles - from 500 Mev to about 10^{12} GeV, insensitives to the magnetosphere state. The main components are protons, electrons and light nuclei. Below about 1 GeV/nucleon the cosmic ray flux is strongly decreased due to adiabatic deceleration with the solar wind, which results into a decreasing flux below this energy at Earth orbit. The intensity of cosmic rays on Earth maximises when solar activity is minimal (quiet Sun) and minimises vice versa (active Sun), with an average variation in intensity of about 20 %.

The main structures or regions present in the solar wind are:

- the high velocity solar wind, associated to the coronal holes,
- the low velocity solar wind,
- the regions of interactions between high and low velocity solar winds,
- the heliospheric current sheet,
- the signatures in the interplanetary medium of the CMEs, associated or not with shocks. In practice, these signatures are observed at large distances from the Sun nearby the Earth or the Lagrange point L1.

The influence of the solar wind results from both its very structure and its interaction with the propagation of solar perturbations, such as energetic particles resulting from solar eruptions or interplanetary shocks or CMEs. The structure of the interplanetary magnetic field lines, which drives the particle propagation, may in given situations dramatically affects this propagation and therefore the resulting effects at Earth. This ambivalent action can be illustrated by examples of major events at the Sun with minor effect at the Earth, or on the contrary of minor events at the Sun resulting in a major perturbation at the Earth.

Solar wind models have been developed to address many aspects of its structure. One class of models treats the solar wind from a hydrodynamic point of view, thus solving the one dimensional equations of motion along a single field line (e.g. Parker, 1963). The main aim of such models is to obtain accurate expressions for the plasma density, velocity, and especially

temperature at 1 AU. They are also amenable to adding multiple ion species and to including quite detailed calculations of different ionisation states and even the effect of plasma instabilities on the temperatures.

However, from the point of view of Space Weather, it is the large-scale multi-dimensional MHD models that are the more relevant. One class of these models examines the global structure of the solar wind plasma and magnetic field in the heliosphere. These models are quasi-steady state, but incorporate solar rotation, and a three dimensional magnetic field. For solar minimum conditions (which they are best suited for), they clearly demonstrate the formation of the familiar co-rotating interaction regions at distances of 1 AU and beyond (Pizzo, 1982, 1991). The current Ulysses mission has permitted a comparison of these results with the three dimensional solar wind structure. The agreement is good, especially in terms of plasma flows upward and downward from the ecliptic plane (Riley et al., 1996).

A second class of models deals with the motion of coronal mass ejections in the solar wind. The goal is, for given plasma and magnetic field conditions at the Sun, to calculate the properties of the CME at 1 AU and beyond. Early models treated the CME as a pressure pulse, but these are now viewed as being not relevant. Other purely hydrodynamic models have been developed by Riley and collaborators during an investigation of so-called over-expanding CMEs. They showed that with a large plasma over-pressure at the Sun, the conditions observed by the Ulysses spacecraft at large distances could be roughly reproduced (Riley et al., 1997).

The most geo-effective type of CMEs are magnetic clouds. Models for these have been developed by a number of groups who have (in general terms) established that magnetic clouds can propagate from the Sun to the Earth while retaining their organised magnetic structure (e.g. Cargill et al., 2000, Odstrcil and Pizzo, 1999, Vanda et al., 1996). However, the clouds interact with the solar wind by two processes. Firstly, the cloud magnetic field can undergo magnetic reconnection with the solar wind field, leading to its ultimate destruction at large distances. Secondly, the interaction of the cloud with the solar wind plasma leads to considerable changes in its shape, as well as leading shock waves. This modelling is plagued by difficulties in initialising the solar wind magnetic field in a way that minimises errors in the $div\mathbf{B}=0$ condition. A proper 3-D model requires that this problem be resolved.

Models describing the propagation of the cosmic rays through the solar wind are based on a second order equation whose main input parameters are the solar wind characteristics and the interplanetary magnetic field. Fisk et al.. (1998) show that most of the observed phenomena can be accounted for within acceptable ranges of these parameters. However no single model, with a single choice for the input parameters has been able to account for all the observed features of galactic and anomalous cosmic ray behaviour. The most highly developed models concern the interpretation of long-term variations of the flux of cosmic rays at Earth.

Among the empirical models, one can quote the Wang-Sheeley one, based upon the discovery of an anti-correlation between the solar wind velocity and the rate of expansion of the magnetic flux tubes (Wang and Sheeley, 1992). The model is based on observations of magnetograhs at the SUN surface and on deduced maps of coronal holes, surface magnetic field sources and solar wind velocity. It forecasts the IMF polarity and the solar wind velocity at the Earth, two parameters that are mandatory for geomagnetic activity forecasting [1].

Finally empirical models of solar energetic protons and cosmic rays are used in radiation environnement models. The CREME96 software (Tylka et al., 1997) include cosmic rays and SEP models. The JPL proton model (Feynman et al., 1990) describes the interplanetary fluences of protons with energies greater than 10 MeV and also of protons with energies greater than 30

[1] http://solar.sec.noaa.gov/~narge/

MeV at a distance of one Astronomical Unit (A.U. = Earth-Sun distance). It is based on riometer, rocket, and balloon measurements from the Earth's surface and from above the atmosphere between 1956 and 1963, and on spacecraft measurements in the vicinity of Earth between 1963 and 1985. Altogether, close to 200 events are considered. In general, the JPL model can be considered the most reliable at this time because of the large data base used.

2.3 THE MAGNETOSPHERE

The magnetosphere is the region of the ionised environment of the Earth where the Earth magnetic field has a dominant control over the motion of charged particles. The boundary layer between the magnetosphere and the solar wind is the magnetopause, at which the dynamic pressure of the solar wind is balanced by the magnetic pressure of the Earth magnetic field[2]. The location of the magnetopause obviously depends on the status of the solar wind. Under typical solar wind conditions, the terrestrial magnetosphere extends up to ~10 R_E in the sunward direction and to several hundreds R_E in the antisunward direction. The solar wind velocity is supersonic at 1 AU[3], and the magnetosphere behaves as a solid obstacle. There is therefore a bow shock upstream from the magnetopause. In the solar direction, the bow shock is located at a distance in the range 2-4 R_E from the magnetopause. The region between the bow shock and the magnetopause is the magnetosheath, in which the shocked solar wind plasma has a lower velocity and a temperature 5 to 10 times higher than in the solar wind.

The inner magnetosphere is the region of major concern for Space Weather issues. Three regions have been there identified following different criteria: the plasmaphere, the radiation belts, and the ring current:

- *the plasmasphere* corresponds to a cold ($T_e \approx 1$ eV) but dense ($n_e \approx 5 \times 10^2$ cm^{-3}) plasma which corotates with the Earth. It is a torus-shaped volume in the innermost magnetosphere. The outer boundary of the plasmasphere is the plasmapause, where the density sharply drops down to about 1 cm^{-3}. In average, the plasmapause is located about 4 R_E in the equatorial plane, i.e. a McIlwain parameter[4] L=4. It may reach out to L=5-6 during periods of magnetospheric quietness and be compressed down to L=3 during periods of intense magnetospheric activity;
- *the ring current* refers to 'those parts of the particles in the inner magnetosphere, which contribute substantially to the total current density' (Hultqvist et al., 1999). It is then defined with regard to its magnetic signature, and corresponds to a toroidal-shaped electric current that flows westwards around the Earth, with variable density at geocentric distances between ~2 R_E and ~9 R_E. During magnetospheric storms, the particles that contribute substantially to the total current density are mainly trapped ions in the medium energy range (few tens of keV to few hundreds of keV) that originate in the solar wind (He^{++}), the plasmasphere and the ionosphere (O^+). During low activity periods, the particles responsible for the ring current are mostly protons. This change in composition impacts on the evolution with time of the ring current, because loss mechanisms (wave-particle interactions, charge exchange, Coulomb collisions, …) depend on the mass and energy of the particles;
- *the radiation belts* generally refer by now to the 'high energy ions and electrons that can penetrate into spacecraft shielding materials and eventually cause radiation damage to

---

[2] The dynamic pressure of the solar wind is $2\rho V^2\cos^2\chi$, where ρ and V are the solar wind density and velocity and χ the angle between the direction of the solar wind velocity and that of the normal to the magnetopause; the magnetic pressure of the Earth magnetic field is $B^2/2\mu$, where B is the tangential component of the Earth magnetic field at the magnetopause. μ is the magnetic permeability of the medium

[3] 1 AU corresponds to the mean Sun-Earth distance, i.e. 149 610 000 km (1,496 10^{11} m).

[4] For a given geomagnetic field line, the Mac Ilwain parameter L is the geocentric distance of the point where it crosses the magnetospheric equator. It is expressed in Earth radii (R_E).

spacecraft instrumentation and to humans' (Hultqvist et al., 1999). The radiation belts are defined with regard to the energy of particles trapped in the geomagnetic field lines, above ≈ 100 keV and reaching values of hundreds of MeV. Most of the trapped particles are protons and electrons, giving rise to the proton and electron radiation belts:

the proton belt has generally one maximum, which corresponds to a McIlwain parameter L that decreases with increasing proton energy. For 1 MeV, the maximum corresponds to L~2.5 (i.e. field lines crossing the equatorial plane at an altitude h_{eq} of ~10 000 km), while it corresponds to L~1.4 (i.e. h_{eq}~2 500 km) for 50 MeV. The proton belt is fairly stable. At low altitude, it is modulated by the solar cycle, in particular in the region of the South Atlantic magnetic anomaly: its intensity is maximum during solar minimum, and minimum during solar maximum. Major magnetic storms (e.g., March 1991) may significantly impact on the proton belts, in particular for high McIlwain parameters values;

the *electron belt* has generally two maximum, giving rise to the internal and external electron belts. The internal belt, with a maximum corresponding to 500 keV around L~1.4 (i.e. h_{eq}~6 400 km), does not significantly vary with time. On the contrary, the external belt, the maximum of which is around L~4 (i.e. h_{eq}~19 000 km) dramatically fluctuates under the control of strong magnetic storms: short term variations of the flux, up to 4 orders of magnitude in a few hours, can be observed during periods of intense magnetic activity. The long term variation of the external belt fluxes is driven by the solar cycle: the annual mean values of the flux are maximum during the descending phase (about 3 years after the maximum), when coronal holes are in good conjunction with the Earth.

It is worth noting that ring current, radiation belts and plasmasphere partially overlap. For instance at L=3, the density of the cold plasma is about 1000 times higher than the density of energetic protons (>100 keV) whereas the energy density of energetic protons dominates by a factor of about 1000. It is also worth noting that trapped radiation belts and ring current are actually closely related because the major part of the ring current is carried by trapped particles and all the trapped particles contribute to the ring current (Hulqvist et al., 1999).

The interaction between singly charged energetic ions and the cold neutral hydrogen of the geocorona results in energetic neutral atoms (ENA). The ENA resulting from H^+ and O^+ charge exchange have an energy between a few eV and a few hundred keV. They are not affected by magnetic or electric field forces, and therefore leave the interaction region in ballistic orbits. Their energy and direction is representative of those of the incident ion, and remote sensing of ENA provide line-of-sight integrated observations of the source population. The geocorona thus acts as an imaging screen for the energetic ions inside the inner magnetosphere.

For a thorough description of the present knowledge on these regions of the magnetosphere, refer to the recently published reviews on the ring current (Daglis et al., 1999) and the inner magnetosphere (Hultqvist et al., 1999).

2.3.1 Global magnetosphere modelling

2.3.1.1 Empirical models

Empirical models for the bow shock and magnetopause have been developed for decades, in the case of the Earth as well as in that of other magnetised planets (e.g. Slavin and Holzer, 1981). Shue et al. (1997) recently published a well documented model, based on fresh data. It has a simple functional form driven by two adjustable parameters: the stand-off distance in the solar direction and the tail flaring.

Empirical models for the magnetic field inside the magnetosphere are based on a statistical analysis of the available magnetic field observations, parameterised by geomagnetic indices. They basically rely

on a combination of the Earth planetary magnetic field – usually described by the IGRF model – and external fields estimated from both in situ magnetic field measurements and mathematical modelling of the current systems (e.g. Tsyganenko, 1990; 1995; Hilmer and Voigt, 1995). These models are continuously updated to account for more and more complex processes in the magnetosphere.

At a given time, the dynamics of the magnetosphere depends on both the present solar wind conditions and magnetosphere status. This status depends on the past history of the magnetosphere, and models that only use present magnetic field values as input cannot provide reliable predictions of the magnetospheric state. In order to develop better predictors, indicators of the magnetosphere history should be added to the inputs.

2.3.1.2 MHD simulations

Fully three-dimensional MHD models of the magnetosphere have already been developed for scientific use. Their input parameters are typically solar wind density, velocity, and interplanetary magnetic field. The inner boundary of the magnetosphere is typically set at somewhat above 3 R_E, and physical quantities are mapped down to the ionosphere along field lines. The output is the dynamic response of the magnetosphere-ionosphere system. These models do not generally provide a proper description of the inner magnetosphere, because of (i) the definition of the inner boundary, and (ii) the presence of dominant non-MHD processes in the inner magnetosphere.

This field is very active. Several groups are developing their own model, and have not yet already published their results. The situation is then expected to evolve rapidly during the next decade. The best known global MHD models of the magnetosphere are those developed at the University of Maryland (see Mobarry et al., 1996) and at the University of California at Los Angeles (see Raeder et al., 1997 for a recent application). Another model developed at UCLA (Walker et al., 1993) is worth being mentioned here. In Europe, a model is currently developed for scientific use only at the Finnish Meteorological Institute (Janhunen, 1996).

2.3.1.3 Kinetic models

The behaviour of the inner magnetosphere cannot be described in the frame of the MHD approximations[5]. Models of the inner magnetosphere should therefore take into account:

- the non-local character of the plasma response for any transport with characteristic time duration longer than the shorter reflection period,
- the effect of the plasma on the magnetic field,
- the interaction between the different waves in the plasma.

Self-consistent kinetic methods properly describe the field-particle interaction and allow to satisfy these requirements, at the expense of very heavy calculations. Le Contel et al. (1999a; 1999b) recently developed a model of substorm growing phases based upon such methods. Their model is based on the approach proposed by Pellat et al (1995) and Hurricane et al. (1995) to describe electromagnetic perturbations in a non-adiabatic[6] plasma. It allows to estimate the adiabatic response of the plasma to a given external electromagnetic perturbation that originates in the solar wind: an East-West current flowing close to the equatorial plane in the far tail.

---

[5] The ideal MHD basically assumes that the plasma is a perfectly conductive medium.

[6] Adiabatic responses of a plasma correspond to situations where the motion invariants defined in the frame of the Hamiltonian mechanics are conserved. For a charged particle in presence of a magnetic field, the first invariant is its magnetic moment μ, the second invariant is the integral along the field line of the component along the magnetic field of the particle momentum, and the third one is the magnetic flux encircled by the particle's periodic drift shell orbits.

The computations could become significantly simpler if one neglects the perturbation generated by the motion of particles. That comes down to assume that the used magnetic field model takes quite satisfactorily into account the existence of the currents associated to the particles whose motion is studied. This approach uses both an Eulerian approach (global model of the magnetosphere) and a Lagrangian one (particle transport). In practice, it provides an efficient tool for describing the trajectories of the particles in the magnetosphere once available an accurate model of magnetospheric magnetic field. Smets (1998) used such an approach to study the particle distribution functions associated to reconnection processes. Numerical simulation of particle transport then allowed him to characterise particle distributions associated inside the magnetosphere to reconnections at sites of different topology and localisation.

2.3.2 Specific models

2.3.2.1 The Magnetospheric Specification and Forecast Model (MSFM)

The MSFM is a large scale physics-based model designed to specify fluxes of electrons, H^+, and O^+ in the energy range responsible for spacecraft charging, ~100 eV to ~100 keV. It is being developed for operational use by the US Air Force, and it is probably the closest large scale physics-based model to being an operational one. Its description is available on the net[7]. It is an update of a series of earlier models. Its predecessor, the MSM (Magnetospheric Specification Model), is routinely used by NOAA/SEC for Space Weather services. Its major improvement compared to the earlier models is the complexity of the electric and magnetic field models and its capability to run in real-time.

The primary input parameters for MSFM are:

- the Kp and Dst geomagnetic indices;
- the polar cap potential drop and the auroral boundary index which specify the polar ionospheric electric field distribution and the auroral precipitation pattern;
- the solar wind density and speed and the interplanetary magnetic field (IMF).

Secondary input parameters include:

- the sum of Kp;
- precipitating particle flux and polar cap potential profiles from the operational DSMP satellites.

The solar wind density and speed define the magnetopause stand-off distance, and the IMF is used to select the appropriate convection pattern in the polar cap. All together, the primary input parameters determine the used electric and magnetic field models. The sum of Kp is used as indicator of the long-term activity level.

The model can operate with reduced sets of input parameters, and in particular with Kp alone. It also includes neural network algorithms that predict the input parameters from solar wind measurements. It has thus some capability for short-term Space Weather forecasting.

MSFM follows particle drift through the magnetosphere using slowly time varying electric and magnetic field models. The electric and magnetic field configurations are updated every 15 minutes. The particle distribution is isotropic, the model keeps track of energetic particle loss by charge exchange and electron precipitation into the ionosphere.

MSFM successfully accounts for most major electrons flux enhancements observed at geosynchronous orbit. Flux dropouts that often precede the flux enhancements are predicted with less confidence, and they are often missed near the dawn meridian.

[7] http://rigel.rice.edu/~ding/msfm95/msfm.html

2.3.2.2 Ring current models

It has already been mentioned that the ring current composition and dynamics particles is driven by the level of the magnetopheric activity. During periods of magnetospheric activity, the ring current dynamics is driven by particle injection: direct ionospheric ion injection, inward transport of plasma-sheet and pre-existing ring current particles. On the contrary, the behaviour of the quiescent ring current is driven by diffusion of low energy protons in presence of convection electric fields (see e.g., Daglis et al., 1999). Different quantitative models have accordingly been developed for storm- and quiet-time ring current.

A family of storm ring current models neglects direct injection of ions from the ionosphere. The main source of ring current particles is then the plasma sheet, and the characteristics of that source enter the models as boundary conditions. At least four groups are at present working along this path. They are located at the University of Michigan, the Aerospace Corporation, NASA-Goddard Space Flight Centre, and Rice University (see Chen et al., 1994 for a review of these works). Differences between their models are mainly related to different selection of aspects of the problem that are treated at a state-of-the-art level or neglected. One of the main difficulties for these models in the context of a Space Weather operational use is the specification of the boundary condition (i.e. the distribution function of the particles at all parts of the boundary where the drift velocity is inward) in absence of adequate real-time data.

More sophisticated simulations have been developed, that involve both global magnetospheric models and Lagrangian models of particle transport. They have been developed to address questions in relation with academic research rather than with Space Weather activities. Such coupled investigation is however very promising for Space Weather activities because it provides an efficient tool for particle distribution function determination in a given region of the magnetosphere.

With the objective of analysing the ring current dynamics, Fok et al. (1993) have developed a kinetic model that simulates the evolution with time of the distribution functions for the dominant ions (H^+, He^{++}, O^+) as a result of charge exchange and Coulomb collisions. Their results show that during the recovery phase of a magnetic storm, Coulomb collisions lead to generation of low energy (< 500 eV) ions and significant heating of plasmaspheric populations. More recently, the model of Fok et al. (1993) and the particle code of Delcourt et al. (1990a) have been coupled to investigate the ring current response to the field line depolarisation observed in the inner magnetosphere during substorm growing phase. The code of Delcourt et al. (1990a) computes the path of charged single particles given time varying electric and magnetic fields, from their injection in the magnetosphere (from the magnetosheath or the ionosphere) to their input in the plasmasphere

In a more recent study, Fok et al. (1999a) used the particle code of Delcourt et al. (1990b) to estimate the particle distribution in the near tail (at a geocentric distance of about 12 Earth radii), by means of back-propagation of particles to their sources. The transport and acceleration of these ions in the inner magnetosphere, as well as their contribution to the ring current are then computed using the kinetic model of Fok et al. (1993), with a magnetic field more realistic than a dipolar one. These simulations account for many characteristic features of substorms. Further refinements of these investigations will involve estimate of the initial particle distribution functions from results of MHD simulations (see e.g. Fok et al., 1999b) for given solar wind situations instead of semi-empirical modelling.

Understanding the loss process in the region where the hot ring current plasma coexists with cold plasmaspheric plasma requires modelling of the interaction between ring current ions and plasma waves resonantly generated by the coexisting hot and cold plasmas. Modelling wave particle interaction on a global scale is very challenging because it needs a self consistent description of

wave and particle behaviour. The models that have already been developed in this field have only academic research objectives.

2.3.2.3 Radiation belt models

2.3.2.3.1 Empirical models

Very early in the space era, it became clear that the average radiation doses received by satellites are key parameters that should be known. United States and former Soviet Union therefore started building empirical models of radiation belts, using data collected for several years onboard a number of satellites.

In the United States, these models were developed for NASA by Aerospace Corporation. The latest versions are the AP8 (Aerospace Protons #8) and AE8 (Aerospace Protons #8) models (Sawyer et Vette, 1976 ; Vette, 1991). They have been built at the end of the 1970s, using data from about 40 satellites that were in orbit between 1961 and 1977, a period that mostly correspond to solar cycle #20. They provide proton flux for energy in the range 100 keV to 400 MeV and electron flux for energy in the range 40 keV to 7 MeV, for altitudes up that of geostationnary orbits (i.e. 36000 km).

The necessity of updating these models led the United States to launch a satellite dedicated to radiation measurements: the NASA/DoD CRRES (Combined Release and Radiation Effect Satellite) satellite. It has been operational for 14 months, between August 1990 and October 1991 that roughly corresponds to the maximum of solar cycle 22. The CRRES data have been used by DoD to develop new empirical models for the proton (CRRESPRO) and electron (CRRESELE) radiation belts (see e.g., Brautigham et al., 1992 and Gussenhoven, 1993). These models do not provide a significant updating of earlier models, because (i) the altitude and energy ranges they cover are not as wide as those covered by the NASA's AP and AE models, and (ii) they rely on data collected by only one satellite during a disturbed period that is probably not representative of the average behaviour of the radiation belts.

On the contrary, the durability of some meteorological satellites gives the opportunity to improve the models for the low altitude range. Boeing is presently preparing for NASA a model using the NOAA/TIROS satellite data (Huston et al., 1998). This model relies on measurements made since 1978, i.e. over almost two solar cycles. Despite its limitation with respect to altitude (< 800 km) and energy (3 ranges for energy larger than 16 MeV), it is a significant improvement compared to earlier models because it describes the evolution with solar cycle of high energy proton fluxes. The authors are now trying to extend the altitude range addressed by the model.

A series of ESTEC Contracts on Trapped Radiation Environment Model Development led to the development of models based upon the AE8 and AP8 models together with the UNIRAD ESTEC radiation software. These models also incorporate the results of the Russian belt modelling effort at the Institute for Nuclear Physics of the Moscow State University, that use data from the Soviet and Russian spacecraft. The application of these developments are included in the Space Environment System (SPENVIS). SPENVIS is a www server (http://www.spenvis.oma.be/spenvis/) that is continuously updated. SPENVIS allows to estimate the value of relevant magnetospheric parameters (such as e.g., magnetic field, McIllwain parameter, trapped proton and electron fluxes, trapped proton flux anisotropy, …) and determine the effects on spacecraft of the ionised environment (e.g., radiation doses, spacecraft charging, damage equivalent fluxes for Si and GaAs solar panels, solar proton fluences…).

In addition to the models described above, nucleus of models appear at many places in the world. Most of them rely on data from only one satellite, and their representativeness is accordingly limited. As a result of these limitations, the AP8 and AE8 empirical models will probably still

remain during the next few years the standard to be used for mission planning, despite their own limitations.

2.3.2.3.2 Physics-based models

Physics-based models have also been developed very early, in order to elucidate the radiation belt sources and their dynamics. Because of limitation in the computer capacities, they did not significantly evolve during the 1980s. The increasing efficiency of computers allowed to restart their development at the beginning of the 1990s. During the last years, they made possible significant breakthroughs in our understanding of the sources and dynamics of the proton and electron belts.

They basically rely on the resolution of the Fokker-Planck diffusion equation in adiabatic conditions. They take into account more and more different physical phenomenon:

- particle-particle interactions
- wave-particle interactions;
- Coulomb interactions;
- plasma influence.

They basically come down to modelling three-dimensional diffusion in the particle phase space density together with local sources or sinks, in terms of the three adiabatic invariants. A numerical code, named Salambô, has been recently developed to treat the three-dimensional diffusion of energetic ions and electrons in Earth's radiation belts. This model is described in annexe A.

One difficulty in the elaboration of a physics-based radiation belt model is the introduction of a wave model. The two models presently used are the Abel and Thorne (1998 – a; 1998 –b) semi – empirical model and the LPCE /CEA empirical model (Baussart et al., 1999; Lefeuvre et al., 2000) mainly based on statistics performed from 3 years of DE-1 data and on wave normal directions estimated from GEOS - 1 and ISEE-1 data. Tests made on the prediction of the time variation of the life time of trapped electrons (i.e. time needed to have the initial flux decreased by a factor e) have shown that radiation belt models are very sensitive to the waves (Baussart et al., 1999).

The input data of the LPCE/CEA wave model are the geomagnetic coordinate (L, MLT, MLAT), the geographic longitude and the Kp value. The output data is the Square root of S(f) the magnetic field power density spectrum. In option, the model provides the Wave distribution Function (distribution of the wave energy density as a function of the wave normal direction and the wave frequency).

Improving the wave models requires the following supplementary observations and developments:

- measurements of one magnetic wave field component in the ULF to VLF frequency domain over several years (if possible a solar cycle), to complete the data bases presently available in order to point out the variation of the field power density spectrum S(f) as a function of the geomagnetic activity. Presently, wave models have been defined for 2 classes of geomagnetic activity ($Kp \leq 3^+$ and $Kp > 3^+$),
- measurements of the three magnetic components below ~ 100 Hz, to point out the righ-handed polarized waves below the local proton gyrofrequency, and so to identify the waves which potentially precipitate the highest energy electrons (presently, in the quasi-absence of relevant data out of L = 6, the S(f) power spectrum below the local proton gyrofrequency is either supposed to be the spectrum of left-handed polarized waves, which means that there is no interaction with trapped electrons above ~ 1 Mev, or the spectrum of right-handed

polarized waves, which means that there is a maximum interaction with trapped electrons above ~1 Mev), measurements of the three magnetic components in a wider frequency range, to provide a more accurate model of the Wave Distribution Function, New developments are necessary:

- development of codes to calculate the pitch angle and energy diffusion rates for important wave modes, including whistler mode, ion cyclotron, magnetosonic, for the general case where fpe ~ fce and f ~ fce, and at large angles of propagation. The development is required to model regions in the heart of the radiation belts and out to geostationary orbit where existing diffusion rates are not valid, and for different geophysical conditions and magnetic local times.
- work to improve the calculation of the radial diffusion co-efficients governing plasma transport and the structure of the radiation belts.

2.4 THE IONOSPHERE-THERMOSPHERE SYSTEM

Above 90 km altitude, the upper thermosphere is characterised by a large density decrease, that implies a decrease of the collision frequency between molecules. The temperature increases rapidly from about 180 K to the thermopause value of about 1000 K. This value, constant above 300 km, is also called the exospheric temperature. It is directly dependent on the solar energy in the UV and EUV bands and on the auroral energy inputs. The main atmospheric constituents, nitrogen and molecular oxygen, are photodissociated and ionised to form the ionosphere. The altitude of the maximum of the electron density is close to 250 km.

The understanding of the physics of this solar-terrestrial sub-system and its effects on technological operations is determined by the ability to model at least the height, geographical and time distributions of the electron concentration and the neutral densities. The modelling effort has started a long time ago, due to the development of our technological society (telecommunications, orbitography,…). However, there is no numerical code or model that is able at present time to describe accurately the three-dimensional and time-dependent distribution of the ionospheric plasma and the thermospheric densities during quiet and disturbed conditions. In other words no model is able to reproduce in a satisfactory way both the climate and the weather of the earth ionosphere-thermosphere. In addition there is no well established experimental database that can be used to verify and test the existing models in order to generate the improvements needed.

At present most models are able only to reproduce consistently the climate of the ionosphere and the thermosphere defined mostly by diurnal, seasonal and solar cycle variations. Serious theoretical and computational efforts supported by complex combinations of experimental techniques are being done to model and predict the weather. This weather is defined as the hour to hour, day-to-day, week-to-week variability of the electron and neutral concentrations within the framework of the climatology.

Three different types of models can be identified, each of them having implicit limitations and advantages:

- semi-empirical and empirical models,
- physics-based models,
- in the case of ionospheric modelling only, analytical "profilers" based on routinely scaled ionospheric data.

The physics-based models of the ionosphere and the thermosphere use as inputs empirical models of convection electric field and auroral precipitations in order to describe the coupling with the magnetosphere. Such models are also presented at the end of this section.

2.4.1 Empirical and semi-empirical Models

2.4.1.1 Ionospheric models

Theses models are based on analytical function to describe the ionosphere. Theses functions are estimated either from experimental data or from results of physics-based models.

A well known empirical model widely used for different applications is the International Reference Ionosphere (IRI) (Bilitza, 1990). This is the result of an international project sponsored by the Committee on Space Research (COSPAR) and the International Union of Radio Science (URSI) to produce a reference model of the ionosphere, based on available experimental data sources. For given location, time and date, IRI describes the electron concentration, electron temperature, ion temperature, and ion composition in the altitude range from about 50 km to about 2000 km; and also the electron content. The solar activity is represented by the sunspot number index. IRI provides monthly averages in the non-auroral ionosphere for magnetically quiet conditions. IRI model can also be used to obtain the profile of electron concentration using the experimental values of F2 peak electron concentration (i.e foF2) and height as inputs.

The major IRI data sources are the coefficients (foF2 and M(3000))produced by the Radiocommunication Sector of the International Telecommunication Union (ITU-R)[8] on the basis of a large set of ground vertical ionosonde data, the powerful incoherent scatter radars (Jicamarca, Arecibo, Millstone Hill, Malvern, St. Santin), the ISIS and Alouette topside sounders, and in situ instruments on several satellites and rockets. IRI is updated periodically and has evolved over a number of years.

At present the major limitation of IRI appears to be its electron distribution in the region above the peak of the F2 region (topside ionosphere). Such distribution gives vertical total electron content (TEC) that for high solar activity has values above the expected ones, particularly at middle and high latitudes. The height limit of 2000 km for the electron concentration calculation with IRI make difficult to use this model for TEC estimates for satellite heights like those of the GPS constellation.

IRI (1) is avalaible from NSSDC's Request Office on tape or on two diskettes (including the ASCII version of coefficients) for use on PCs; (2) is retrievable from NSSDC's anonymous FTP site; (3) can be run via the WWW.

A group of semi-empirical models have been developed by D. N. Anderson of the Phillips Laboratory of the USAF and others. There are based on the combination of databases of coefficients that reproduce theoretically calculated profiles based on physics-based models.

- The Semi-Empirical Low-Latitude Ionospheric Model (SLIM) (Anderson et al, 1987) is based on a theoretical simulation of the low latitude ionosphere. Electron concentration profiles are determined for different latitudes and local times by solving the continuity equation for O^+ ions. The profiles are normalised to the F2-peak concentration and are then represented by Modified Chapman function using six coefficients per individual profiles. Input parameters used in the theoretical calculation include the MSIS model neutral temperatures and densities (see below), the IRI model temperature ratios and the diurnal ion drift patterns observed by the Jicamarca incoherent scatter radar for the different seasons.

[8] http://www.itu.int/ITU-R/index.html

- The Fully Analytical Ionospheric Model (FAIM) (Anderson et al, 1989) uses the formalism of the Chiu model (Chiu, 1975) with coefficients fitted to the SLIM model profiles. The local time variation is expressed by a Fourier series up to order 6 and the variation with dip latitude by a fourth order harmonic oscillator function (Hermite polynomial).
- The same group developed a Parameterised Real-time Ionospheric Specification Model (PRISM) (Daniell et al, 1993) that consists of two segments. One is the Parameterised Ionospheric Model (PIM) and the other incorporates near-real-time data from ground and satellite sensors. PIM is a relatively fast global ionospheric model. It is based on the output of physics-based ionospheric models developed by Utah State University and Boston College. It consists of a source code and a large database of runs of ionospheric specification codes. From a given set of geophysical conditions (day of the year, solar activity index $f_{10.7}$, geomagnetic activity index Kp…) and positions (latitude, longitude, and altitude), the model can produce critical frequencies and peak heights for the ionospheric E and F2 regions as well as electron concentration profiles from 90 to 1600 km and TEC.

2.4.1.2 Thermospheric models

Thermospheric semi-empirical models are based on the hypothesis of independent static diffusive equilibrium of the different thermospheric constituents above 120 km altitude. The density of each constituent decrease exponentially with altitude with its own scale height that depends on its mass and on the temperature. The temperature variation is described by the Bates profile that is function of the exospheric temperature, and the temperature and its gradient at the lower limit. The temperature and the gas concentration evolve depending on season and solar local time, on latitude and on solar flux represented by the $f_{10.7}$ index and magnetic activity represented by Ap or Kp indices. Periodic functions are used to represent the diurnal and seasonal variations. Latitudinal, solar activity and magnetic activity variations are represented by non-periodic functions that may differ from one model to another.

The DTM-78 model (Drag Temperature Model, Barlier et al., 1978) has been developed at the Centre d'Etudes et de Recherches Geodynamiques (CERGA, France) in a co-operative effort with the Institut d'Aéronomie spatiale in Belgium and the Service d'Aéronomie du CNRS in France. It is based on temperature measurements by the OGO-6 satellite and density data from drag observations. The version DTM-94 (Berger et al., 1998) include data from the micro-accelerometer CACTUS (1975-1979) and from the Dynamic Explorer 2 satellite (1981-1983). This version is actually used for various applications: trajectory computation for satellites such as SPOT or TOPEX/POSEIDON and developments of gravity models. A new version is under development by CNES/GRGS and Service d'Aéronomie in order to better describe the variations in the lowest altitude region (120 to 150 km).

MSIS, the most widely used model in the scientific community, has been developed by GSFC (Goddard, Maryland). MSIS (Mass Spectrometer and Incoherent Scatter) is based on satellite mass spectrometer data and ground incoherent scatter data. The version MSIS-86 (Hedin, 1987) became the highest part (altitude above 90 km) of the COSPAR International Reference Atmosphere (CIRA). The version MSISE-90 (MSIS Extented, Hedin, 1991) describes the atmosphere from the ground level. Above 72,5 km altitude, it is a revised version of MSIS-86 that include new data. Above 120 km, MSIS-86 and MSISE-90 are identical. These models can be retrieved from NSSDC's anonymous FTP site or can be run via the WWW.

An empirical model of the thermospheric winds has also been developed by GSFC, using data from the AE-E and DE-2 satellites in the first version HWM-87 (Hedin Wind Model). Ground based measurements by incoherent scatter radars and Fabry-Perot interferometers have been added in the version HWM-90 (Hedin et al. 1991) to lower the altitude limit at 100 km. The last

version HWM-93 (Hedin et al., 1996) describes the winds almost from the ground using data from MF and meteor radars. This model is also available on the NSSDC servers.

The MSIS and HWM models are often used as inputs for physics-based modelling, for example ionospheric and radiation belt models. MSISE-90 will be used for orbit prediction of the TIMED spacecraft. Current development efforts have been transferred at NRL (Washington, DC) and are focused on the improvement of the solar and geomagnetic input specifications and on the incorporation of new data sources (Picone et al., 2000).

2.4.2 Physics-based models

Global or limited area models that use basic physical principles controlling the ionospheric plasma have been developed in recent years as well as coupled thermosphere-ionosphere 3-dimensional time-dependent models. They make use of empirically specified input data. The main ones are: the solar EUV/UV radiation, the thermospheric winds, the ion convection pattern and the auroral precipitation pattern (see description below). The accuracy of these inputs limits the ability of these physics-based models to reproduce climatic and weather conditions. Shunk and Sojka (1992) have given a good review on the situation up to 1992. Among the models reviewed are the NCAR Thermosphere-Ionosphere Electrodynamics Global Circulation Model (TIE-GCM), the Utah State Time Dependent Ionospheric Model (TDIM) and the University of Alabama Field Line Integrated Plasma (FLIP).

In UK, Zhang et al (1993) and Zhang and Radicella (1993) developed a time dependent ionospheric model limited essentially to middle latitudes. This model has the advantages of being fast in comparison with global model calculations and suitable for the investigation of the influence of different physical processes that define the electron concentration distribution and - to a certain extent- its variability.

In France, a collaboration between CESR and LPG has led to the TRANSCAR ionospheric model, developed specifically to describe the high latitude ionosphere as observed by the EISCAT incoherent scatter radars. It couples a time-dependant fluid description of the thermal components of the plasma and a steady-state kinetic description of the hottest population that originates either in the magnetosphere (electron and proton precipitation) or in the atmosphere, through photo-ionisation. A full description of TRANSCAR is given in annexe B.

Finally a Coupled Thermosphere-Ionosphere-Plasmasphere (CTIP) model has been developed in UK. CTIP is one of the most comprehensive upper atmosphere models currently available, covering the region from 80 km to 450 km altitude in the neutral atmosphere, 120 km to 10,000 km in the ionosphere. It solves self-consistently the 3-dimensional time-dependent equations of momentum, energy and continuity for neutral particles (O, O_2 and N_2) and ions (O^+, H^+) on an Eulerian co-rotating spherical grid spaced 2 degrees in latitude and 18 degrees in longitude. Parameters relevant to the ion-neutral and neutral-ion coupling are exchanged at every few time steps between the thermospheric and ionospheric codes. The CTIP full description can been found in annexe C.

2.4.3 Ionospheric profilers

An additional way to calculate the electron concentration distribution with height is based on data assimilation techniques. It uses ionospheric characteristics routinely scaled from the ionograms to generate the profile by means of simple mathematical expressions. The advantage of this type of profile modelling is that it can in principle use as inputs experimental values of basic ionospheric characteristics for both quiet and disturbed conditions. The profilers share with the other types of models the difficulty to describe well the topside ionosphere. This is due essentially to the absence of a well-established experimental database of topside profiles that allow a clear definition of the topside ionosphere behaviour.

The Bradley and Dudeney (1973) "profiler" describes the electron concentration profile up to the peak of the F2 region and consists of two parabolic layers one each for the E and F2 layer and a linear segment to unite both layers. This profile generation is still used by the ITU-R HF propagation prediction method. Dudeney (1978) has later developed a more refined profile using routinely scaled characteristics incorporating combinations of trigonometric-function segments and providing optional valley and F1-ledge description. The main advantage of this profile over the previous one is the continuity of the gradient of electron concentration with height across the segment boundaries.

The DGR model, a "profiler" originally introduced by Di Giovanni and Radicella (1990) and improved by Radicella and Zhang (1995), is able to describe the electron concentration profile in the E-F1-F2 regions of the ionosphere by using simple analytical expressions. It is essentially based on the Epstein layer introduced by Rawer (1983) and considers the existence of characteristic points in the profile with co-ordinates (values of electron concentrations and its height) calculated by means of empirical expressions. The model is constructed as the sum of three Epstein layers that are formally identical. The model calculates the electron concentration profile above the F2 peak making use of an effective *shape parameter* empirically derived for the topside ionosphere. The total electron content is computed with an analytical expression obtained from the Epstein layers formulation of the model. The input parameters are: foF2, M(3000)F2, foF1, foE and the geomagnetic dip angle. This model of electron concentration profile has been adopted by the European Commission COST 238 (PRIME) action and it is part of the computer program produced by the action.

A new family of electron concentration "profilers" which differ in complexity and which have different but related application areas has been developed, based on the DGR "profiler" concept (Hochegger et al. 2000). They allow also the use of median or instantaneous values, or maps based on regional or global experimental data, of the ionospheric parameters needed for the characteristic points determination.

The three models are:

- NeQuick : is a quick-run model for ionospheric applications. This model has been adopted in the ionospheric specifications for the European Space Agency EGNOS project.
- COSTprof : a model that can be used for ionospheric and plasmaspheric satellite to ground applications. This model has been adopted by the COST 251 action of the European Commission as the profiler for its electron concentration distribution.
- NeUoG-plas: a model that can be used particularly in assessment studies involving satellite to satellite propagation of radio waves.

The basic input parameters are values foF2 and M(3000)F2. The output of the models is the electron concentration in the ionosphere as a function of height, geographic latitude and geographic longitude, solar activity (given by sunspot number or by 10.7 cm solar radio flux), season (month) and time (Universal Time UT or local time LT). The models permit also to calculate electron concentration along arbitrarily chosen ray paths and slant or vertical total electron content up to heights in the plasmasphere as those of GPS satellites. The profiles are continuous in all spatial first derivatives (a necessity in applications like ray tracing and location finding).

Above 100 km and up to the F2 layer peak all three models are identical using a modified DGR formulation. Models use the ITU-R coefficients for foF2 and M(3000)F2 and simplified models for foF1 and foE, that take into account solar zenith angle, season and solar activity. The topside F layer for the NeQuick model is again a semi-Epstein layer but with a height dependent thickness parameter (Radicella and Zhang, 1995). For the COSTprof the topside ionosphere formulation uses three physical parameters, namely the oxygen scale height at the F2 peak, its height gradient, and the O^+- H^+ transition height. These three parameters are modelled according

to solar activity, season, local and ”modified dip latitude”. NeUoG-plas has an additional geomagnetic field aligned third part for the “plasmasphere” to model this region in a more realistic way.

2.4.4 Convection electric field and auroral precipitation models

Several empirical models have been developped. Only the most recent and well known models are presented below.

The Heppner-Maynard-Rich Electric Field Model (1990) is a software package that includes several empirical electric convection field models, and the AFGL Precipitation and Conductivity Model; the latter for obtaining conductances, currents, and heating. The Heppner-Maynard models are based on OGO 6 and DE 2 electric field measurements and provide the electric potential and field poleward of 60 geomagnetic latitude. Seven different models were generated for different Interplanetary Magnetic Field (IMF) conditions. Spherical harmonics to order 11 in magnetic local time and latitude are used in each case. For southward IMF, an explicit variability with geomagnetic activity is included. The Heelis Electric Convection Field Model (Heelis et al., 1982) is included in this package for comparative purposes. Rich and Maynard (1989) illustrate the improvements of their model in relation to the Heelis model and point out the differences to the Millstone Hill Electric Field Model (Holt et al. 1987) in the region of the Harang discontinuity and near the dayside cleft.

The Izmiran Electrodynamic Model (Feldstein et al. 1984) is based on the inversion of geomagnetic groundbased observations. The 1985 version of the IZMEM is parameterized by the interplanetary magnetic field (IMF) strength and direction and available for three seasons of the year (summer, winter, equinox). Seven parameters of the high-latitude ionospheric electrodynamics can be determined for the specific IMF strength and orientation (Bx, By, Bz): geomagnetic perturbation vectors at the Earth's surface, electrostatic field potential at the ionospheric altitude, as well as electric field vectors, field-aligned currents, ionospheric current vectors, equivalent current vectors, and Joule heating rate. The new IZMEM / DMSP model produces patterns obtained after recalibration of the IZMEM model by the observed DMSP electrostatic potentials (Papitashvili et al., 1999) and can be run at http://www.sprl.umich.edu/MIST/spw.html using real time IMF data from the ACE satellite.

The AFGL Electron Precipitation Model (Hardy et al. 1987) and the AFGL Ion Precipitation Model (Hardy et al. 1989) provide the integral energy and number flux of precipitating auroral electrons and ions as a function of corrected geomagnetic latitude (CGL), magnetic local time (MLT), and magnetic activity (Kp). There are based on millions of spectra from the DMSP F2 F4 F6, and F7 satellites and the P78-1 satellite. At each level of activity the high-latitude region was separated into 30 zones in corrected geomagnetic latitude (from 50 to 90) and 48 one-half-hour zones in magnetic local time. The electron model provides also Pedersen and Hall conductivities, using empirical relationships between the conductivities and the electron energy flux and average energy.

For space weather applications, it should be noted that now real time global convection maps, or the equivalent electrostatic potential maps, constrained by SuperDARN radar measurements, are avalaible at http://superdarn.jhuapl.edu/index.html (Shepherd and Rhuohoniemi, 2000). Convection pattern and auroral precipitation pattern can also be deduced from all available data (geomagnetic and radar ground based observations and in situ measurement of electric field and auroral precipitation) using the AMIE procedure (Richmond and Kamide, 1988) which is not today a real time procedure. The use of such time dependant auroral inputs has dramatically increased the physics-based model reliability for describing the ionosphere and thermosphere during disturbed conditions.

2.4.5 EUV/UV models for aeronomy

The ultraviolet (UV) / extreme ultraviolet (EUV) solar flux is energetic enough to ionize the upper atmosphere. It constitutes the major source for the diurnal ionosphere. Most of the current models rely on few experiments taken onboard the Dynamics Explorer missions (Hinteregger,1973). A first representation of Solar EUV fluxes for aeronomical applications was given by Hinteregger (1981) and Hinteregger et al. (1981). A first reference flux SC#21REF was assembled from measurements performed in july 1976 ($f_{10.7}$ = 70), and given in 1659 wavelengths. An extrapolation model (SERF 1) allows to estimate the flux during other periods of solar activity.

Torr and Torr (1979, 1985) proposed two reference fluxes for aeronomy called F79050N ($f_{10.7}$ = 243) and SC#REFW ($f_{10.7}$= 68). The UV spectrum was divided in 37 bins. Some bins correspond to intense spectral lines but the bright Lyman α line at *121,565* nm does not show up because it is not energetic enough to ionise the terrestrial ionosphere. This work revealed to be extremely useful. One of its qualities was that the authors proposed the corresponding absorption and ionisation cross sections for the major thermospheric species.

Its main limitation is that the measurements do not allow to reach a good estimate of the flux variability for different solar activity conditions. Since then, several authors developed their codes in order to take better advantage of the AE data base. Amongst them, two must be emphazised. Tobiska (Tobiska , 1991; Tobiska and Eparvier, 1998) developed a model called EUV, which takes data from other sources into account (SME, OSO; AEROS; rockets and ground-based facilities). This model takes into account the solar emission zone of each line, through a parameter. It proposes a formula to retrieve a solar flux from the gift of the decimetric index and its average.

The second improved model is EUVAC (Richards, Fenelly and Torr, 1994). Its main difference with previous models is the reference flux choosen, and the interpolation formula. The coronal flux is also constrained to be at most 80% of the total.

Those models are very important for aeronomic computation. They allow to develop a fairly good physics. However, they cannot take into account the variability at different wavelengths. Indeed, specific full measurements (for example onboard the space shuttle) clearly show that there is no linear variation with the decimetric index. At the contrary, some lines of the solar flux may increase with solar activity or decrease, sometimes drastically.

Finally, a radically different approach has been undertaken by Warren and co-authors (Warren et al., 1996, 1998). They combined a spectral emission line database, solar emission distributions, and estimates from ground-based solar images of the fraction of the Sun covered by the various types of activity to synthesise the irradiance. The goal was to give a way to estimate the irradiance from EUV line emission formed in the upper chromosphere and lower transition region from the Ca II K-line through the model. Based on this approach, they could derive the emission measure from a spectrum of a portion of the quiet solar disk measured with the Harvard instrument on Skylab and compilations of atomic data (Warren et al, 1998 paper I). The irradiance spectrum from 50-1200 A was then computed for the quiet Sun, with the contributions of optically thick emission lines and continua included empirically. A comparison with the empirical models described above indicates relatively good agreement among fluxes of emission lines formed in the solar chromosphere and transition region. A factor of typically 2 is found with the fluxes for coronal emission lines.

In the frame of space weather, several questions have to be addressed : what is the contribution of each different zone of the sun to the global flux ? Can we find one index, a mixing of several indexes, or a selection of thin lines (to be monitored) allowing to determine the flux on top of the

Earth atmosphere with a much better precision than the decimetric index (and its mean) ? Can we forecast the solar flux hours in advance ?

2.5 METEOROIDS AND SPACE DEBRIS

Debris are a growing preoccupation of space environment users. Some 300 active satellites are close to a graveyard orbit region reserved for even more defunct satellites. Many are not parked in this graveyard orbit. Launch activity into GEO has and will continue to contribute to the injection of matter into the region and depletion mechanisms are in most cases slow to remove fragments. The knowledge of the debris population has greatly increased over the last years, especially with the in-situ impact detector GORID and the data taken onboard LDEF.

Several models predict the location of the space debris and meteoroids. To the difference of the models listed elsewhere in this report, their aim is not to reproduce one or several geophysical parameters, but to predict the location of the space debris and meteoroids. In this sense, they can be considered as "technological" models, or operational models. This is why they appear in two separate tabs. Two documents make a good cross comparison of these models : Sdunnus et al., 1998 and McDonnell et al., 2000. This paragraph takes their outputs into consideration, with some updates when updates occur.

2.5.1 Space debris models

ORDEM96 is a semi-empirical, computer-based orbital-debris model which combines direct measurements of the environment with the output and theory of more complex orbital-debris models. It approximates the environment with six different inclination bands. Each band has a unique distribution of semi-major axis, for near circular orbits, and a unique perigee distribution, for highly elliptical orbits. In addition, each inclination band has unique size distributions which depend on the source of debris. Collision probability equations are used to relate the distributions of orbital elements to flux on a spacecraft or through the field of view of a ground sensor. The distributions of semi-major axis, perigee, and inclination are consistent with the U.S. Space Command catalogue for sizes larger than about 10 cm, taking the limitations of the sensors into account. For smaller sizes, these distributions are adjusted to be consistent with the flux measured by ground telescopes, the Haystack radar, and the Goldstone radar as well as the flux measured by the LDEF Satellite and the Space Shuttle. The computer program requires less than one second to calculate the flux and velocity distribution for a given size debris relative to an orbiting spacecraft. It can be retrieved at URL : http://www.orbitaldebris.jsc.nasa.gov/model/ordem96.html

EVOLVE is the primary NASA orbital debris environment model for short-term (a few decades to a few centuries) evolution of the orbital debris environment. EVOLVE is a simulation model, in that it places launched objects, explosion or collision breakup fragments, and non-fragmentation debris in specific orbits, calculates how these orbits will change in time, and calculates from these orbits debris environment characteristics such as orbital debris flux as a function of time, altitude, and debris size. A fast orbit propagator, which accounts for J_2 and lunar-solar gravitational perturbations and aerodynamic drag, has been developed for EVOLVE.

EVOLVE places breakup fragments in the environment according to the mass and velocity distribution in the NASA breakup models, and debris from non-fragmentation sources are placed in orbit according to specific models for each debris deposition process. Debris mitigation measures are modeled in EVOLVE through the scenario definition file. Scenarios have been run controlling future launch rates, accidental explosions, and post mission orbit lifetime for payloads and upper stages. Launched objects are placed in orbit in accordance with historical data or, for environment projections, with mission model data that specifies the launch date, orbit, and payload and upper stage data for future launches.

The typical EVOLVE environment projection is started by calculating the current environment, using the historical record of launches and breakup events, where fragments from these events are placed in orbit using the breakup model. This current environment is then used as the initial environment for debris environment projections. Because EVOLVE calculates the current environment, comparisons between this environment and measurements of the current environment can be used to provide confidence that historical sources of orbital debris are being handled properly and that similar sources are being handled correctly in the environment projections. EVOLVE results are periodically compared with the US Space Command satellite catalog and the Haystack radar data. It can be retrieved at URL http://www.orbitaldebris.jsc.nasa.gov/model/evolve.html

ESA's MASTER (Meteoroid and Space Debris Terrestrial Environment Reference) model is based on quasi-deterministic principles, using orbit propagation theories and volume discretisation techniques to derive spatial densities and velocity distributions for particles larger than 0.1 mm in a 3D spherical control volume ranging from LEO to GEO. Space debris are generated for historic fragmentation events, and orbit states are propagated to a reference epoch, before they are merged with data of tracked objects. Collision flux from debris and meteoroids can be recovered for any (also highly eccentric) target orbits between LEO and GEO altitudes. The only source term considered by the current version of the MASTER model are breakup fragments. Update activities aiming for a consideration of other source terms including very small fragments down to 1 micron, paint flakes, AL_2O_3 particles and NaK droplets are currently going on.

The semi-deterministic approach used here implies the propagation of individual particles by means of 'classic' orbit propagation tools. Solar activity here is considered in terms of measured or projected cycles.

MASTER consists of two branches. The developer's branch of MASTER is used to establish a population of particles at a given reference epoch, which is further processed to act as the database for the MASTER user's branch. The user's branch is distributed to the model users on a CD ROM. Up to the reference epoch, classic and proven orbit propagation methods including the forces induced by the solar cycle are used for orbit propagation. ESA/ESOC's FOCUS orbit propagation routine is applied for this task. FOCUS combines the analytical integration method according to King-Hele with a quick access density model based on the MSIS-77 atmosphere. A rotating and oblate atmosphere, the density scale height variation with respect to altitude, and the diurnal bulge are considered by FOCUS. Historic solar activity values and future projections are obtained from NOAA data.

The MASTER model is not intended to render long term (> 10 years) flux predictions. To compute impact fluxes at epochs different from the MASTER reference epoch, the model does not perform the complex and time consuming orbit propagation process. Instead, an approach proposed in the former NASA engineering model is applied to extrapolate reference results with respect to time.

The Integrated Debris Evolution Suite (IDES) depicts objects larger than 10 microns in the debris environment. IDES is used primarily to predict directional collision flux to a satellite orbit for debris sizes larger than 1 mm over the next 50 years by simulating the long-term evolution of the debris environment. The only source term considered by the current version of the IDES model are breakup fragments. Update activities aiming for a better representation of other source terms, e.g. paint flakes and NaK droplets, are currently going on. As the MASTER model, IDES uses classic orbit propagation models applied to individual particles larger than 10 cm, and to classes of particles having comparable orbital elements at sizes between 10 microns and 10 cm.

As MASTER, IDES is based on semi-deterministic modelling and orbit propagation techniques. IDES propagates the orbits of individual large objects with respect to atmospheric drag, geopotential, luni-solar and solar-radiation pressure perturbations. Small objects are binned by their values of relevant orbital parameters and propagated sample-wise. For each sample object representing a certain number of real objects propagation is performed over a period Δt and results are applied to all objects represented by the sample. Historic solar activity values are obtained from /6/ and used for future projections. Atmospheric drag perturbations on the particle orbits are predicted by employing the complex, analytical expressions developed by King-Hele. Look-up tables are used to obtain atmospheric density/density scale

The presence of the in-situ microparticle detector GORID has stimulated understanding of the relationships between solid particles and the low energy radiation and plasma environment. Mc Donnel and co-authors have developed quantitative assessments of the interactions and modelling of population dynamics and, especially, a model for predicting GEO populations is developed and tested (DIADEM) which is linked to Master 99, ESA's comprehensive space debris tool. The GEO data from GORID prompted study of the role of electrostatic charges, closely linked to the orbital dynamics for the smaller particles which may achieve surface potentials exceeding some 20 KV. The DIADEM cloud model provides the user with the opportunity to determine particle flux to a HEO orbiting spacecraft resulting not only from the almost static 'background population' but also from highly dynamic sporadic 'particle clouds' (e.g. from solid rocket motor firings). Particle clouds are groups of orbiting objects with the same origin. This leads to well-defined distributions of their orbital parameters. Especially the inclinations of the cloud particles should have a very narrow distribution. The complete particle diameter range from 1 μm to 100 m.

EVOLVE	Kessler et al., 1996	Analytical
ORDEM 96	Kessler et al., 1996	Semi-empirical
MASTER	Klinrad, 1997	Semi deterministic
IDES	Walker et al., 1996	Semi deterministic
DIADEM	Mc Bride et al., 1999	Semi deterministic

Table 2 : models for debris location prediction

2.5.2 Meteoroids models

Cour-Palais derived a mass-dependent meteoroid flux distribution by considering various photographic data and information from space borne meteoroid detectors. In the mass range below 10-6 gram, the flux model has been developed from direct measurement data as a result of penetration damage from various sources such as the Explorer spacecraft mentioned above and converted to a corresponding mass by applying an empirical formula. The Grün Model expresses the averaged flux resulting from meteoroids in terms of integral flux F(>m) (impacts per sqare meter and year resulting from particles of mass m and larger) impacting a randomly oriented plate under a viewing angle of 2π in the ecliptic plane at 1 AU. Both, the Cour-Palais and the Grün model assumes an isotropic flux environment and does not give directional information. Contributions from streams or other sources are implicitly contained and would have to be removed when applied together with a stream model.

The derivation of the Grün flux required an assumed meteoroid mean speed and in recent ESA supported studies the velocity distribution has been developed using the Harvard Radio Meteor Project (HRMP) data where ~20000 meteor observations were taken so offering a statistically reliable data set, but reappraised the data using an improved analysis of ionisation probability and mass distribution index. To deduce the 1 A.U. distribution, the gravitational enhancement (and increase in speed) that is implicit within the 'atmosphere' data set is be taken out. The Divine Model (and the Divine-Staubach Model) developed a mathematical model using measurements of interplanetary dust to determine the orbital distributions of particles. As a starting point the model takes the particle phase space density. The model assumes the meteoroid environment to be comparable to a 'charged plasma' in which gravity - as the principle acting force - varies with the inverse of the distance between interacting objects. A simplified approach to consider solar pressure is also implemented. The model gives describes the meteoroid population at a given epoch. Time dependant effects such as collisions between particles, the change of orbital elements due to the Poynting Robertson effect or other perturbing forces induced by light pressure and electrostatic forces are neglected by Divine, though these may be very important, especially for the smaller particles. In the Taylor/McBride model, a meteoroid model that accounts for the variation of flux with respect to the viewing direction is presented.

While the background flux is known to remain fairly constant over the year, the individual stream activity is characterised by a seasonal dependent appearance. The meteoroid streams are caused by the intersection of orbits of existing or disintegrated comets with the Earth's ecliptic plane. The Jenniskens stream model takes into account meteoroid stream fluxes resulting from particles larger than 10^{-4} kg and is recommended to use the Jenniskens model.

Grün	Grün et al 1985
Cours Palais	Cour Palais, 1968
Divine	Divine 1993
Divine / Straubach	Divine 1993
Taylor / Mc Bride	Taylor and McBride, 1997
Jenniskens stream	Jenniskens, 1994

Table 3 : models for meteoroids location prediction

3 THE PARAMETERS

The large variability of the Solar Terrestrial system limits the efficiency of empirical models while progress in Space Weather requires the development of models that rely on basic physical principles controlling the behaviour of the Sun Earth interaction. Achieving the development of such quantitative physics-based models is one of the main challenge for Space Weather issues. However one can foresee a long time before this achievement. The short overview of the state of the art presented in the previous section shows that this delay is highly dependant on the considered sub-system. In the meantime, more developments and improvements of empirical models remain mandatory.

In the Space Weather perspective the ultimate goal of Modelling is to routinely produce forecasts of relevant parameters. That implies routine availability of key parameter measurements. The definition of these parameters should arise from the analysis of the inputs necessary to run operational Space Weather models. Before to summarised the input and output key parameters for each sub-system of the Solar Terrestrial system, we present tables that synthesise information on models presented in section 1.

Table 4 and 5 summarise the main models described in section 1, their inputs and their outputs. The tables do not include the technological models which estimate the effects of our environment on a given system as for example radiation doses, spacecraft charging, proton fluences or atmospheric drag. These models are presented in WP 3220 and in table 2 and 3 of the previous section for the meteoroid and space debris specific models.

Table 4 presents the pre-operational and operational models. The models are not restricted to the ones that are effectively used in operational centres, but include the models that could be today used operationally, as are for example most of the empirical models. This table does not however include all the models described in section 1 but is limited to either recent models or the most used ones for the same outputs. A letter indicates if the model is a physical one (P) or a semi-empirical or empirical one (E). We have also indicated whether development of the model itself or availability of new observations is the most crucial for its improvement. Column 3 indicates the type of data on which the model is based upon and finally some remarks are added in a last column. Most of these models use the geomagnetic indices as inputs. The SuperDARN convection model and the ionospheric profilers are based on data assimilation techniques in order to provide a 3D description of a given parameter using localised observations as inputs. It should be noted here that the development of ionospheric profilers is co-ordinated by the new European action COST271, and that within this action, one working group aims at developping methods to extract thermospheric parameters (neutral composition, temperature, total density, winds) from routine ionospheric observations (ground-based vertical sounding, TEC data).

Table 5 presents a summary of non-operational physics-based models. Contrarily to table 4, this table deals with classes of models and not specific models. All models require either improvements or new observations (including for validation purposes), or both. Most of them are today scientific codes developed for research purposes. The last column states their operational potentialities as foreseen today, if resources are available for operational development. Ring current models, as defined in section 1, are not included in this table, because the data needed at the boundary make almost impossible their use for operational Space Weather applications.

	Models	Based on	Inputs	Outputs	P or E	Model development needed	Observations needed for improving the model	Remark
Sun	Torr	DE satellite data	$F_{10.7}$	EUV/UV spectrum	E		X	New models under construction
	JPL Proton model	ground based and space data from 1956 to 1985		Proton fluences for E >10 Mev and for E>30 Mev	E			
Magnetosphere	Shue et al.	Satellite data	IMF Bz Solar wind density and velocity	magnetopause size and shape	E		X	
	Tsyganenko	IGRF Satellite magnetic field data	Geomagnetic Indices IMF Solar wind density and velocity	Magnetic Field	E			
	MSM	IGRF	Geomagnetic indices IMF Solar wind density and velocity	Magnetospheric particle fluxes : 0.1-100 Kev Magnetospheric E and B Precipitating electrons Ionospheric convection	P			Next generation : MSFM
	AP8-AE8	Satellite data from 1960 to 1975	Solar activity : min or max	Particle fluxes Protons : 0.1-400 MeV Electrons : 0.1-7 MeV	E		X	Magnetic storm effects non included
	LPCE/CEA Wave model	Satellite data : DE-1	Geomagnetic indices	Magnetic field power density spectrum Wave distribution Function	E		X	Presently only 2 Kp classes
Ionosphere	Heppner-Maynard-Rich	Satellite data	Geomagnetic indices IMF	Convection electric field	E			
	SuperDARN	Radar data assimilation	IMF SuperDARN radar data	Convection electric field	E		X	Real time
	AFGL precipitation models	Satellite data	Geomagnetic indices	Ion and electron auroral precipitation Conductivities	E			
	IRI	Ionosondes, IS data Topside sounders	$F_{10.7}$ or Sunspot number [NmF2 and HmF2, or TEC]	Electron and ion densities and temperatures	E	X		Valid in non auroral zone and for quiet conditions
	SLIM-FAIM PIM	outputs of physics-based models	$F_{10.7}$ Geomagnetic indices	Electron density profiles	E	X		
	Profilers	Data assimilation (Ionosondes)	$F_{10.7}$ or Sunspot number Ionosondes data	Electron density profiles	E	X	Mainly topside densities	Development co-ordination by COST271
Thermosphere	MSIS DTM	Satellite data from 1975 to 1983 + IS data for MSIS	$F_{10.7}$ Geomagnetic indices	Neutral densities and temperature	E		X	Mostly valid at mid and low latitudes
	HWM	Satellite data from 1975 to 1983 IS and interferometer data	$F_{10.7}$ Geomagnetic indices	Neutral wind	E		X	Mostly valid at mid and low latitudes

	Models	Method	Inputs	Outputs	Operational potentialities
Sun	Solar atmosphere	MHD	Photospheric magnetic field	Coronal magnetic field; Eruptive phenomena	Long term
Interplanetary medium	Solar Wind Global Structure	MHD	Plasma and magnetic field at the Sun	IMF, Plasma velocity, density and temperature at 1 AU	Long term
	propagation of CMEs	MHD	Plasma and magnetic field at the Sun	Properties of CMEs at 1 AU and beyond	Long term
Magnetosphere	Global models	MHD and/or Kinetic	IMF, solar wind velocity and density at 1 AU Present status of the magnetosphere	Magnetic field and particle distribution in the magnetosphere	Depend on the model
	Radiation belt	Adiabatic invariants Fokker Planck diffusion equation	Geomagnetic indices Thermospheric neutral densities Cosmic neutron flux, Waves Plasmaphere position	Particle fluxes Protons: 0.1-300 MeV Electrons: 0.1-10 MeV	Short term for Salammbô
Ionosphere Thermosphere	Ionosphere 1D and 3D models	Fluid description (+Kinetic Transport)	$F_{10.7}$ Thermospheric neutral densities, temperature and winds Geomagnetic indices or Convection pattern and Auroral Precipitation	Electron and ion densities and temperatures Ion velocity	Short term
	Coupled Ionosphere Thermosphere	Fluid description Eulerian approach	$F_{10.7}$ Geomagnetic indices or Convection pattern and Auroral Precipitation	Neutral densities, temperature and wind	Mid term

Table 4: Synthesis of model inputs and outputs of pre-operational and operational models. Only the most used ones in a given category are indicated. A column indicates if the model is a physics-based one (P) or a semi-empirical or empirical one (E) and 2 columns state whether development of the model itself or availability of new observations is the most crucial for its improvement.

Table 5: Summary of non-operational physics-based model classes. The last column states their operational potentialities as foreseen today, if resources are available for operational development.

3.1 THE SUN

With regard to the physics of the Solar-terrestrial relations the key parameter is indisputably **the solar magnetic field** : only the phostospheric magnetic field can be mesaured and MHD modelisation aimed to reconstruct from such observations the coronal magnetic field and its geographic variations (coronal holes, sunspots…).

For Space Weather applications, modelling should forecast the eruptive phenomena, mainly Solar Eruptions and Coronal Mass Ejections. Today their monitoring is required by the Space weather users. Solar eruptions are clearly associated with an increase of the **solar X and UV/ EUV fluxes**, and with an accelerations of electrons, protons, and heavy ions resulting in **solar energetic particle** events **(SEPs)**. CMEs correspond to ejection of mass and associated magnetic field which move away from the Sun at speeds ranging from 250 to 950 $km.s^{-1}$. **CME onset times - CME velocities and directions** are important parameters to be observed, or predicted for Space Weather applications.

3.2 THE INTERPLANETARY MEDIUM

The key parameters for global modelling of solar wind behaviour and propagation of CMEs in the interplanetary medium are:

- **the magnetic field** conditions **at the Sun**,
- **the Solar wind density and velocity**
- **the Interplanetary Magnetic Field** (IMF)

For Space Weather applications, one of the main goals of modelling the solar wind flow through the interplanetary medium is the forecast at the Earth of hazards related to e.g., magnetic clouds which are the most geo-effective types of CMEs, high speed solar winds, or shock interactions with the magnetosphere which may result in geomagnetic storms and substorms. Therefore **irregularities in the electronic density**, **suprathermal electron beams, shock waves** need to be monitored.

The cosmic ray and Solar energetic particle fluxes whose intensity are highly dependant on the solar wind conditions, is also an important parameter for Space Weather applications, as for example to evaluate the radiation hazards on board aircrafts.

3.3 THE MAGNETOSPHERE

The global status of the magnetosphere is determined and controlled by the interaction between the interplanetary and the Earth magnetic fields. The key parameters are therefore:

- the **Solar wind density and velocity** at Earth orbit, that allow to calculate its hydrodynamic pressure,
- the **Interplanetary Magnetic Field** at Earth orbit and specifically its vertical component which control the reconnection between the interplanetary and Earth magnetic field lines,
- the **Earth magnetic field**,
- the auroral boundary conditions that specify the present status of the magnetosphere: the **polar cap potential pattern** (or equivalently the convection electric field pattern) and the **auroral precipitation pattern** or the **geomagnetic indices** used as proxies.

In the Space Weather context, global models of magnetosphere are mostly used as inputs for more specific models with more straightforward applications.

One of the main difficulties for physics-based models aiming at describing a given region of the magnetosphere (e.g., the inner magnetosphere) is the specification of the boundary condition (e.g., the distribution function of the particles at all parts of the boundary where the drift velocity is inward). The adequate real-time data that are needed in the context of a Space Weather operational use are actually almost impossible to acquire. One must consider the use of physical quantities that are easier to observe and that reflect the behaviour of the modelled region. For instance **Energetic neutral atoms** (ENAs) allow to image the energetic ions in the inner magnetosphere.

The case of the radiation belts is worth being considered separately.

3.3.1 The radiation belts

Many parameters are involved in the physics-based modelling of radiation belts. The particle sources are mostly in the magnetosphere tail, the particle losses take place in the upper atmosphere and ionosphere through collisions, and in the magnetosphere through pitch angle diffusion by electromagnetic waves. Moreover particle transport depends on electric and magnetic field perturbations and is thus much controlled by magnetic storms and substorms.

The key parameters for radiation belts modelling are therefore:

- the **Earth magnetic field** (geometry and temporal variations) for Mac Ilwain parameters smaller than 10,
- the **electromagnetic wave spectrum** (energy density and $\underline{k}$ vector) in the range 100 Hz to 20 kHz,
- the **plasmasphere characteristics** and more particularly the plasmapause radial distance. They depend on events that may have occurred a long time ago,
- the **atmosphere characteristics** (density of each constituent),
- the **cosmic neutron flux**

The quantities to be monitored and predicted are the **particle distribution spectrum** with respect to energy and altitude. The distribution of energetic electrons is driven by radial diffusion and by particle acceleration and loss caused by waves in several different wave modes, including the whistler mode, ion cyclotron, magnetosonic wave modes. Particularly important are whistler mode waves at frequencies of 100 Hz.

The **magnetic index Dst** is a proxy of radiation belt behaviour.

3.4 THE IONOSPHERE-THERMOSPHERE SYSTEM

The key parameters for modelling are linked to the energy inputs in the ionosphere-thermosphere system. They are:

- the **UV/EUV solar flux**, that defines the electromagnetic energy input;
- the **auroral precipitations** (electrons and protons with energy smaller than about 100 keV) that define the particle energy input;
- the **convection electric field** (i.e. the polar ionospheric electric field distribution) that define the Joule energy input.

Although limited to auroral zones, particle and Joule energy inputs have effect on the whole globe. Their increases during periods of high geomagnetic activity leads to heating and expansion of the thermopshere and consequently to ionospheric density changes.

Today, ionosphere and thermosphere modelling is however still based on indices that define theses energy inputs. The **$F_{10.7}$ cm index** and the **sunspot number** are the most widely used proxy for the electromagnetic energy input. The **magnetic indices Ap** (or equivalently Kp) are

used to define the high latitude energy inputs, but other proxies may be used as for example the polar cap potential (i.e. a measurement of the potential drop between the two cells of the convection pattern), the auroral boundary index (which specify the equatorial limit of the auroral oval.) or local magnetic indices (Al, AE, An, As…).

The quantities that are modeled are the **altitude profiles** of:

- the **neutral and ion densities and compositions**;
- the **neutral, ion and electron temperatures**;
- the **neutral and ion velocities**.

Improvement of the physics-based modelling requires observations of all the above parameters. However, the set of parameters that need to be monitored and forecasted for Space Weather applications is much smaller:

- the **total neutral density**, that increases during magnetic storms as does **the exospheric temperature**. It is responsible for an increase of the atmospheric drag on the satellites but also on the space debris whose tracking may be lost.
- the **electron density profile** and the **total electron content** affect the communications and the GPS observations; the **ionospheric irregularities** are responsible for the scintillation in GPS signals,
- finally the time varying ionospheric currents, that depends on the convection electric field and the ionospheric conductivities (i.e. the electron density) result in geomagnetically induced currents (GICs) which affect the power distribution networks, the pipeline corrosion and possibly the railway signalling.

4 THE OBSERVATIONS

Some of the parameters listed in the previous section are not yet observed and most of them will probably never be measured with the necessary space and time resolution. However these parameters can be monitored by physical quantities that are easier to observe and that reflect the behaviour of one or more parameters. Some of these quantities, whose importance is acknowledged by the whole scientific community, are routinely measured and made available. Among them are "indices", presented in the next section. Some others are at present measured only in the frame of scientific experiments of limited duration.

In this section, we present rapidly observations that are of interest for Space Weather. They are classified according to the sources of the associated physical processes and summarised in table 6.

More detailed information about space observations and ground-based measurements will be given in workpackages 2200-2300 and 3120 respectively. The choices of the measurements that are necessary for a Space Weather programm will be made in these reports according to different strategies.

4.1 THE SUN

The solar activity is monitored with indices that are presented in the next section. Observations of solar flares, of CMEs, and of their proxies are reviewed in WP-3120 and complement therefore this first catalogue.

White-light and Hα coronal images are obtained by means of ground and space coronographs. Images measured from ground, which allow to deduce the sky projection of the velocity, are not very useful for CMEs coming towards the Earth. Coronal images obtained onboard SOHO have outlined the different behaviours of CMEs: some are very rapid as soon as they are visible, some are accelerated while others disappear as they go away from the Sun.

The outer corona is also observed at *radio wavelengths* (between 0.6 and 2 meters) by the Nancay radioheliograph, since 1967. A complete mapping of the emissive sources is possible since 1996. Images are obtained daily for distances above the photosphere in the range 50 000 to 500 000 km. Radio bursts, i.e. abrupt increases in the solar radio emission, can be associated with various phenomena: sunspots with strong magnetic field; shock waves caused by chromospheric eruptions; ejection of beams of energetic electrons at relativistic velocities; synchrotron emission of electrons at the top of magnetic loops in the corona, or in plasma bubbles moving at a speed of about 100 km/s; high energy electrons enclosed in coronal magnetic loops.

X/EUV/UV full disc images are obtained by several satellites including SOHO, TRACE and Yohkoh.

Figure 1 shows the time and wavelength coverage of solar *EUV/UV spectrophotometric measurements* from satellites. Today, measurements are obtained by the SOHO spacecraft (ESA-NASA) and very recently by TRACE (NASA).

The knowledge of the whole EUV spectrum integrated over the entire solar disc is mandatory for the ionosphere-thermosphere modelling. The presently avalaible measurements do not correspond to a significant range of solar activity conditions. New spectrometric measurements will be done onboard the TIMED spacecraft from NASA (launch scheduled in 2001) and the Solar platform on the International Space Station (2002). In addition, a new instrument will be flown on the GOES spacecrafts that already monitored the *X-rays.*

	Observed quantity		Measurement	I -M
Sun	Flux EUV/UV for aeronomy		Satellite spectrophotometry	I
	Flux UV, EUV et X		Satellite imaging	M
	Solar magnetic field		Ground based and satellite	M, I
	CMEs proxies		magnetograph, Hα and EUV telescopes	M
	CMEs onset times and velocity		Coronograph (ground based and satellite) EUV and X-ray telescopes, radio imaging	M, I
	Shocks		Hα and EUV telescopes, radio	M
	Energetic particles interacting in the atmosphere		Radio, X, gamma diagnostics	M
Interplanetary medium	Solar wind density and velocity		In situ, at the Lagrange point L1	M, I
	Interplanetary Magnetic Field			M, I
	Irregularities in the electronic density		Thomson diffusion in white light (satellite)	M
	Suprathermal electron beams and shock waves		Radio emission (satellite)	M
	InterPlanetary Scintillation		Radio emission (ground based)	M
	Cosmic rays		Neutron and muon monitors (ground based and satellites)	M
Magnetosphere	Spectrum of magnetospheric particles 1 eV ≤ E ≤ 500 MeV		Satellite observations	I
	High energy Solar Protons and heavy ions			M, I
	Electromagnetic ULF/VLF waves			I
	Energetic Neutral Atoms			M
Ionosphere	Spectrums of auroral precipitations e^-, H^+: 0.1 eV ≤ E ≤ 500 keV		Satellite observations	I
	Image of auroral ovals		Satellite observations	M
	Convection electric field		Satellite observations High latitude radars (EISCAT, SuperDarn, …) Deduced from the magnetic activity	M
	Electron density	variation with altitude	Incoherent scatter radars	I
		TEC, foF2 and hmF2	GPS, Ionosondes	M
Thermosphere	Neutral wind		Optical interferometry (ground based and satellite) Incoherent scatter radars	I
	Neutral density		Spectrometry (satellite) Accelerometry (satellite)	I
	Neutral temperature		Optical interferometry (ground based and satellite) Incoherent scatter radars	I
	Meteoroids and Space debris	Large debris	Radar, optical telescopes (ground)	M
		Dust	Satellite observations	I
	Main Earth magnetic field		Magnetic observatories and dedicated satellites	I
	Magnetic activity at the Earth surface		Magnetic observatories and network of variometers	M

Table 6 : *Summary of available observations. The last column indicates if observations are used for model improvement (I) or for monitoring (M).*

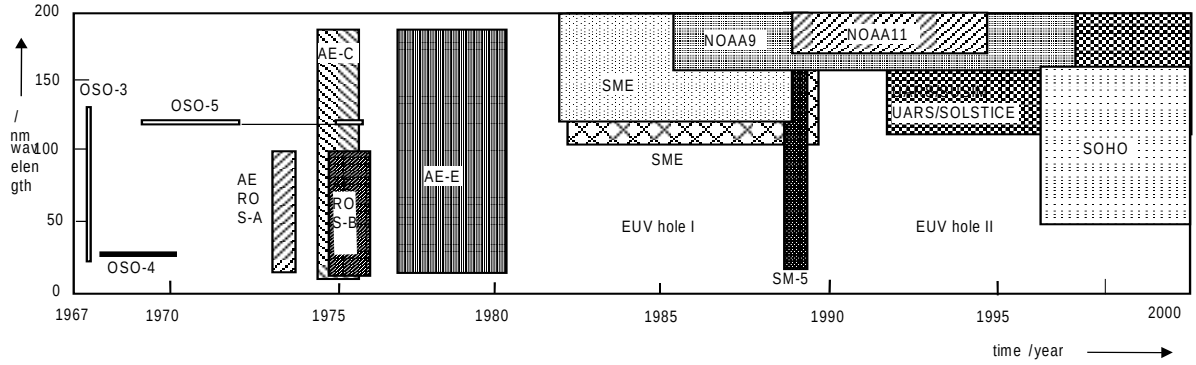

Figure 1: *Time/wavelength coverage of solar EUV/UV spectrophotometric measurements from satellites (from Schmidtke, 2000)*

The Photospheric magnetic field is measured onboard the SOHO satellite and from the ground. The THÉMIS Franco-Italian Solar telescope (Télescope Héliographique pour l'Etude du Magnétisme et des Instabilités Solaires) provide high spatial resolution, accurate polarisation measurements and simultaneous observations in several spectral lines. However, ground measurements of full-disk magnetographs are only provided the USAF Improved Solar Observing Optical Network and by SOLIS-VSM.

4.2 THE INTERPLANETARY MEDIUM

Measurements of the Interplanetary Magnetic Field (IMF) and of the solar wind parameters should be made in situ, upstream enough from the magnetosphere to be in regions not perturbed by the magnetosphere itself and by upstream phenomenon. The Lagrange point L1 is an ideal location to make these measurements. At the moment in situ measurements of the IMF and solar wind parameters are made at the Lagrange point by the NASA ACE and WIND probes. In addition to them, celerity and density of solar wind protons are measured by CELIAS experiment onboard SOHO.

Data from four ACE instruments are sent in real time to the SEC (for Space Environment Centre) of NOAA. These data are circulated as RTSW (for Real Time Solar Wind) packages containing:

- *energetic ions and electrons* (EPAM experiment),
- *magnetic field vector* (MAG experiment),
- *fluxes of high energy particles* (SIS experiment),
- *solar wind ions* (SWEPA experiment).

Apart from in situ measurements in the solar wind, possible observations are in quite limited numbers, and in general difficult to interpret. They amount to optical and radio techniques:

- optical techniques aim to observe white light Thomson diffusion related to *irregularities in the electronic density*. Present instruments (SOHO/LASCO) allow observations up to 30 Ro, i.e. 0.14 AU[9]. Instruments under development (e.g. SMEI) will allow to observe up to distances

[9] The Sun radius Ro is 696 000 km, and 1 UA corresponds to about 215 Sun radius.

from the Sun larger than 1 AU, as already demonstrated by HELIOS observations. Such an instrument will flow onboard STEREO;

- radio techniques are of two types:

  observations of coronal and interplanetary bursts, that are the signature of *suprathermal electrons beams and shock waves* (Mann et al., 1999)

  IPS (for *Inter Planetary Scintillation*) measurements, that allow to derive maps of solar wind velocity and density projected onto the sky.

  The combination of these two techniques with a heliospheric density model may allow to determine the radial velocity of the radio sources and therefore their arrival time at Earth

The *cosmic ray flux*, as well as the most energetic solar particles issues from solar flares[10], are measured by neutron monitors on board satellites and on the ground. The heliocentric potential measures the difficulty for the cosmic ray travelling through the heliosphere to reach the Earth environment. It is deduced from measurements by ground neutron monitors of the secondary cosmic rays that reach the ground. The heliocentric potential intensity is modulated by the solar cycle, as shown on figure 2 which compares the behaviour of cosmic rays measured at Kerguelen (a station of the "Institut Polaire Français") between 1964 and 1995, and the solar index RI_{12} .

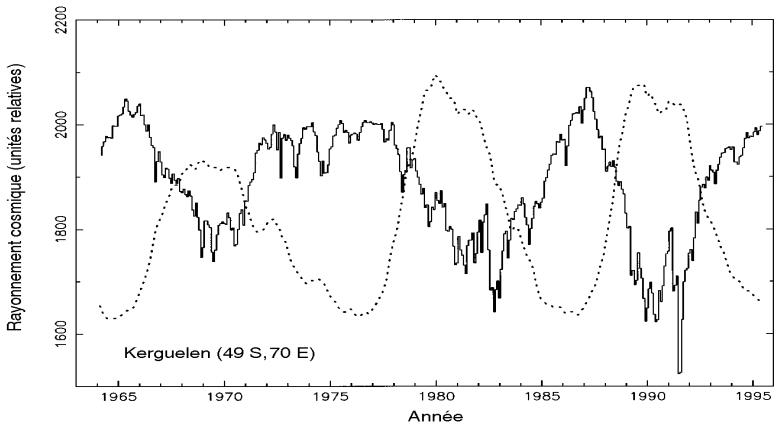

Figure 2 : *Comparison of cosmic rays measured at Kerguelen (heavy line) and the solar index RI_{12} (dotted line)*

4.3 THE MAGNETOSPHERE

Fluxes of particles of energy up to 500 MeV and *high energy protons and heavy ions* from SPEs (with energies of hundred of Mev) are routinely measured at various points of the magnetosphere with sensors installed onboard satellites whose main objective is not the study of the magnetosphere. These measurements which are routinely performed, are not continuous both in time and in space. Therefore they are difficult to use for short term predictions.

- on geostationary orbits, e.g. GOES and LANL satellites,
- on polar orbits, e.g. POES satellites,
- on orbits with mean inclination, e.g. GPS satellites.

[10] In solar energetic particle (SEP) events, solar particles are accelerated due to fast CME-driven shocks up to several hundreds of MeV/nuc and all species from H to Fe reach energies in the order of the lower energy limit of cosmic rays (about 1 GeV). The temporal evolution in the spectra of gradual SEP events may be used as a kind of 'remote sensing', in which the conditions in the shock region are studied, even when the shock is still far away from Earth (Tylka et al., 2000).

Energetic particles observations observations are also made onboard science research satellites (e.g. INTERBALL, FAST, CLUSTER…).

Like energetic particles observations, *ELF/VLF wave observations* can be found on research spacecraft. Wave models, used for example in the Salammbo code, are based on data from OGO5, ISEE1, GEOS1, DE1 and CRESS.

Energetic neutral atoms (ENAs) allow to image the energetic ions in the inner magnetosphere. Three instruments onboard the research satellite IMAGE provide images of the ring current, the near-Earth plasma sheet, the nightside injection boundary, the ion populations of the cusp and finally the outflow of low-energy ions from the polar ionosphere.

4.4 THE IONOSPHERE

The *convection electric field* is measured on board spacecraft, in particular the American DMSPs, and from the ground using high latitude radars: incoherent scatter radars like EISCAT and HF SuperDARN radars. It can also be inferred from magnetic activity measurements.

Spectra of auroral particle precipitations (electrons and protons of energy smaller than or equal to 100 keV) are routinely measured onboard DMSP and NOAA satellites. Observations are also made onboard science research satellites (e.g. INTERBALL, FAST, CLUSTER…).

Visible and UV *images of the auroral ovals* are obtained by the POLAR spacecraft.

The *altitude variation of the electron density* is monitored by incoherent scatter radars, which therefore could become validation instruments for Space Weather. Ionosondes provide the peak and the altitude of the maximums of the E and F2 layers. Such measurements have been done on a regular basis since about half a century. GPS measurements allow to deduce the total electron content, that is directly important for users in communication, navigation and satellite altimetry.

In addition polar cap riometers measures the Polar Cap Absorption (PCA) related to the solar proton fluxes following solar flares, and all-sky cameras provide images of the auroras produced by the precipitating particles.

4.5 THE THERMOSPHERE

The *thermospheric neutral wind* is measured from the ground by optical interferometers: About 10 Fabry-Perot interferometers are working in the world now. A new French Michelson interferometer EPIS will be installed in Svalbard in 2001. The neutral wind is also measured by optical interferometers on board satellites (UARS ; TIMED). From ground, its meridional component can be inferred from incoherent scatter measurements and at middle latitude from ionosonde measurements.

The *neutral densities* and composition can be measured by spectrometry. They will be deduced from an UV imager onboard TIMED. The total density can also be inferred from satellite drag and from accelerometers. The ONERA accelerometer is flown on the German CHAMP satellite (2000-2005). The routine analysis of these accelerometric measurements in term of neutral density is now considered by CNES. The joint US-German two satellite mission GRACE (2001-2006) will also provide thermospheric data.

The *neutral temperature* is measured by ground optical interferometers and satellite ones. Temperature observations by the WINDII experiment on board UARS are currently under validation. Such observations will also be done by the TIMED spacecraft. In addition, the neutral temperature can be deduced from incoherent scatter observations under specific assumptions.

4.6 THE EARTH MAGNETIC FIELD AND THE MAGNETIC ACTIVITY

The *Earth magnetic field* is mainly described from measurements made at:

- geomagnetic observatories, that constitute a network of about 200 permanent stations distributed over all the world , where continuous recordings are made;
- satellites on polar orbit, and in particular the American MAGSAT (1980) and Danish ØRSTED (launched in January 1999) satellites.

All the available data are used to derive models of the main magnetic field and of its secular variation close to the Earth. A provisional model, the IGRF (for International Geomagnetic Reference Field), is computed on a five year basis[11]. The definitive models, called DGRF (for Definitive Geomagnetic Reference Field), are derived when the necessary data are available. These models are used to build the magnetic field models inside the magnetosphere.

The variations with time and space of the *geomagnetic activity* are described from recordings made at the geomagnetic observatories, and at networks of magnetic stations. These networks are mainly located in auroral zones. Data are now available on line, at the Web homepage of the networks, e.g. CANOPUS[12] or IMAGE[13], and at those of the INTERMAGNET[14] network that links about 70 observatories.

4.7 METEOROIDS AND SPACE DEBRIS

The usage, when a satellite arrives to death is to leave it to fall in the atmosphere where it burns. This fall is often slow: a geostationnary rocket stage needs between 10 years and 10 000 years to fall down, for perigees varying from 200 to 600 kilometres. Today, amongst the known space objects, only 6% are functional satellites. 22% are satellites having finished their operations, 17% are the superior stages of rockets, and the remainder 55% is made of fragments and various debris.

While dispersing itself in the atmosphere, a spatial vehicle generates debris that can be as dangerous as projectiles for the other satellites or worse, a space station. In 1990, the American satellite LDEF was recovered by the spatial shuttle after 6 years of flight. His examination revealed more of 30 000 visible debris impacts, perforations up to 3 millimetres, and degradation of the Mylar and Teflon cover. Another famous example is the French satellite Cerise, of which the stabiliser mast was cut in July 1996 by the collision with a debris originating from an Ariane rocket. Since then, Arianespace proceeds to the passivation of the rockets after the placement in orbits. The geostationnary satellites in life end are pushed up of about 200 kilometres, so that they gently escape to the attraction of the Earth. But no solution has been found yet to make inoffensive the satellites in low orbit.

It therefore becomes necessary to maintain these debris under high supervision. That is possible for those bigger than ten centimetres. There are about 8500 of them, facing the 110 000 debris of 1 to 10 centimetres, what is almost 300 time less that the smallest debris, impossible to localise. Altogether, this makes 2 millions of kilograms that orbit above our heads. The loss risk of a satellite by collision with one of these debris is for the moment of 1/10 000, but it grows exponentially with time.

---

[11] For instance, the IGRF 2000, published at the end of 1999, provides an extrapolation of the main field variations for the period 2000-2005.

[12] www.dan.sp-agency.ca/www/canopus_home.html.

[13] http://www.geo.fmi.fi/image/

[14] European data centres (GINs): par_gin@ipgp.jussieu.fr and e_gin@ub.nmh.ac.uk.

The NORAD centre mission is to follow the space debris in real time and to forecast their orbit moves. In spite of multiple efforts, space debris fluxes of millimetre or smaller sizes are basically unknown for orbits above 600 km. The data sources are of different types. Space based measurements mainly provided by passive sensors contribute to the knowledge in the small size particle region. Ground based measurements provide a picture of the larger particles. The most important space missions that contributed to the knowledge of the dust (meteoroids and space debris) distribution are Explorers 16 and 23, Pegasus 2 and 3, Solar Max, STS-MFE, LDEF, EURECA and ESA's HST array studies.

For the ground based measurements, the most important source is from the United States Space Command's Space Surveillance Network. It makes use of electro-optical and radar sensors located all over the world. It reveals a large population of debris between 850 and 1000 km altitude in an inclination band centered near 65° inclination, mostly of spherical shape sizing less than 3 cm.

5 THE INDICES

It is sometimes necessary to use summarised quantities, the indices, that provide a relevant synthetic information. Despite the simplifications they involve in the description of the solar-terrestrial system and in its interactions, indices do remain basic data in Space Weather. Furthermore, their very definition make them impossible to bypass for long term studies.

5.1 WHAT IS AN INDEX

Indices have been introduced in order to give a simple yet almost exact description of massive data ensembles which vary with time (and eventually in space). Basically, an index is made up from a set of discrete values which provide as pertinent and reliable information as possible about the phenomenon in question by characterising it as a whole. Of course, the validity of the index basically depends on its definition, and on the choice of the described aspect of the phenomenon.

A good index must be:

- *relevant*, i.e. the parameters used to derive the index are clearly related to the considered phenomenon. If not obvious, this relation must be clearly established before any use of the index to monitor a given phenomenon;
- *routinely computed*, i.e. values are continuously derived in order to make the index available to anyone who wants to use it. The computation is made on a permanent basis, even if there is no specific request at a given time;
- *consistent*, i.e. during the whole time span over which the index has been computed, it has the same meaning. Two equivalent situations would correspond to the same value of the index, whatever may be their epoch of occurrence;
- *objective*, i.e. the value of the index does not depend on the observer who derives it. In particular, it implies a clear definition relying on as simple and unambiguous operations as possible;
- *of clear meaning*, i.e. the aspect of the phenomenon described by the index can be clearly identified. If this is not the case, the possible quantitative investigations based on the index should be limited;
- *free of assumptions*, i.e. its derivation should not rely on some theoretical assumption which may be proved to be false afterwards, thus implying the irrelevance of the index;
- *available*, i.e. the index should be published in such a way that everybody can find and use it without difficulties. In particular, the index must be available both in computer compatible and printed forms;
- *reliable*, i.e. the published values have been effectively computed according to the rules established in defining the index. As for quick-look and provisional values, their status should be clearly indicated, and the underlying approximations clearly described.

5.2 THE SOLAR INDICES

5.2.1 The solar activity level : direct monitoring

5.2.1.1 Sunspot number index (Ri)

The simplest index -and therefore the oldest- is the number of sunspots and groups of sunspots. The relative international index monitoring the sunspots was set back in the years 1700'. The confidence in its monthly value started to be good after 1750, and after 1850 for the daily one. Today, it is called Ri. It is computed at the « Observatoire Royal de Bruxelles[15] » from the daily observations of several tens of ground stations. The index is the weighted mean of these observations. The weight of each observation depends on the instrument used. The number of groups of sunspots multiplied by a factor of ten is added to the number of sunspots itself. Therefore, the commonly used « sunspot index » denomination is wrong and particularly ambiguous for the journalists and the public.

The solar cycle is usually studied and predicted through the Ri_{12} index. This one is a 13 months weighted average, the two extreme values being divided by 2 :

$$RI_{12} = \frac{1}{12}\left(\sum_{m=-5}^{m=5} RI_m + \frac{RI_{-6}}{2} + \frac{RI_{+6}}{2} \right),$$

where Ri_m is the observed monthly mean of Ri. Therefore, it can only be available with a delay of seven months. The Ri_{12} index is of general use as soon as the studies are of long term purpose, including the ionospheric propagation studies. However, it should be noted that the CNET-Lannion rather uses a 5 months index Ri_5, which is considered as more efficient for the predictive models of the ionosphere :

$$RI_5 = \frac{1}{5}\left(\sum_{m=-3}^{m=+1} RI_m \right)$$

The sunspot index is not as arbitrary as it could seem : Indeed, the measurements of the areas of spotted sun made at the Greenwich Observatory from 1874 to 1976 and then at the Debrecen Observatory (Hungary) are reasonably well correlated with the sunspot index Ri (figure 3).

5.2.1.2 The $f_{10.7}$ cm index.

A second solar index is well correlated with the Ri one. It is the solar flux measured at the radio wavelength of 10.7 cm ($f_{10.7}$) (figure 4a). The correlation coefficient is 0.982 for the monthly mean values and 0.996 for values such as Ri_{12}. The $f_{10.7}$ index is now used in most of the operational thermospheric models (aerobreaking...) to determine the full X and UV/EUV spectrum. In its thesis, published in 1948, J.F. Denisse showed that the centimetric flux is correlated (with a coefficient of 0.87) to $\sum_k \sqrt{A_k} H_{0k}$ where A_k is the area of a sunspot k, Ho_k is its magnetic field strength, and the summation is made on all active regions on the solar disk.

[15] http://www.oma.be/KSB-ORB/SIDC/index.html

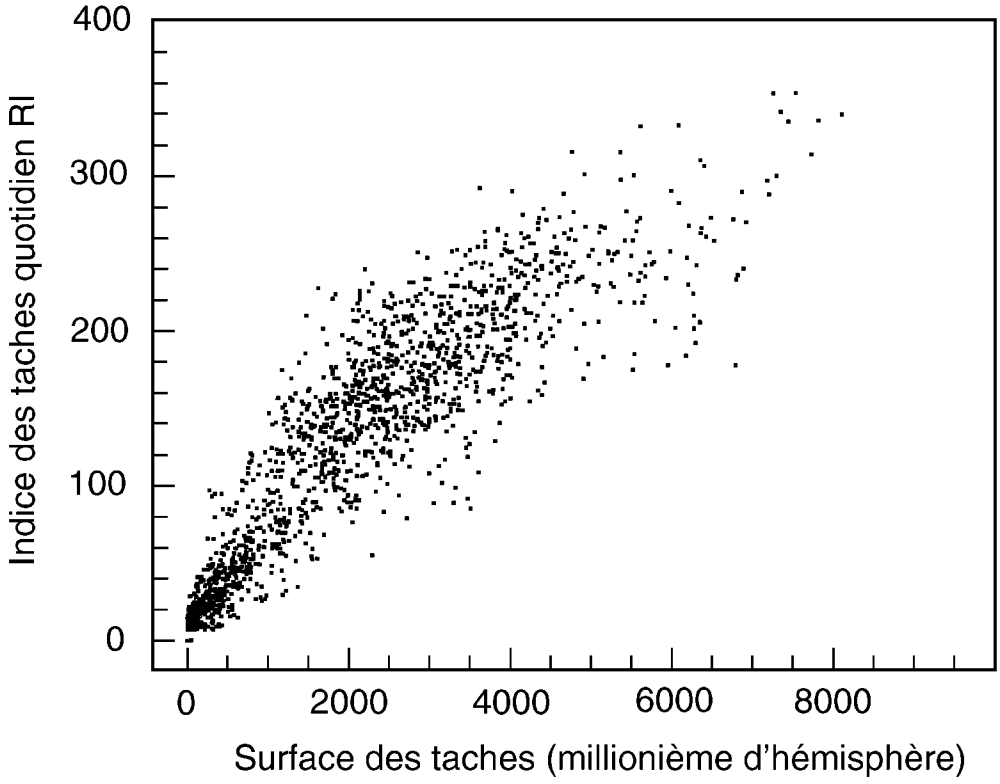

***Figure 3** : comparison of the daily values of the sunspot number index with the area of the spotted sun*

Today, one knows that the slowly variable component of the centimetric flux is due to the thermal electrons of the coronal loops above the sunspots, as it is the case for the UV/EUV flux. In the case of the centimetric flux, the emission mechanism is either a free-free emission, or a gyromagnetic emission. It is measured each day at the Penticton Observatory near Vancouver[16]. The daily measurements exist almost since the beginning of the radio astronomy in 1947. That explains partially the interest of this index in the conception of the empirical models. Since the energy of the solar radio spectrum is too small to have any impact on the terrestrial atmosphere, the $f_{10.7}$ index is interesting for the physics-based models only because it is used in most of the empirical modelling of the UV/EUV and X fluxes.

5.2.2 The solar activity level: other indicators

Apart from the indices that we just described, one can find several routine measurements that give access to simple parameters at the Sun scale (heliocentric potential, total solar flux, Lyman α flux : see previous chapter). Many other indicators have been suggested in order to characterise the solar activity level. None have proved to be convincing enough to set an international network of measurements. In particular, they do not succeed in satisfying the criteria proposed in the introduction of this chapter. Two families can be frequently met in the literature :

- Those using measurements of the H and K lines of the Calcium, or h and k of the Magnesium
- The coronal ones using measurements of different highly ionised elements.

[16] http://www.drao.nrc.ca/icarus/www/sol_home.shtml

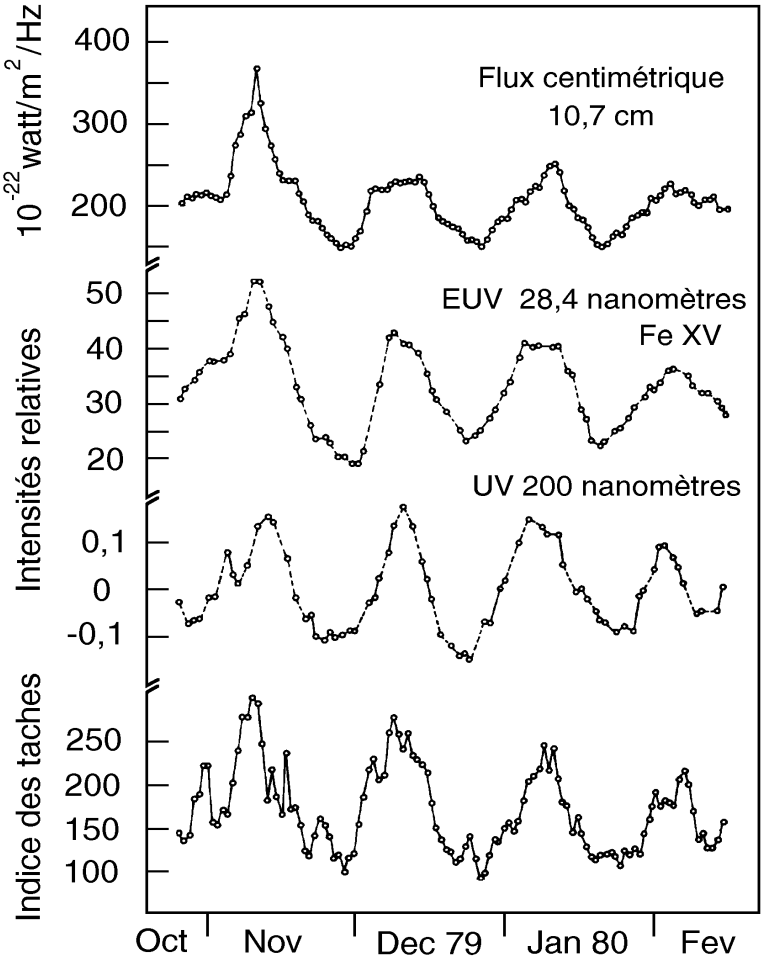

Figure 4a : *comparison between the sunspot index, the solar flux in a line of Fe XV, the UV flux at 200 nm and the centimetric index ($f_{10.7}$) on four solar cycles*

5.2.2.1 The calcium and magnesium lines

As many chromospheric lines, the H and K CaII lines (at 396.8 nm. and 394.4 nm. in the visible spectrum) and the h and k MgII lines (around 280 nm. in the ultraviolet spectrum) have a complicated profile. Indeed, they present a double emission peak in the centre of the line, of which the amplitude varies with the solar activity. Figure 5 shows the difference between the K Ca line profile as observed on a quiet Sun zone and on a chromospheric plage. A similar situation occurs for Mg II. The total flux of these lines is used in stellar physics to study the star activities. In the case of the Sun, the measurement of the energy ratio between the centre and the wings of the line allows determination of a precise index that characterises magnetic activity. This ratio is measured from the ground for the calcium lines and in orbit for the magnesium ones (Heath and Schlesinger, 1986). The correlation between the centimetric flux and the Ca or Mg indices for the undecennal flux is about 0.99. However, this correlation coefficient decreases when one considers smaller duration such as the 27 days solar rotation (figures 4a and 4b). At the undecennal cycle scale, the centimetric flux represents fairly well the intensity variations of the EUV lines, which are responsible of the high altitude atmosphere heating. Therefore, it is used in the modelling of the thermosphere or ionosphere. At the solar rotation time scale though, some

differences appear, as it is seen in the figures 4 when comparing the variations of the centimetric index and those of the Fe XV line.

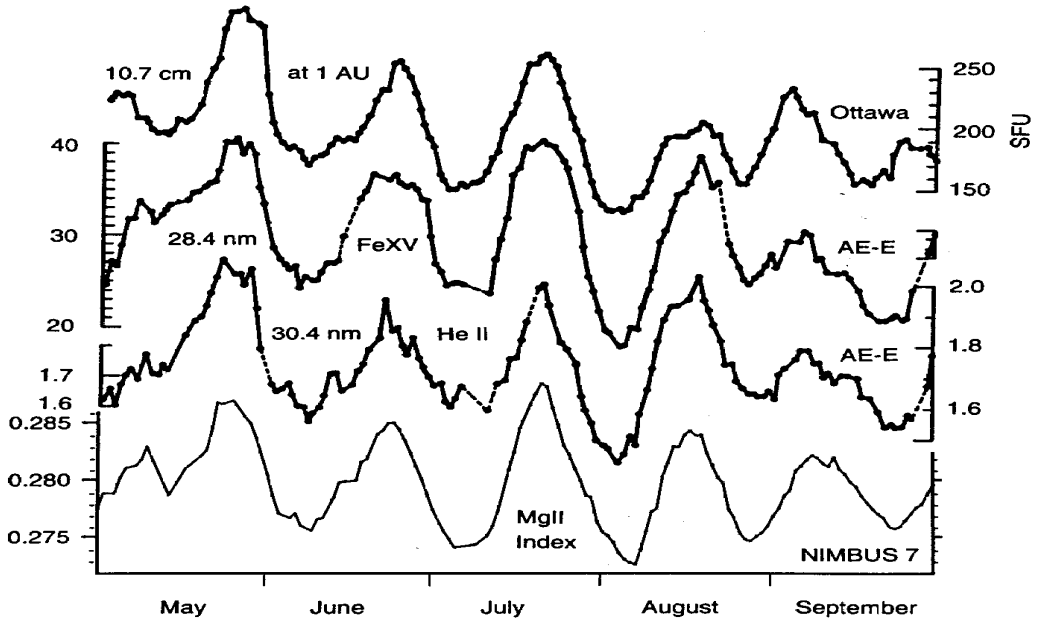

Figure 4b : *Comparison of the Mg index, the EUV flux at 30.4 nm. (He II), 28.4 nm. (Fe XV), and the centimetric index on five solar cycles*

Recent results show that the Mg II index simulates the UV flux better than the centimetric one (Lean et al., 1992). Figure 4b shows a comparison of the Mg index, the EUV flux at 30.4 nm (He II), 28.4 nm (Fe XV), and the centimetric index on five solar cycles. The best correlation is obtained between the EUV emissions and the Mg II index. This comes probably from a better proximity between the emission zones of the EUV and ionised magnesium than between the EUV and centimetric emission zones. Indeed, the centimetric flux originate at higher altitude (upper chromosphere / lower corona). Therefore, it is foreseen to introduce the Mg II index in the future empirical models of the thermosphere. The first results confirm this analysis (Thuillier and Bruinsma, 2000).

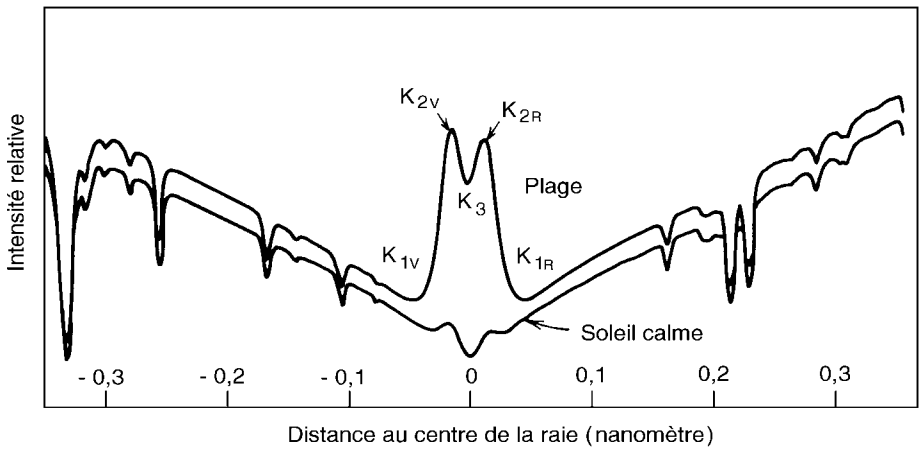

Figure 5 : Spectral profiles of the K line of the ionised calcium in the case of the quiet Sun and emitted in a chromospheric plage

Regular measurements of the Mg II lines started only in 1978, and are actually not immediately available. However, they are easy to get upon demand[17]. When the modelling requires previous values, the statistical relationship between the Mg II and the centimetric indices remains usable. MgII is measured by the instrument SBUV onboard the NOAA spacecrafts (NASA), and by SUSIM and SOLSTICE onboard UARS (NASA). Latter on, it will be measured by the SOLSPEC and SORCE instruments onboard the International Space Station. Because of its importance, the problem of its long term computation and its routine diffusion clearly appears.

5.2.2.2 Highly ionised species lines

The intensity of the coronal lines could also witness the solar activity level. It could be for example lines observed from ground with a coronograph, or UV lines observed from a spacecraft (i.e. EIT onboard SOHO). As an example, the Fe XV line is plotted in figures 4.

At the moment, only one line in the visible domain was sufficiently observed to be used as a coronal index : the XIV iron line at 530.2 nm. In 1956, Treillis showed that the most intense emissions of this line were localised above the plages. The Tatranská Lomnicka Observatory (Slovakia) regularly performs these observations since 1964. But in the absence of an international network, these coronographic observations from the ground depend on the local meteorological conditions.

5.3 THE GEOMAGNETIC INDICES

The magnetic field measured at the Earth surface is the sum of an internal planetary magnetic field and of components of primarily external origin, including those due to currents induced in the conductive Earth. While the planetary magnetic field has a slow or 'secular' variation, the external components are characterised by transient variations with a time scale in the order of days to minutes, and even less.

The transient variations of the geomagnetic field at the Earth surface are the signature of the currents taking place in the entire magnetosphere, as the result of the solar wind magnetosphere coupling processes. The high degree of complexity of the solar wind - magnetosphere - ionosphere coupling results in a large variety of magnetic signatures, depending upon the state of the magnetosphere, and differing with the geographic and geomagnetic location of the observatory. Thanks to decades of observation, it is possible to delineate the main morphological features of the ground observed perturbations, and, to a certain extent, to relate them to ionospheric and magnetospheric sources.

A fundamental starting point in the studies of transient variations is their decomposition into a regular and an irregular part. 'Regular' means that the variations have both a smooth shape and a regular occurrence, every day, while 'irregular' refer to both a great variability in shape and intensity, and an irregular occurrence of the variations. Such a distinction is linked to the discrimination between two different physical processes. The regular variations are mainly related to the atmospheric dynamo processes, while the irregular variations are mostly due to the energy input in the magnetosphere related for instance to magnetospheric storms and substorms. It is important to note that the terms magnetically quiet or disturbed only refer to irregular variations, i.e. indicate the absence or presence of irregular variations respectively.

Since the beginning of continuous recordings of the Earth's magnetic field variations, many indices have been derived to monitor its complex perturbations. At present, geomagnetic indices and remarkable events that are considered as relevant are acknowledged by the *International Association of Geomagnetism and Aeronomy* (*I.A.G.A.*). The reason for defining indices is twofold: on

[17] cebula@ssbuv.gfsc.nasa.gov

the one hand, to separate and quantify the variations representative of an isolated effect, as for example the ring current axis-symmetric variations (Dst index) or the auroral electrojet activity (AE indices) and, on the other hand, to estimate the global energy input in the magnetosphere, which is the purpose of the planetary indices. A synthetic presentation of the indices and remarkable events acknowledged by *I.A.G.A.* is given in Annex.

The summary of the derivation of the *I.A.G.A.* geomagnetic indices is shown in Table 2 and Figure 6 shows the network of stations.

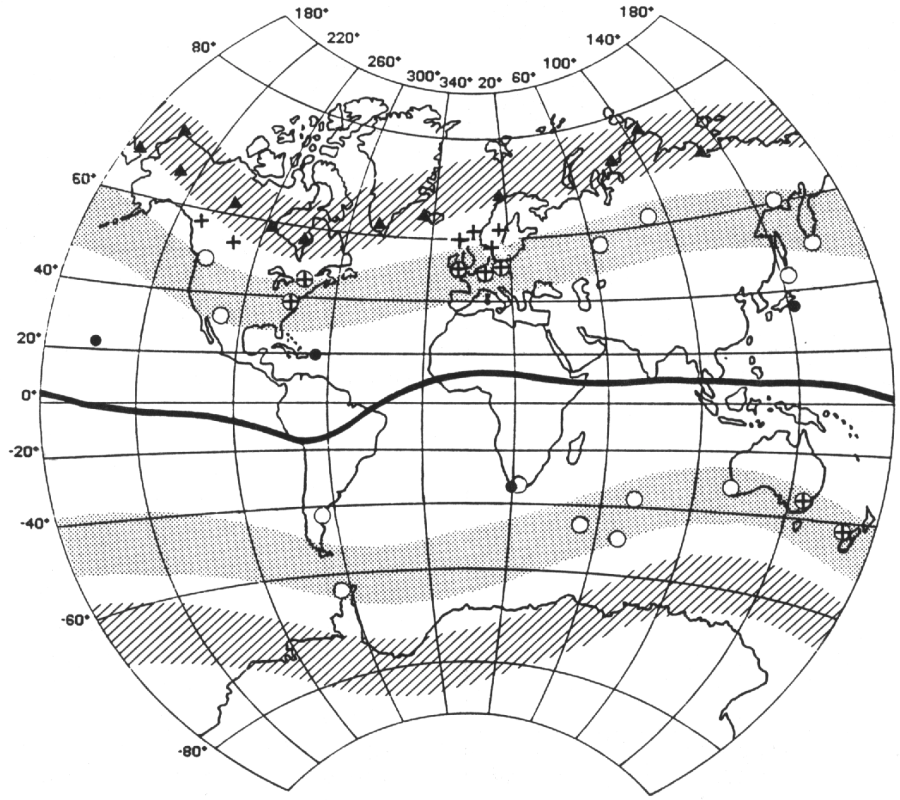

Figure 6: *Geographical world map on which are indicated the positions of stations belonging to the different networks used in deriving geomagnetic indices: ▲ for AE, ● for Dst, + for Kp, ap, ○ for am, Km, and ⊕ for stations belonging to both Kp, ap, and am, Km networks. A solid line indicates the position of the dip equator. The average extension of the auroral zone is sketched by the hatched area, that of the subauroral region by the shaded area (after Berthelier, 1993).*

-

Indices ***(beginning of the data series)***	**(1) Measured quantity Baseline**	**(2) Time interval**	**(3) Network**	**(4) Derivation process**
Auroral indices AE, AU, AL, A0 *(Since July 1957 ; missing data in 1976-1977)*	Deviation ΔH (nT) of the horizontal component Baseline: Sq* variation (see text)	1 minute (since 1978)	Network of stations in the boreal auroral zone Modification of the network in 1966 (see Figure 8 the network since 1966)	AU : largest observed value of ΔH(*t*) at the network stations and at time *t* (upper envelope) AL : smallest observed value of ΔH(*t*) (lower envelope) AE = AU + |AL| A0 = (AU + AL) / 2 *Unit: nT*
Equatorial index Dst *(since 1957)*	ΔH (nT) variation of the horizontal component; Baseline: secular variation	1 hour	Network of 4 low latitude stations (see Figure 8)	Hourly values of the perturbation D are computed at each station : D = ΔH - Sq** (see text) Dst = *Moy*(D) / *Moy*(cosϕ) ϕ : dipolar latitude of the stations *Unit: nT*
Local indices K	Amplitude of the irregular variations: ranges Baseline: S_R variation (see text)	3 hours (UT) : 00-03, 03-06, … …, 18-21, 21-24	K indices are defined everywhere, but their meaning is the best at subauroral latitudes	K is a code (a number: 0 to 9) corresponding to the class in which falls the measured range. The limits of the classes are defined according to a quasi logarithmic scale (see text and Figure 8) a_K(nT) is the mid-class amplitude associated to the K value.
Planetary indices Kp ap, Ap *(since 1932)*	K indices	3 hours (UT) (*cf.* K indices)	Network of 13 stations : 11 boreal ones and 2 austral ones. (see Figure 8)	K codes from each station are converted to standardised codes "3Ks" 3Kp=Σ3Ks/12 3Ks et 3Kp : integers, 0 to 27 Kp: 0o, 0+, 1-, to 9o ap: deduced from Kp through conversion tables *(unit: 2nT)* Ap: daily mean value of ap
Planetary indices an, as and am An, As and Am Kpn, Kps and Kpm *(since 1959)*	Amplitudes deduced from K indices	3 hours (UT) (*cf.* K indices)	Network of subauroral latitude stations: 13 boreal ones and 10 austral ones arranged in groups each group representing a longitude sector (see Figure 8)	For each longitude sector Gi, the average of Ks in converted to equivalent amplitudes: a_{Gi}(nT) an: $\Sigma\lambda_{Gi}a_{Gi}$ (boreal hemisphere) as: $\Sigma\lambda_{Gi}a_{Gi}$ (austral hemisphere) λ_{Gi} : weighting factor accounting for the longitude width of Gi am = (an + as) / 2 An, As, Am: daily mean values of an, as, am Kpn, Kps, Kpm: deduced from am, an, as through conversion tables *Unit for am, an, as: nT* *Unit for Kpn, Kps, Kpm: Kp unit*
Planetary index aa *(since 1868)*	Amplitudes deduced from K indices	derivation: 3 hours (UT) meaningful when averaged over at least 4 intervals	Network of 2 antipodal subauroral latitude stations: HAD and CAN (see Figure 8)	For each station, the a_K values are corrected to take into account the small differences between the latitudes of the 2 stations aa: average of the 2 corrected amplitudes *Unit: nT*

Table 2: Derivation processes of geomagnetic indices (after Berthelier, 1993)

6 SPACE WEATHER VERSUS CLIMATOLOGY

Geophysical and historical records show that mankind already experienced several climatic changes, i.e. on long time scale, or meteorological changes, i.e. on time scales of some years. Several phenomena contribute to these changes. Some have a geophysical terrestrial origin, such as the continental drift, oceanic dynamics, or the volcanism. Some others have an extraterrestrial origin, such as the position of the Earth in space, the fall of bodies in the atmosphere (asteroids, meteors…). Those sources are not a priori linked to the solar activity, nor to the space weather, although it is certain that we will have soon or later to unify our knowledge in order to understand the global Earth system.

6.1 IMPACT OF THE SOLAR CONSTANT AND SOLAR ENERGY

The fluctuations of the solar source have a preponderant impact on the terrestrial climate. This influence can be direct : a change of the total irradiance produces an immediate effect on the terrestrial temperature. The solar flux varies in function of the emission source : a sunspot does not radiate as a facula nor as a coronal hole. Therefore, the climate is directly linked to the solar activity. A variation of 0.3% of the solar constant (i.e. 4 $W.m^{-2}$) implies a variation of the average temperature on the Earth of 0.4 °C. The solar constant is linked to the sun diameter, which is not know with a sufficient precision. The existence of a diameter variation is itself a source of debates. From 1650 to 1760, J. Picard, P. La Hire and T. Mayer tried to answer this question. From their measurements and from recent measurements, it seems that the sun diameter diminishes by about 350 km each century, and that very poorly known oscillations occur (periods 3, 120, 400 years) (Rozelot, 2001).

Several studies demonstrate an influence of the solar cycle on some meteorological phenomena. A very good correlation between the averaged temperature and the sunspot number has been found over the last 5 centuries (Friis-Christensen and Lassen, 1991, Lassen and Friis-Christensen,1995). A discrepancy over the last years could be interpreted as an effect of the greenhouse gases. There also exists clues that the solar activity interacts with the Earth climate in the past history. For example, the small glaciation age (1550-1750) is probably linked to the Maunder minimum (1645-1715), during which there was no sunspot (E. Nesme-Ribes and G. Thuillier, Belin, janvier 2000).

6.2 IMPACT OF THE COSMIC RAYS

The cosmic rays are high energy particles (several MeV) that penetrate deeply in the atmosphere. They could be a source of condensation nucleus, and therefore of clouds formation (the physico-chemical process in not well established). One explanation could be that when the sun is active, the magnetosheat becomes broader, and screens the cosmic rays more efficiently. At the contrary, when the sun is quiet, the cosmic rays cross the magnetosheat more easily and can create more clouds. That could be an explanation for the anticorrelation recently found between the solar activity and the clouds coverage (Svensmark and Friis-Christensen, 1997, 1999, Svensmark 2000)

6.3 IMPACT OF THE GREENHOUSE GAZES

Brasseur and Hitchman suggested that the increase of the greenhouse gazes, and in particular CO2 could generate a decrease of the temperature of the middle atmosphere (Brasseur, 1993 and references herein). With the assumption of a doubling of the methane concentration at 60 km, they showed that the mesosphere would cool by about 5 K and that the thermosphere above 200

km would cool by about 40 K. From simulations (Roble and Dickinson, 1989) this would lead to a decrease of the F peak altitude by about 15 to 20 km. This is not yet measurable, and the effects of this thermospheric variation are not known. If confirmed, this would have a direct effect on the drag ant thus on the trajectory of the spacecrafts.

6.4 WHERE SPACE WEATHER STANDS IN CLIMATOLOGY ?

The items described above show that they may be some relations between solar activity and climatology, and that it is still a research activity. However any monitoring of solar activity in the space weather context could be useful for climatology studies. Therefore any Space Weather centre should keep open relationships with weather and climate centres.

7 BIBLIOGRAPHY

7.1 MODELLING SECTION

Abel B., and R.M. Thorne, Electron scattering loss in Earth's inner magnetosphere. 1. Dominant physical processes, J. Geophys. Res., 103, 2385-2396, 1998a

Abel B., and R.M. Thorne, Electron scattering loss in Earth's inner magnetosphere. 2. Sentivity to model parameters, J. Geophys. Res., 103, 2397-2407, 1998 b

Alissandrakis, C.E., On the computation of constant alpha force-free magnetic field, Astron. Astrophys., 100, 197-200, 1981.

Amari, T., et P. Démoulin, in Proceedings of the Workshop ``Méthodes de détermination des champs magnétiques solaires et stellaires", Observatoire de Paris, 187, 1992

Amari, T., J.-J. Aly, J.-F. Luciani, T.Z. Boulmezaoud et Z. Mikic, Reconstructing the solar coronal magnetic field as a force-free magnetic field, Solar Physics. 174, 129-149, 1997.

Amari, T., T.Z. Boulmezaoud et Y. Maday, A regularization method for the extrapolationbreak of the photospheric solar magnetic field. I. Linear force-free field, Astron. Astrophysis., 339, 252-260, 1998

Anderson, D. N., M. Mendillo, and B. Herniter, A Semi-Empirical Low-Latitude Ionospheric Model, Radio Sci. 22, 292, 1987.

Anderson, D. N., J. M. Forbes, and M. Codrescu, A Fully Analytical, Low- and Middle-Latitude Ionospheric Model, J. Geophys. Res. 94, 1520, 1989.

Aulanier, G., P. Démoulin, B. Schmieder, C. Fang, Y.H. Tang, Magnetohydrostatic Model of a Bald-Patch Flare, Solar Physics, 183, 369-388, 1998.

Barlier, F., C. Berger, J.-L. Falin, G. Kockarts et G. Thuillier, A thermospheric model based on satellite drag data, Ann. Geophys., 34, 9-24, 1978.

Baussart N. , F. Simonet, T. Réveillé, P. Bertrand, A. Gjizzo, R. André, and F. Lefeuvre, Investigation of the dynamics of enhanced natural and artificial electron fluxes in the radiation belts : influence of the whistler mode wave model, , Fifth European Conference on Radiation and its Effects on Components and Systems (RADECS 99), pp 1 – 5, IEEE, Piscataway, NJ, USA, 2000.

Berger, C., R. Biancale, M. III et F. Barlier, Improvement of the empirical thermospheric model DTM : DTM94 - a comparative review of various temporal variations and prospects in space geodesy applications, J. of Geodesy, 72, 161-178, 1998

Bilitza, D.(ed.) International Reference Ionosphere 1990, NSSDC 90-22, Greenbelt, Maryland, 1990.

Bradley, P.A. and J. R. Dudeney, A simple model of the vertical distribution of electron concentration in the ionosphere", J. Atmos. Terr. Phys., 35, 2131, 1973.

Cargill P.J., J. Schmidt, D.S. Spicer, S.T. Zalesak, Magnetic structure of overexpanding coronal mass ejections: Numerical models, J. Geophys. Res., 105, 7509, 2000.

Chen, M.W., L. Lyons, and M. Schultz, Simulation of phase and space distributions of storm time proton ring current, J. Geophys. Res., 99, 5745-5759, 1994

Chiu, Y. T., An Improved Phenomenological Model of Ionospheric Concentration, J. Atmos. Terr. Phys. 37, 1563, 1975.

Chiu, Y.T. et H.H. Hilton, Exact Green's function method of solar force-free magnetic-field computations with constant alpha. I -Theory and basic test cases, Astrophysis. J., 212, 873-885, 1977.

Cour-Palais, B.G. , Meteoroid environment model 1969 , NASA SP-8013 , NASA JSC, Houston TX 1969

Cuperman, S., L. Ofman et M. Semel, The absolute value and sign of the function alpha(r) in the force-free magnetic field modelling of photospheric observations, Astron. Astrophysis., 227, 227-234, 1990.

Daglis, I.O., R.M. Thorne, W. Baumjohann, and S. Orsini, The terrestrial ring current: origin, formation, and Decay, Rev. Geophys., 37, 407-438, 1999

Daniell, R. E., W.G. Whartenby, L. D. Brown, D. N. Anderson,M. Fox, P. Doherty J. J. Sojka, and R. W. Schunk, PRISM: A Parameterized Real-time Ionospheric Specification Model , Radio Sci, 1993.

Delcourt, D.C., J.-A. Sauvaud et T.E. Moore, Cleft contribution to ring current formation, J. Geophys. Res., 95, 20937, 1990a.

Delcourt, D.C., J.-A. Sauvaud et A. Pedersen, Dynamics of single-particle orbits during substorm expansion phase, J. Geophys. Res., 95, 20853, 1990b.

Demoulin, P., S. Cuperman, M. Semel, Determination of force-free magnetic fields above the photosphere using three-component boundaryconditions. II - Analysis and minimization of scale-related growing modes and of computational induced singularities, Astron. Astrophysis., 263, 351-360, 1992.

Demoulin P., L.G. Bagala, C.H. Mandrini, J.C. Henoux, and M.G. Rovira, Quasi-separatrix layers in solar flares. II. Observed magnetic configurations, Astron. Astrophysis., 325, 305-317, 1997.

Di Giovanni, G. and S. R. Radicella, An analytical model of the electron concentration profile in the ionosphere, Adv. Space Res., 10, No. 11, 27-30, 1990.

Divine N., Five Populations of Interplanetary Meteoroids , Journal Geophysical Research 98, 17, 029 - 17, 048 1993.

Dudeney, J. R., An improved model of the variation of electron concentration with height in the ionosphere, J. Atmos. Terr. Phys., 40, 195, 1978

Feldstein Ya. I., A. E. Levitin, D. S. Faermark, R. G. Afonina, B. A. Belov, and V. Y. Gaidukov, Electric fields and potential patterns in the high-latitude ionosphere for different situations in interplanetary space, Planet. Space Sci. 32, 907, 1984.

Feynman J., T. P. Armstrong, L. Dao-Gibner, and S. Silverman, Solar Proton Events During Solar Cycles 19, 20, and 21, Solar Phys., 126, 385-401, 1990.

Fisk, L. A.; Wenzel, K.-P.; Balogh, A.; Burger, R. A.; Cummings, A. C.; Evenson, P.; Heber, B.; Jokipii, J. R.; Krainev, M. B.; Kóta, J.; Kunow, H.; Le Roux, J. A.; McDonald, F. B.; McKibben, R. B.; Potgieter, M. S.; Simpson, J. A.; Steenberg, C. D.; Suess, S.; Webber, W. R.; Wibberenz, G.; Zhang, M.; Ferrando, P.; Fujii, Z.; Lockwood, J. A.; Moraal, H.; Stone, E. C., Global Processes that Determine Cosmic Ray Modulation, Space Science Reviews, **83** , 179-214, 1998.

Fok, M.-C., J.U. Kozyra, A.F. Nagy, C.E. Rasmussen et G.V. Khazanov, Decay of equatorial ring current ions and associated aeronomical consequences, J. Geophys. Res., 98, 19381, 1993.

Fok, M.-C., T.E. Moore et D.C. Delcourt, Modeling of inner plasma sheet and ring current during substorms, J. Geophys. Res., 104, 14557, 1999a.

Fok, M.-C., T.E. Moore, S. Slinker, J.A. Fedder et D.C. Delcourt, Nonadiabatic behavior of heavy ions in the magnetotail during IMF southward turning, AGU Fall Meeting, San Francisco, EOS Trans. AGU (abstract), 1999b.

Grad, H. et H. Rubin, Proc. 2nd Intern. Conf on Peaceful Uses of Atomic Energy, 31, 190, Geneva, United Nations, 1958.

Grün, E., Zook, H.A., Fechtig, H., Giese, R.H., Collisional Balance of the Meteoritic Complex, ICARUS 62, pp 244-277, 1985

Hardy D. A., M. S. Gussenhoven, and R. Raistrick, Statistical and Functional Representations of the Pattern of Auroral Energy Flux, Number Flux, and Conductivity, J. Geophys. Res. 92, 12275, 1987.

Hardy D. A., M. S. Gussenhoven, and D. Brautigam, A Statistical Model of Auroral Ion Precipitation, J. Geophys. Res. 94, 370, 1989.

Hedin A.E., MSIS-86 Thermospheric Model, J. Geophys. Res. 92, 4649, 1987.

Hedin A.E., Extension of the MSIS Thermospheric Model into the Middle and Lower Atmosphere, J. Geophys. Res. 96, 1159, 1991.

Hedin A.E., et al., Revised Global Model of Thermosphere Winds Using Satellite and Ground-Based Observations, J. Geophys. Res. 96, 7657-7688, 1991.

Hedin A.E., E.L. Fleming, A.H. Manson, F.J. Schmidlin, S.K. Avery, R.R. Clark, S.J. Franke, G.J. Fraser, T. Tsuda, F. Vial et R.A. Vincent, Empirical wind model for the upper, middle and lower atmosphere, J. Atmos. Terr. Phys. 58, 1421-1447, 1996.

Heelis R. A., J. K. Lowell, and R. W. Spiro, A Model of the High-Latitude Ionospheric Convection Pattern, J. Geophys. Res. 87, 6339, 1982.

Hilmer, R.V., and G.-H. Voigt, A magnetospheric magnetic field model with flexible internal current systems driven by independent physical parameters, J. Geophys. Res., 100, 5613, 1995

Hinteregger, H.E., D.E. Bedo, and J.E. Manson, The EUV spectrophotometer on Atmosphere Explorer, *Radio Sci.*, **8**, 349-354, 1973

Hinteregger, H.E., Representation of solar EUV fluxes for aeronomical applications, *Adv. Space Res*, **1**, 39-52, 1981.

Hinteregger, H.E., and F. Katsura, Observationnal, reference and model data on solar EUV, from measurements on AE-E, *Geophys. Res. Lett.*,**8**,1147-1150, 1981

Hochegger,G. Nava, B., Radicella, S., Leitinger, R., A family of ionospheric models for different uses, Phys. Chem. Earth, 25, 4, 307-310, 2000

Holt J. M., R. H. Wand, J. V. Evans, and W. L. Oliver, Empirical Models for the Plasma Convection at High Latitudes from Millstone Hill Observations, J. Geophys. Res. 92, 203, 1987

Hultqvist, B. M. Øieroset, G. Pashmann and R. Treumann (eds.), Magnatospheric plasma sources and losses, Space Science Series of ISSI, vol. 6, 482 pp., Kluwer Academic Publishers, 1999 (published also in Space Sci. Rev., 88, 1999)

Hurricane, O.A., R. Pellat et F.V. Coroniti, A new approach to low-frequency « MHD-like » waves in magnetospheric plasmas, J. Geophys. Res., 100, 19421, 1995.

Janhunen, P., GUMICS-3 – A global ionosphere-magnetosphere coupling simulation with high ionospheric resolution, in Environmental modelling for Space-based applications, ESA SP-392, 233-239, 1996.

Jenniskens, P.; Meteor Stream Activity – I. The annual meteor streams, Journal of Astron. And Astrophys. 287, pp 990-1013, 1994

Kessler D.J., J. Zhang, M. J. Matney, P. Eichler, R.C. Reynolds, P.D. Anz-Meador, and E.G. Stansbery, A Computer-Based Orbital Debris Environment Model for Spacecraft Design and Observations in Low-Earth Orbit, NASA Technical memorandum 1048825, 1996

Klinkrad H., J. Bendisch, H. Sdunnus, P. Wegener and R. Westerkamp, An Introduction to the 1997 ESA MASTER Model, Proc. of the 2nd European Conf. on Space Debris, pp. 217-224, ESA SP-393, May 1997.

Le Contel O., R. Pellat et A. Roux, Self-consistent quasi-static radial transport during the substorm growth phase, J. Geophys. Res., 105, 12929-12944,1999a.

Le Contel O., R. Pellat et A. Roux, Self-consistent quasi-static parallel electric field associated with substorm growth phase, J. Geophys. Res., 105, 12945-12955, 1999b

Lefeuvre, F., R. André, F. Simonet and N. Baussart, On the modelling of low frequency waves in the equatorial regions of the plasmasphere, Fall meeting of AGU, SM52A – 31, 2000.

Low B.C., Three-dimensional structures of magnetostatic atmospheres. IV - Magnetic structures over a solar active region, Astrophys. J., 399, no. 1, 300-312, 1992.

McBride N., S.F. Green & J.A.M., McDonnell. Meteoroids and small sized debris in Low Earth Orbit and at 1 AU: results of recent modelling, Advances in Space Research, 23, 73-82, 1999.

McDonnell J.A.M., D. J. Catling and M. A. Fowler , Update the statistical Meteoroid/debris models for GEO, UniSpace Kent, contract No 13145/98/NL/WK, ESA, december 2000

Mobarry, C.M., J.A. Fedder, and J.G. Lyon, Equatorial plasma convection from global simulations of the Earth's magnetosphere, J. Geophys. Res., 101, 7859, 1996.

Odstrcill D and V. Pizzo, Distortion of the interplanetary magnetic field by three-dimensional propagation of coronal mass ejections in a structured solar wind, J. Geophys. Res., 104, 28225, 1999.

Papitashvili, V. O., F. J. Rich, M. A. Heinemann, and M. R. Hairston, Parameterization of the Defense Meteorological Satellite Program ionospheric electrostatic potentials by the interplanetary magnetic field strength and direction, J. Geophys. Res., 104, 177-184, 1999.

Parker E.N., Interplanetary Dynamical Processes, 1963.

Pellat R., O.A. Hurricane et F.V. Coroniti. Multipole stability revisited, Phys. Plasmas, 1, 3502, 1994.

Picone, J.M., A.E.Hedin, D.P. Drob, R.R. Meyer, J. Lean, A.C. Nicholas and S.E. Thonnard, Enhanced empirical models of the thermosphere, Phys. Chem. Earth, 25, 5-6, 537-542, 2000.

Pizzo V.J., A three-dimensional model of corotating streams in the solar wind. III - Magnetohydrodynamic streams J. Geophys. Res, 87, 4374, 1982.

Pizzo, V.J., The evolution of corotating stream fronts near the ecliptic plane in the inner solar system. II - Three-dimensional tilted-dipole fronts J. Geophys. Res., 96, 5405, 1991.

Pridmore-Brown, D., Aerospace report no ATR-81(7813)-1, The Aerospace Corporation, El Sequndo, Californie, USA, 1981.

Radicella, S. M. and M. L. Zhang, The improved DGR analytical model of electron concentration height profile and total electron content in the ionosphere" Annali di Geofisica, 38, 1, 35-41, 1995.

Raeder, J., J. Berchem, M. Ashour-Abdalla, L.A. Franck, W.R. Paterson, K.L. Ackerson, S. Kokubun, T. Yamamoto, and J.A. Slavin, Boundary layer formation in the magnetotail: geotail observations and comparisons with a global MHD simulation, Geophys. Res. Lett., 24, 951-954, 1997

Rawer, K., Replacement of the present sub-peak plasma concentration profile by a unique expression", Adv. Space Res., 2, 183, 1983.

Rich F. J. and N. C. Maynard, Consequences of Using Simple Analytical Functions for the High- Latitude Convection Electric Field, J. Geophys. Res. 94, 3687, 1989.

Richard P.G., Fennelly and D.J. Torr, EUVAC : a solar EUV flux model for aeronomic calculation, *J. Geophys. Res.* **99**, 8981-8992, 1994

Richmond, A. D., and Y. Kamide, Mapping electrodynamic features of the high-latitude ionosphere from localized observations: Technique, J. Geophys. Res., 93, 5741, 1988.

Riley P. et al., J. T. Gosling, L. A. Weiss, V. J. Pizzo, The tilts of corotating interaction regions at midheliographic latitudes, J. Geophys. Res., 101, 24349, 1996.

Riley P., J. T. Gosling, V.J. Pizzo, A two-dimensional simulation of the radial and latitudinal evolution of a solar wind disturbance driven by a fast, high-pressure coronal mass., J. Geophys. Res., 102, 14677, 1997.

Roumeliotis, G., The ``Stress-and-Relax'' method for reconstructing the coronal magnetic field from vector magnetograph data, Astrophys. J., 473, 1095, 1997

Sakurai, T., Computational modeling of magnetic fields in solar active regions, Space Sci. Rev. 51, 11-48, 1989.

Sakurai, T., Calculation of force-free magnetic field with non constant alpha, Solar Phys., 69, 343, 1981.

Schunk, R. W. and J. J;. Sojka, Approaches to ionospheric modelling, simulation and predictions, Adv. Space Res. 12, (6)317, 1982

Schmidt, H.U., in Physics of Solar Flares, NASA SP 50, 107, 1964.

Sdunnus H. , H. Stokes, R. Walker, J. Bendisch, H. Klinkrad, Consideration of Solar Activity in Models of the Current and Future Particulate Environment of the Earth, ESA Proceedings WPP 155, 1998

Shepherd S.G.and J. M. Rhuohoniemi Electrostatic potential patterns in the high latitude ionosphere constrained by SuperDARN measurements, J. Geophys. Res., 2000.

Shue, J.-H., J.K. Chao, H.C. Fu, C.T. Russel, P. Song, K.K. Khurana, and H.J. Singer, A new functional form to study the solar wind control of the magnetopause size and shape, J. Geophys. Res., 102, 9497-9511, 1997

Slavin, J.A., and R.E. Holzer, Solar wind flow about terrestrial planets – 1. Modelling bow shock position and shape, J. Geophys. Res., 86, 11401-11418, 1981

Smets, R., Dynamique des electrons dans les regions de transitions de la magnetosphere terrestre, Thèse de l'Université Paris Sud XI, 1998.

Taylor, A.D., McBride, N. A radiant-resolved Meteoroid Model; Proceedings of the second European Conference on Space Debris; ESOC, Darmstadt/Germany, 03/97

Tobiska, W.K., revised solar extreme ultraviolet flux model, *J. Atmos. Terr. Phys.*, **53**, 1005-1018, 1991

Tobiska, J.R., and Eparvier, EUV 97 : improvements to EUV irradiance modeling in the soft X-ray and FUV, *Sol. Phys.*, **177**, 147-159, 1998

Torr, M.R., and D.J. Torr, Ionization frequencies for major thermospheric constituents as a function of solar cycle 21, *Geoph. Res. Lett.*, **6**, 771-774, 1979.

Torr, M.R., and D.J. Torr, Ionization frequencies for solar cycle 21: Revised, *J. Geophys. Res.* **90**, 6675-6678, 1985

Tsyganenko, N.A., Quantitative models of the magnetospheric magnetic field: methods and results, Space Sci. Rev., 54, 75, 1990

Tsyganenko, N.A., Modelling of Earth's magnetospheric field confined with a realistic magnetopause, J. Geophys. Res., 100, 5599-5612, 1995

Tylka et al., J.H. Adams, Jr.,P.R. Boberg, B. Brownstein, W.F. Dietrich, E.O. Flueckiger, E.L. Petersen, M.A. Shea, D.F. Smart, and E.C. Smith, CREME96: A Revision of the Cosmic Ray Effects on Micro-Electronics Code, IEEE Trans. Nucl. Sci. 44, 2150-2160, 1997.

Vandas M.., S. Fischer, M. Dryer, Z. Smith, T. J. Detman, Simulation of magnetic cloud propagation in the inner heliosphere in two dimensions 2. A loop parallel to the ecliptic plane and the role of helicity, J. Geophys. Res., 101, 2505, 1996.

Walker, R.J., T. Ogino, J. Raeder, and M. Ashour-Abdalla, A global magnetohydrodynamic simulation of the magnetosphere when the interplanetary magnetic field is southward: the onset of magnetotail reconnection, J. Geophys. Res., 98, 17235, 1993

Walker, R., Hauptmann, S., Crowther, R., Stokes, H., Cant, A., Introducing IDES: Characterising the Orbital Debris Environment in the Past, Present and Future, AAS 96-113, Advances in the Astronautical Sciences, Space Flight Mechanics 1996, Vol. 93, Part I, pp. 201-220, 1996.

Wang, Y.-M., and N. R. Sheeley, Jr., On potential field models of the solar corona, Astrophys. J., 392, 310, 1992.

Warren H.P., Mariska J.T., Lean J., Marquette W. and A. Johannesson, Modeling solar extreme ultraviolet irradiance variability using emission measure distribution, *Geoph. Res. Lett.*, **23**, 2207-2210, 1996.

Warren H.P., Mariska and J.T., Lean J., A new reference spectrum for the EUV irradiance of the quiet sun. 1. Emission measure formulation, *Journal Geoph. Res.*, **103**, 12077-12089, 1998.

Wu, S.T., M.T. Sun, H.M. Chang, M.J. Hagyard et G.A. Gary, On the numerical computation of nonlinear force-free magnetic fields, Astrophys. J, 362, 698-708, 1990

Zhang S. R., X. Huang, Y. Su and S. M. Radicella, A physical model for one-dimension and time-dependent ionosphere. Part I. Description of the model, Annali di Geofisica, 36, 5-6, 105,1993.

Zhang S. R. and S. M. Radicella, A physical model for one-dimension and time-dependent ionosphere. Part II. Results and discussion, Annali di Geofisica, 36, 5-6, 111, 1993.

7.2 OTHER SECTIONS

Berthelier, A., The geomagnetic indices: derivation, meaning and uses in Solar Terrestrial physics, in STPW-IV proceedings, Hruska, J., M.A. Shea, D.F. Smart et G. Heckman éditeurs, 3-20, Vol. 3, US Gov. Publications Office, Boulder, 1993.

Berthelier, A. et M. Menvielle éditeurs, IAGA Bulletin 40, ISGI Publication Office, Paris, 1991

Campbell, W.H., The regular geomagnetic field variations during quiet solar conditions, in Geomagnetism, Jacobs, J.A. éditeur, 385-460, Vol. 3, Academic Press, London, San Diego, 1989.

Friis-Christensen E. and K. Lassen, Length of the solar cycle : an indicator of solar activity closely associated with climate, Science, 1991.

Heath, D.F. et B.M. Schlesinger, The Mg 280 nm doublet as a monitor of changes in solar ultraviolet irradiance, J. Geophys. Res., 91, 8672-8682, 1986.

Lassen, K. and E. Friis-Christensen, Variability of the solar cycle length during the past five centuries and the apparent association with terrestrial climate, Journal of Atmospheric and Terrestrial Physics, **57** (8), 835-845, 1995

Lean J., M. Vanhoosier, G. Brueckner et D. Prinz, SUSIM/UARS observations of the 120 to 300 nm flux variations during the maximum of the solar cycle: inference for the 11-year solar cycle, Geophys. Res. Let., 19, 2203-2206, 1992.

Mann, G., Jansen, F., MacDowall, R.J., Kaiser, M.L., Stone, R.G., A heliospheric density model and type III radio bursts, Astron. Astrophys., **348 ,** 614

Mayaud, P.N., Derivation, meaning and use of geomagnetic indices, Geophys. Monogr 22, 154 p., AGU, Washington DC. 1980.

Menvielle, M., Derivation and dissemination of geomagnetic indices, Revista Geofisica, **48**, 51-66, 1998.

Menvielle, M. et A. Berthelier, The K-derived planetary indices: description and availability, Rewiews Geophys. Space Phys., **29,** 415-432, 1991.

Menvielle, M. et A. Berthelier, The K-derived planetary indices: description and availability (erratum), Rewiews Geophys. Space Phys., **30,** 91 1992.

Nesme-Ribes E. and G. Thuillier, Histoire solaire et climatique, Belin, 2000, ISBN 0993-4812

Rangarajan, G.K., Indices of geomagnetic activity, in Geomagnetism, Jacobs, J.A. éditeur, 323-384, Vol. 3, Academic Press, London, San Diego, 1989.

Rishbeth H, a greenhouse effect in the ionosphere ?, *Planet Space Sci*, **38**, 945-948, 1990.

Roble, R.G. and R.E. Dickinson, How will changes in carbon dioxide and methane modify the mean structure of the mesosphere and thermosphere ?, *Geoph. Res. Letters*, **16**, 1441-1444, 1989.

Rozelot, J.P., Possible links between the solar radius variations and the Earth's climate evolution over the past four centuries, Journal of Atmospheric and Terrestrial Physics, **63**, 375-386, 2001.

Samson, J.C., Geomagnetic pulsations and plasma waves in the Earth's magnetosphere, in Geomagnetism, Jacobs, J.A. éditeur, 481-592, Vol. 4, Academic Press, London, San Diego, 1991.

Schmidtke G., TIGER: A Program for Thermospheric-Ionospheric GEospheric Research, Physics and Chemistry of the Earth, 2000.

Svensmark H. and E. Friis-Christensen, Variation of Cosmic Ray Flux and Global Cloud Coverage - a Missing Link in Solar-Climate Relationships, Journal of Atmospheric and Solar-Terrestrial Physics, **59**, 1225-1232, 1997.

Svensmark H. and E. Friis-Christensen, Reply to comments on « Variation of Cosmic Ray Flux and Global Cloud Coverage - a Missing Link in Solar-Climate Relationships », Journal of Atmospheric and Solar-Terrestrial Physics, **62**, 79-80, 1999.

Svensmark H., Cosmic rays and Earth's Climate, Space Science Review, **93,** 155-166, 2000.

Sugiura, M. et T. Kamei, The Equatorial Dst index, in Equatorial Dst index: 1957-1986, Berthelier, A. et M. Menvielle éditeurs, IAGA Bulletin 40, ISGI Publication Office, Paris, 1991

Thuillier, G. et S. Bruinsma, The Mg II index for the upper atmosphere modelling, submitted to Ann. Geophys., 2000.

Tylka et al. in Acceleration and Transport of Energetic Particles Observed in the Heliosphere, eds. Mewaldt J.R., AIP Conference Proc. (2000), in press

8 ANNEXE A: THE SALAMMBÔ MODEL OF THE RADIATION BELTS

Salammbô is a set of codes devoted to the understanding of high energy charged particle transport in the inner part of the magnetosphere, in particular during magnetic activity periods. It is now composed of three different codes.

8.1 SALAMMBÔ-3D (2D IN SPACE)

The first one, called Salammbô-3D, was the first written. It solves the classical Fokker-Planck diffusion equation, either for proton or electron radiation belts, in the 3-D phase space. The equation is written in terms of the three adiabatic invariant, corresponding to energy, pitch angle and L McIlwain parameter, so this version is a real 2D in space, where the results are averaged on the longitude (local time).

For the protons, sources were taken as night side injections occurring during magnetic storms or substorms, and the well known CRAND (Cosmic Ray Albedo Neutron Decay) phenomenon. Particle transport were assumed to be due to radial diffusion, either given by magnetic or electric perturbations, and to frictional process related to Coulomb interaction with neutrals from the exosphere and cold electrons from the plasmasphere. Losses correspond to the charge exchange phenomenon, a proton giving its energy to a cold hydrogen atom, the resulting cold proton being lost from the radiation belt point of view. Other losses are efficient when the particle precipitates on the Earth (in fact, on the high atmosphere, near 100 km). The precipitation in this code are related to the loss cone, because when radial diffusion acts, particles are carried from one L shell to another, the two shells corresponding to different loss cones (on the shell L = 1, no particle can subsist). All these processes are well known from the physical point of view, so they are exactly calculated in the code. Nevertheless, their inputs are less known and they come from different models in the code. For the injections, in the first version, distribution functions derived from the NASA AP8 (min or max) model were used as the boundary condition, set at L = 7. For the CRAND process, an incident cosmic neutron flux is needed. It was taken from calculations. For the friction process, exosphere neutral model is needed. From MSIS-86 (better at high altitudes than MSIS-90), and using a hydrostatic model, all the neutral constituents were determined. As for the plasmasphere, we used a Carpenter model, though difficult to extrapolate to non equatorial regions. The charge exchange coefficients also need a Hydrogen atom model, the MSIS-86 plus the hydrostatic extrapolation was also used here. Finally, the most uncertain coefficients are the radial diffusion ones. There were in this first step taken from Schulz. The results of this code were compared to AP8 maps in Beutier et al. (1995).

From this version, different improvements were made. The first one was to replace a simple dipole magnetic field to an eccentric tilted dipole, the coefficients of which were calculated from the year dependent International Geomagnetic Reference Field (IGRF), updated every 5 years. The second one corresponds to the adding of losses due to inelastic nuclear interaction, using the same neutral atom model, this being important for high energy protons (energies greater than 50 MeV). Finally, we have begun to see the influence of the solar cycle on the radiation belts. To do that, the CRAND source terms were set solar cycle varying by the neutron flux, this being modelled from the Climax neutron monitor. Moreover, all the coefficients depending on the MSIS+hydrostatic model were taken solar cycle dependent by using, instead of a $f_{10.7}$ and Ap mean fluxes, those averaged year by year. Finally, the secular drift of the magnetic field was also taken into account, calculating all the coefficients year by year, because the same L shells do not correspond in this case to the same geographic surface, the densities then varying with time. The

results of this version were presented for the equatorially mirroring protons at EGS (Vacaresse et al., 1998), and the full treatment (with all the non equatorial particles), is planned to be presented at COSPAR (Boscher et al., 1998). In the final version, it can run for protons between 1 keV and 300 MeV,

For the electrons, the first version was published in 1995 (Beutier and Boscher, 1995). For these particles, CRAND is not efficient, so the only source corresponds to storm and substorm injections. Frictions due to Coulomb interactions are once more used, derived from MSIS+hydrostatic model. But pitch angle diffusion is here added. This can be due to Coulomb interactions with the neutral atoms or cold plasmaspheric electrons. These particles being many times ligther than protons, they can undergo changes in the pitch angles when interacting with electric field surrounding free electrons or bounded electrons from neutrals. They undergo also pitch angle diffusion when interacting with electromagnetic fields related to the presence of waves. In the first version of the code, only plasmaspheric hiss in the 100 Hz range was considered. These two pitch angle diffusions directly precipitate electrons into the loss cone. This is an efficient process for the electron loss, especially in the slot region. Radial diffusion is also used here to transport particles across L shells. Using a boundary condition derived from NASA AE8 electron model, results were compared with AE8 maps within all the inner magnetosphere by Beutier and Boscher (1995). With this version, dynamics of the outer belt during a storm was calculated and the results compared with in-situ measurements (Bourdarie et al., 1996). Improving the resolution of the code, it was even possible to compare results at low altitudes (in the range 400-800 km) to satellite average measurements and this was made by Boscher et al. (1997). From then, some improvements were made. First, synchrotron losses were added (Pugacheva et al., 1998), showing the influence of these internal losses to radiation belt electrons. Then, using Abel and Thorne calculations, pitch angle coefficient due to different kind of waves were added, including not only hiss, but also whistlers in the 1 kHz range and VLF transmitters in the 10 kHz range (Boscher et al, 1998). The final version runs with particles between 1 keV and 10 MeV.

8.2 SALAMMBÔ-4D (3D IN SPACE)

The Salammbô-4D version is an extended version of Salammbô-3D, taking into account the longitude (local time), so it is a real 3D in space. It was developed to understand injections during substorm periods, and their effects, like drift echoes or the growth of the ring current. In this version which is a full 3D in space code, it is possible to follow particles in their drift around the Earth. This drift was first calculated using an eccentric tilted dipole, but the inward or outward motion of the particle (convection) can be included as they drift around the Earth by adding an electric field which can vary with time. Using a Volland-Stern electric field, the results of this code were calculated (Bourdarie et al., 1997). In particular, drift echoes seen on board synchronous orbit satellites were well reproduced, as well as precipitation of low energy particles on the Earth. It is even possible with this code to reproduce radial diffusion by modifying the electric field as the time evolves. This version, using the same losses and sources than Salammbô-3D, works for both protons and electrons. For the 100 keV range protons, this code reproduces also quite well the increase of ring current particle, responsible for the growth of the Dst index.

A second version of this code was developed in order to take into account magnetic field variability, in particular during the growth phase of a substorm and the dipolarization. This code is now available only for equatorially mirroring particles, but it allows to reproduce the decrease of the fluxes during the growth phase and the injection of "new" particles during the dipolarization, when induced electric field are highest. It reproduces also loss of particles during these periods, related to the moving shape of the drift shell, intercepting or not the

magnetopause. This was made using a Mead-Williams field, with a ring current field added. The results are encouraging (Bourdarie et al., 1998).

8.3 SALAMMBÔ-2D

Finally, a third version of the code was developed, rather incorrectly called Salammbô-2D (so the 2D in the phase space correspond to only 1D in space, the L value). It only runs for low energy equatorially mirroring protons. In this code, the magnetospheric index Kp is a parameter used to modify the plasmapause location (L-boundary of the code) as well as radial diffusion coefficients. One of the properties of this code is that it can be used to reproduce large periods of time. For instance, this code was globally compared to CRRES MEB measurements, giving a first step of what could be a forecasting model for the radiation belts.

8.4 APPLICATIONS OF THE SALAMMBÔ CODES

The different Salammbô codes have different capabilities in terms of applications: scientific or engineering.

From the scientific applications, Salammbô-4D is the most well suited. It is able to localize the particles in the space (altitude, latitude, and longitude or local time), and for energies between 1keV and 10 MeV for electrons and 1 keV and 300 MeV for protons. From this, it is first easy to derive the low energy population, which will be seen by neutral imagers, like on the IMAGE satellite, which will be launched in 1999. Up to now, some neutral images were recorded, for instance on DE1, on Astrid or on POLAR, but the resolutions were too low to understand clearly the location of the particles. From the same range of energy, perturbation of the magnetic field due to the increase of the ring current can also be determined, this being recorded on the Earth by the Dst index. The results of this code can also be compared to in-situ measurements, this being very useful to adjust some parameters in the code, especially during substorms and storms, or for studying particle losses occurring frequently at high L shells.

For the engineering applications, and also for Space Weather forecasting, though Salammbô-3D gives only average values of the fluxes on L shells, this code seems better suited to give fluxes along a satellite trajectory. First, for engineering applications, only high energies are needed, and the average value is not too far from instantaneous values due to the mixing of fluxes for a large range of energies (drift echoes rapidly vanish for high energies). Second, for most important applications, only orders of magnitudes are needed, and Salammbô-3D can give easily this, depending on a lower number of parameters than Salammbô-4D. Finally, the CPU time needed to run the code is much lower than for the 4D version, and information on pitch angle and energy are still there, allowing to determine fluxes along any satellite trajectory, even Low Earth Orbit ones. Moreover, it is easier with that code to interpolate between satellite measurements, giving easily if the satellites are well located fluxes along other satellite trajectories, with no detectors on board.

8.5 LIMITATIONS AND PROSPECTS

Some of the entries of the codes are uncertain, like the ionosphere high altitude densities, the field (magnetic as well as electric) fluctuations, or the wave characteristics (hiss, whistlers or VLF transmitters). The most uncertain coefficients are certainly the radial diffusion coefficients, which can drastically vary with magnetic activity.

For the future development of nowcasting, these codes will be very helpful because up to now all the physical phenomena needed for the creation and dynamics of radiation are modelled in the

codes. Once the parameters adjusted, these codes will permit to determine in the internal magnetosphere (L < 7) the fluxes along any satellite trajectory.

For the forecasting, some entries for studying dynamics are already in the codes, like the influence of the secular drift of the magnetic field, those of the solar cycle (by the intermediate of the neutral model and the neutron flux occurring in CRAND), but we are now studying the effect of storms, like with the Salammbô-2D version.

8.6 REFERENCES

Beutier T., D. Boscher, M. France, « Salammbô: A three-dimensional simulation of the proton radiation belt », J. Geophys. Res. 100, 17181, 1995.

Vacaresse A., D. Boscher, S. Bourdarie, "A long term physical model for high energy low altitude protons", EGS XXIII General Assembly, Nice, France, 20-24 April 1998.

Boscher D., A. Vacaresse, S. Bourdarie, "Contribution for a high energy low altitude proton model", 32nd COSPAR Scientific Assembly, Nagoya, Japan, 12-19 July 1998.

Beutier T., and D. Boscher, "A three-dimensional analysis of the electron radiation belt by the Salammbô code", J. Geophys. Res. 100, 14853, 1995.

Bourdarie S., D. Boscher, T. Beutier, J.-A. Sauvaud, M. Blanc, "Magnetic storm modeling in the Earth's electron belt by the Salammbô code", J. Geophys. Res., 101, 27171, 1996.

Boscher D., S. Fung, L. Tan, "Spatial distributions of the inner radiation belt electrons: a comparison between observations and radial diffusion theory predictions", Adv. Space Res., 20-3, 369, 1997.

Pugacheva G., A. Gusev, I. Martin, D. Boscher, S. Bourdarie, W. Spjeldvik, "Numerical modeling of magnetospheric electron radial transport with accounting synchrotron radiation losses", Geophys. Res. Lett., 25-9, 1519, May 1998.

Boscher D., S. Bourdarie, R. Thorne, B. Abel, "Influence of the wave characteristics on the electron belt distribution", 32nd COSPAR Scientific Assembly, Nagoya, Japan, 12-19 July 1998.

Bourdarie S., D. Boscher, T. Beutier, J.-A. Sauvaud, M. Blanc, "Electron and proton radiation belt dynamic simulations during storm periods: a new asymmetric convection-diffusion model", J. Geophys. Res., 102, 17541, 1997.

Bourdarie S., D. Boscher, A. Vacaresse, "A radiation belt model based on convection-diffusion theory including a time dependent magnetic field", EGS XXIII General Assembly, Nice, France, 20-24 April 1998.

Bourdarie S., D. Boscher, T. Beutier, J.-A. Sauvaud, M. Blanc, R. Friedel, "A physics based model of the radiation belt flux at the day timescale", in Environment modelling for space-based applications, ESA SP-392, 159, 1996

9 ANNEXE B : TRANSCAR : AN EXAMPLE OF THEORETICAL IONOSPHERIC CODE

9.1 PHYSICAL CONCEPTS

As far as energy is concerned, the ionospheric population is mainly made of two kinds of particles. The most abundant one is the thermal population. It is usually understood to be characterised by a Maxwellian energy distribution. Each ion may have its own distribution, different from the electron one. The processes driving this population are strongly time dependant : chemical reactions with their reaction rates, collision frequencies, dynamics (neutral winds)... The behaviour of this population is global. Therefore, a time-dependant fluid description is well suited to describe it.

The hottest population is mainly made of electrons with non-Maxwellian distributions, and energies many times greater than the mean thermal energy. It originates either in the magnetosphere (electron and proton precipitation) or in the atmosphere, through photoionization. Each of these primary particle can create many ionizations and excitations. But their transport along a magnetic field line is so fast that it can be considered as instantaneous in front of the time of the precipitated event or solar intensity changes. Therefore, a steady-state kinetic description is required for this population.

9.2 NUMERICAL SCHEME

The TRANSCAR developped jointly at the CESR and LPG laboratories in France model closely follows the energetic description of the ionosphere above. At a time *t,* the « hot » population is described by a kinetic Boltzmann equation : EUV solar flux, or particle precipitation are given as inputs. They interact with the neutral atmosphere with regard to the absorption and collision cross sections of each neutral constituent. Also as inputs are the electron densities and temperatures, which are computed by the fluid part. The kinetic code computes (within other parameters) the ions and electron production rates, which feed the fluid part of the model.

The fluid part is based on an eight-moment approximation of Boltzmann's equation. The resulting set of equations projected along the magnetic field line allows the determination of the density, velocity, temperature and heat flow of each species. Electron density and velocity are solved assuming charge neutrality and ambipolar flow. Electric field effect is taken into account. The model describes the ionosphere from 90 to 3000 km, solving the set of equations for molecular and atomic ions.

A flow chart of the coupling is shown in figure 1. It has proven to be able to describe the ionosphere both on a statistical point of view and when comparing specific measurements with computations. On a statistical point of view, it could successfully compare computed electric conductivities with 3 years of EISCAT measurements. On the other hand, it was tested versus sporadic events, by comparing electron density and temperature, and ion temperature and composition to several EISCAT experiments. In order to do a successful comparison during quiet day time and during night time precipitation, the neutral atmosphere was adjusted. *Therefore, such an ionospheric code turns out to be a useful tool in estimating the neutral atmosphere, when used for simulating real experiments.* This may be of primary importance for Space Weather applications such as orbitography.

This code has also been used in order to model the TEC and f0F2 parameters at high latitude. Its results have been compared to EISCAT measurements up to 700 km. Above this altitude, the

code has been used to infer what is the influence on the TEC results of the electron density integration (up to 3000 km).

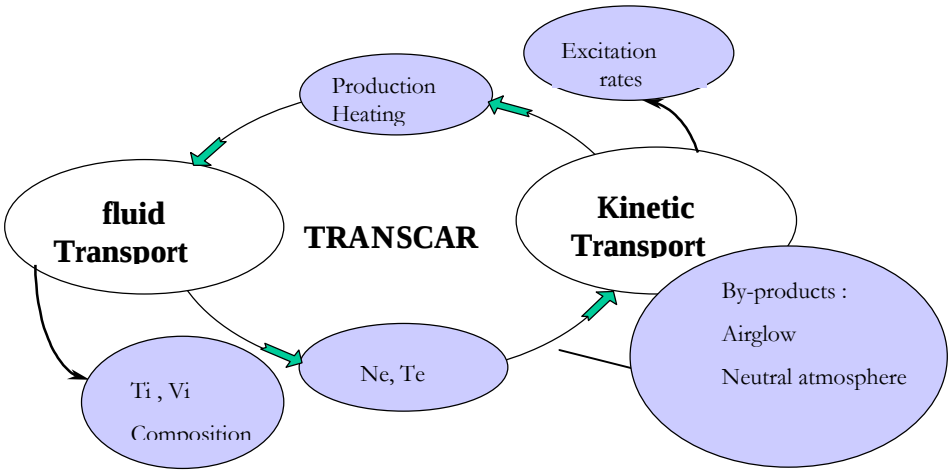

To summarize,

The external inputs are :

- The solar flux on top of the ionosphere
- The neutral atmosphère
- The topside downward electron heatflow imposed on the fluid model ; this accounts for thermal conduction effects
- The number flux and mean energy of precipitating electrons imposed on the kinetic code, corresponding to suprathermal energy exchanges

The main outputs, at a time resolution of about 1 s at fastest and over an altitude range of 90 to 3000 km are :

- Electron and ion productions, compositions, and concentrations
- Excitation rates
- Electron heating rate, electron and ion temperatures
- Ion velocity and heat flux
- A by-product is the neutral atmosphere estimate, when the model is used to reproduce experimental measurements.

9.3 BIBLIOGRAPHY :

Blelly, P-L, J. Lilensten, A. Robineau, J. Fontanari, and D. Alkaydé, Calibration of a numerical ionospheric model using EISCAT data : effect of the neutral atmosphere and the suprathermal electrons on the ionospheric plasma structure, accepted in *Ann. geophysicæ*, 1996

Diloy P.Y., A. Robineau, J. Lilensten, P.L. Blelly and J. Fontanari, A numerical model of the ionosphere including the E-region above EISCAT, *Ann. geophysicæ*, 14, 191-200,1996

J. Lilensten, P-L. Blelly, W. Kofman and D. Alcaydé, Auroral ionospheric conductivities : A comparison between experiment and modeling, and theoretical f107 dependant model for EISCAT and ESR, accepted in *Ann. geophysicæ*, 1996

Lummerzheim D., and J. Lilensten, Electron transport and energy degradation in the ionosphere : evaluation of the numerical solution, comparison with laboratory experiments and auroral observations, *Ann. Geophysicae*, 12, 1039-1051, 1994.

O. Witasse, J. Lilensten, C. Lathuillère and P.L. Blelly, Modeling the OI 630.0 and 557.7 nm thermospheric dayglow during EISCAT-WINDII coordinated measurements, submitted to *J. Geophys. Res*

Galand M., J. Lilensten,D. Toublanc and M. Sylvestre, The ionosphere of Titan : ideal diurnal and nocturnal cases, accepted in Icarus, 1999

10 ANNEXE C : UCL-SHEFFIELD 3-D NUMERICAL MODELS OF THE EARTH'S UPPER ATMOSPHERE

10.1 HISTORY AND PURPOSE

Modelling of the terrestrial atmosphere started at UCL in the late 1970s with the first published work by Fuller-Rowell and Rees (1980). Since then the Atmospheric Physics Laboratory of the Department of Physics and Astronomy at UCL has taken a key role in the use and development of atmospheric models. The Coupled Thermosphere-Ionosphere-Plasmasphere Model (CTIP) is one of the most comprehensive upper atmosphere models currently available, covering the region from 80km to 450km altitude in the neutral atmosphere, 120km to 10,000km in the ionosphere. It solves self-consistently the 3-dimensional time-dependent equations of momentum, energy and continuity for neutral particles (O, O2 and N2) and ions (O+, H+) on an Eulerian co-rotating spherical grid spaced 2 degrees in latitude and 18 degrees in longitude. Parameters relevant to the ion-neutral and neutral-ion coupling are exchanged at every few time steps between the thermospheric and ionospheric codes. These originally separate codes originate from two models developed by different groups in the UK, the thermosphere model by Fuller-Rowell and Rees (1980) and high-latitude ionosphere model by Quegan et al. (1982). They were fully coupled by Fuller-Rowell et al (1987) to form a version commonly referred to as the Coupled Thermosphere-Ionosphere Model (CTIM). This model was later extended to form the Coupled Thermosphere-Ionosphere Plasmasphere Model (CTIP), described by Fuller-Rowell et al (1996) and Millward et al (1996). CTIM uses ionospheric parameters from the empirical model by Chiu(1975) equatorward of an adjustable boundary which is commonly set to 35 degrees geographic latitude. CTIP, in contrast, solves the equations of momentum, energy and continuity for ions along closed magnetic flux tubes also at low to mid latitudes, calculating self-consistently plasma densities, temperatures and velocities.

10.2 PRESENT EVOLUTION

A number of important modifications have been added over the years to CTIM and CTIP as described by Millward et al (1996). More recent code development includes the addition of tidal and planetary wave forcing at the CTIP model's lower boundary (Muller-Wodarg et al, 2000), self-consistent calculation of the E-region dynamo electric field (Millward et al, 2000),

flexible high-latitude auroral precipitation and convection electric field (Schoendorf et al, 1996) and downward extension of the lower boundary from 80km to 30km - below the stratopause (Harris, 2000 - PhD in preparation). The extension into the middle atmosphere including full mesospheric energetics, dynamics and chemistry, is intended to study vertical coupling mechanisms. The model version extending into the lower mesosphere and stratosphere is named the Coupled Middle Atmosphere and Thermosphere model (CMAT), and includes:

1) a factor of three increase in vertical resolution.
2) A more detailed treatment of the calculation of thermospheric solar heating, and extensive additions to the mesospheric energetics
3) Extension of the thermospheric chemistry scheme to include the N(4S), N(2D) and NO, as well as existing O, O2 and N2 and D-region ion chemistry
4) Mesospheric chemistry scheme, which solves for O_3, HO_x (=OH + HO_2 + H), H_2O, H_2, CO, CO_2, CH_4, NO_2, OD, H_2O_2 and He

5) Lower boundary forcing from MSIS-E90 and tidal forcing from the Global Scale Wave Model (GSWM)
6) Middle atmosphere gravity wave drag

The aim in creating this model is to solve how upper atmospheric phenomena such as solar variability and high-latitude particle precipitation may propagate downwards, and how they might affect the middle and lower atmospheres. The emphasis is on potential mechanisms that may have impact on climate, or be associated with anthropogenic induced changes. "Space Weather" effects can be traced from their impact on the magnetosphere and exosphere right down to nearly ground level.

The model simulations are delimited by the parameters controlling the runs. Inputs are basic controlling factors like $f_{10.7}$ cm flux, an activity index (essentially Kp) and the time/date. The high-latitude energy and momentum inputs are via models of the precipitation and plasma flow patterns, and these can be modified for specific studies. The tidal input can be either as a Hough Mode expansion, or as a more structured self-consistent set of velocity, density and temperature oscillations. Solar insolation variability is parameterised, but the routines used can be easily modified to use improved absorption cross-sections, say, or solar flux in any number of discrete bands through the uv, euv and xray bands.

10.3 BIBLIOGRAPHY :

Chiu Y.T. "An improved phenomenological model of ionospheric density", J.atmos.terr Phys 37,1563 (1975)

Fuller-Rowell T.J. and D.Rees, "A three-dimensional time dependent global model of the thermosphere", J.Atmos.Sci. 37 2545-2567 (1980)

Fuller-Rowell T.J., Rees D., Quegan S., Moffett R.J. and Bailey G.J, "Interactions between neutral thermospheric composition and the polar ionosphere using a coupled global model", J.geophys.Res. 92, 7744-7748 (1987)

Fuller-Rowell T.J., Rees D., Quegan S., Moffett R.J., Codrescu M.V. and Millward G.H., "A Coupled Thermosphere-Ionosphere Model (CTIM)", STEP Handbook, pp 217-238, Ed R.Schunk (1996)

Millward G.H., Moffett R.J, Quegan S. and Fuller-Rowell T.J., "A Coupled Thermosphere-Ionosphere-Plasmasphere Model (CTIP)", STEP Handbook of Ionospheric Models 239-279, Ed R.W.Schunk (1996)

Millward G.H.,Muller-Wodarg I.C.F. and Aylward A.D., "The influence of thermospheric tides on equatorial dynamics: CTIP model results" , J.geophys. Res (in press) (2000)

Muller-Wodarg I.C.F., Aylward A.D. and Fuller-Rowell T.J., "Tidal oscillations in the thermosphere: a theoretical investigation of their sources", J.atmos.terr Phys (in press) (2000)

Quegan S., Bailey G.J., Moffett R.J., Heelis R.A., Fuller-Rowell T.J., Rees D. and Spiro A.W.

"A theoretical study of the distribution of ionisation in the high-latitude ionosphere and the plasmasphere: first results on the mid-latitude trough and the light-ion trough", J.atmos.terr.Phys 44,619-640 (1982)

Schoendorf J., Aylward A.D. and Moffett R.J., "Modelling high-latitude electron densities with a coupled thermosphere-ionosphere model" , Ann.Geophys. 14, 1391-1402 (1996)

11 ANNEXE D : THE GEOMAGNETIC INDICES

The following synthetic presentation deals with geomagnetic indices and remarkable events acknowledged by the *International Association of Geomagnetism and Aeronomy* (*I.A.G.A.*). It does not intend to give a detailed or exhaustive review of past and present geomagnetic indices. The reader can refer to e.g.:

- Mayaud *(1980)*, Rangarajan *(1989)*, Berthelier *(1993)* and Menvielle *(1998)* for general reviews;
- Menvielle and Berthelier *(1991)* about *K*-derived indices (*aa*, *am*, *Kp* and *Kp*-related: *ap*, *Cp*, *C9*);
- Sugiura and Kamei *(1991)* for the derivation of *Dst*.

IAGA Bulletin 32 series also contain short but precise definitions of geomagnetic indices and remarkable events acknowledged by I.A.G.A.

The International Service of Geomagnetic Indices (*I.S.G.I.*) and the *ISGI Collaborating Institutes* are in charge of the derivation of *IAGA* geomagnetic indices and lists of remarkable events with data provided by geomagnetic observatories, and of their dissemination.

Indices are intended to describe defined phenomena from a set of measurements. There are in fact two complementary standpoints:

- one consists in starting from a given phenomenon, for which one then describes the measurements to be made (or used) for deriving relevant indices;
- the other starts from the analysis of the available measurements of a given physical quantity, which is directly or easily observed, and the description of the phenomena that can thus be characterised goes with it.

In the case of geomagnetic indices, the second point of view was historically adopted, and the measured physical quantity is made of magnetic field perturbations recorded at a number of observatories all over the world. In fact, at the early beginning there was no real understanding of the link between these measurements and such or such related phenomenon. From further analysis of magnetic perturbations, it was progressively understood that they reflect distinct phenomena of ionospheric and magnetospheric origin, and more precise or elaborated indices were defined in order to account for well defined magnetospheric phenomena.

However, even if the understanding of the links between magnetic perturbations and magnetospheric phenomena significantly increased during decades of geomagnetic studies, it was not always possible to isolate, and even sometimes recognise the magnetic signature of a given phenomenon. It therefore appears easier and more helpful to adopt the second point of view as done in historical developments, and then to present the derivation of the indices as based on the description of the magnetic perturbations.

11.1 THE TRANSIENT VARIATIONS OF THE GEOMAGNETIC FIELD

The magnetic field measured at the Earth surface is the sum of an internal planetary magnetic field and of components of primarily external origin, including those due to currents induced in the conductive Earth. While the planetary magnetic field has a slow or 'secular' variation, the external components are characterised by transient variations with a time scale in the order of days to minutes, and even less (Figure A-1).

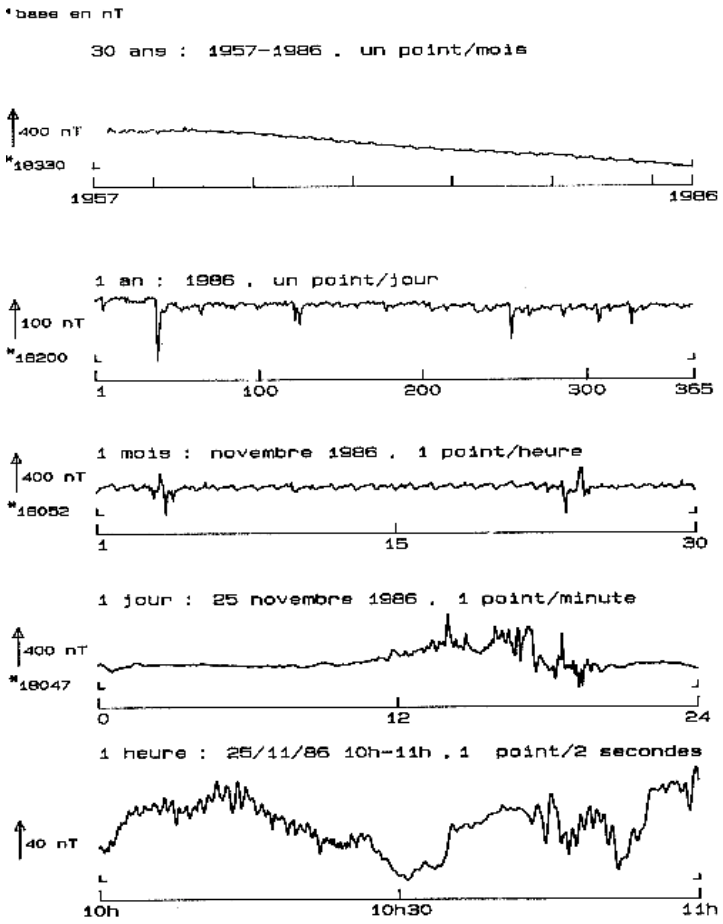

Figure A-1 *: Variations of the horizontal component of the Earth magnetic field observed at the Port aux Français (Kerguelen island, Terres Australes Françaises) French magnetic observatory (from Bitterly and Menvielle, 1987).*

The transient variations of the geomagnetic field at the Earth surface are the signature of the currents taking place in the entire magnetosphere, as the result of the solar wind magnetosphere coupling processes. They result from both external currents flowing in the ionosphere and in the magnetosphere, including field aligned currents and magnetopause currents and internal induced currents. The high degree of complexity of the solar wind - magnetosphere - ionosphere coupling results in a large variety of magnetic signatures, depending upon the state of the magnetosphere, and differing with the geographic and geomagnetic location of the observatory. Thanks to decades of observation, it is possible to delineate the main morphological features of the ground observed perturbations, and, to a certain extent, to relate them to ionospheric and magnetospheric sources.

A fundamental starting point in the studies of transient variations is their decomposition into a regular and an irregular part. 'Regular' means that the variations have both a smooth shape and a regular occurrence, every day, while 'irregular' refer to both a great variability in shape and intensity, and an irregular occurrence of the variations. Such a distinction is linked to the discrimination between two different physical processes. The regular variations are mainly related

to the atmospheric dynamo processes, while the irregular variations are mostly due to the energy input in the magnetosphere related for instance to magnetospheric storms and substorms. It is important to note that the terms magnetically quiet or disturbed only refer to irregular variations, i.e. indicate the absence or presence of irregular variations respectively.

11.1.1 Regular variations

Regular variations are related to permanent sources, the main one being ionospheric tidal currents caused by the heating and ionisation of the day-side atmosphere. These sources are observed alone during quiet periods, but they are actually present during both quiet and disturbed times. Their shape and position are roughly constant in a reference system fixed with respect to the Sun and they have a non negligible day to day variability. *[see Campbell (1989) for a recent review]*. One denotes S_R (for Solar Regular) the solar regular variation observed during a given day and S_q (for Solar quiet) the variation deduced from the S_R curves by averaging them over a given time interval during which it thus represents the most likely S_R variation.

11.1.2 Irregular variations

A striking illustration of the observed diversity in magnetic perturbations and of their variability both with time and with geomagnetic latitude is given in Figure A-2 which presents the variations versus universal time (UT) of one horizontal component of the magnetic field recorded at different observatories, for a given UT period. This figure shows the large range of possible morphologies of the irregular magnetic variations, and their variability with respect to time and geomagnetic latitude.

Figure A-2 illustrates the following important features of magnetic perturbations:

- the typical time scales of the irregular variations range from a few minutes to some hours;
- the intensity of the perturbations observed at a given time considerably varies with latitude, the largest variation being observed at geomagnetic latitudes in the range 60 to 75°, corresponding to the auroral zone (curves 10 to 14). Typical amplitudes of variations are from some nanoTeslas (nT) to some hundreds of nT;
- the latitudinal extension of the irregular variations depends on the time period: one can see on Figure A-2 a period when perturbations extend down to equatorial latitudes (around 14:00 UT), and another when their intensification is limited to the highest latitudes (around 01:00 UT).

Higher frequency fluctuations and rapid variations are also part of the geomagnetic transient variations. It is the case in particular of storm sudden commencements (*ssc*), which are sudden variations followed by a magnetic storm, or by an increase in activity lasting at least one hour.

The so-called magnetic pulsations are also part of the rapid variations. They have quasi-periods of the order of minutes to seconds, or less, and their average amplitude, generally lower than 10 nT or so, decreases with period *[see e.g., Samson (1991) for a review on geomagnetic pulsations]*. They are clearly a non negligible part of geomagnetic activity, although a universal index does not exist for them.

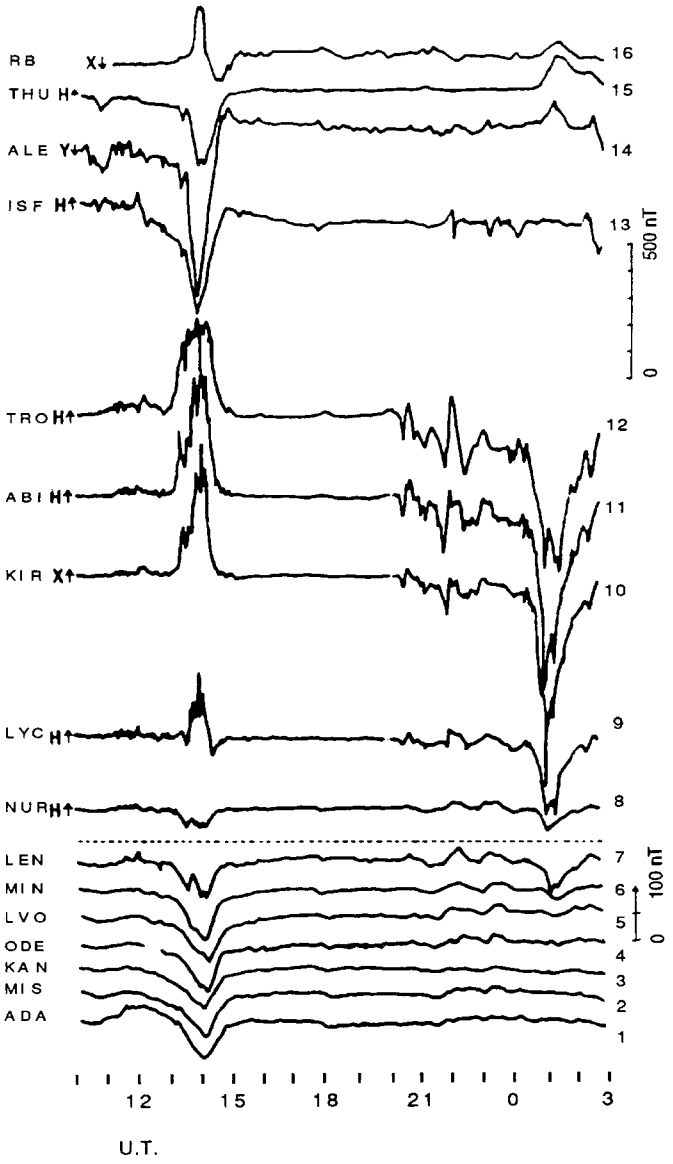

Figure A-2: *Variation of the H (or X) horizontal component of the Earth magnetic field observed at a roughly North-South chain of magnetic observatories during the same U.T. time period. Curves are ordered according to the geomagnetic latitude of the observatories, ranging from ~5° (lower curve) to ~88° (upper curve). Note the change in the scale between the lower (1 to 7) and the upper (8 to 16) latitude stations (after Kamide and Fukushima, 1972).*

11.2 THE *I.A.G.A.* GEOMAGNETIC INDICES

Following Berthelier *(1993)*, let us describe the processes of derivation of geomagnetic indices in terms of four components:

- (1) the quantity to be measured, or estimated, which can be either the range of variation or the derivation from a base value;
- (2) the time interval over which it is measured;
- (3) the location of the station or network of stations;

- (4) the method of derivation.

1. *The measured quantity* is either the deviation ΔH, or the range, depending on the indices:

- for *K* and *K*-derived planetary magnetic indices, the measured quantity is the range *r* of the irregular variations during a given time interval. The base value is the S_R variation of the day under consideration. It can be identified by taking into account the neighbouring quiet days, and is allowed to have a day to day variability. *K* is a code characterising the class in which falls the observed range, and the equivalent amplitude a_K is the mid-value of the class. Given the quasi-logarithmic scale used for deriving *K*-indices, the increasing uncertainty in S_R determination with increasing levels of activity does not significantly affect the precision in the *K* determination *(Mayaud, 1967)*;
- for *AE* and *Dst*, the measured quantity is the deviation ΔH of the horizontal component. In both cases, the base values are average S_q monthly estimates based on the 5 international quietest days[18] of the month.

2. *The time interval*

The time interval on which the index is estimated depends on the measured quantity. One can theoretically reach continuous information in the case of indices based upon the measure of a deviation (*AE* and *Dst*), provided that one has access to continuous recordings. However, using the range intrinsically gives rise to discrete values according to the time interval of derivation.

The three-hour interval used to derive *K* indices is the most suitable for characterising geomagnetic activity in subauroral regions (~ 40 to 55° in magnetic latitude, shaded area on Figure 8) *(Mayaud, 1967)*. At these latitudes the observed morphology of the irregular variations is actually such that the *K*-equivalent mid class amplitudes a_K are related to the energy density embedded in the irregular geomagnetic variations. *(Menvielle, 1979)*.

3. The location of stations

It tends to favour the regions where one expects to observe the phenomena under consideration. Obvious limitations come from:

- the difficulties in precisely determining the region of observation of the phenomenon: e.g., for *AE*, variable geographical position of the auroral electrojets, due to the expansion of auroral oval with increasing magnetic activity for instance;
- the distribution of existing observatories: e.g. the network of observatories available at the time of definition of *Kp* in 1949 was not truly world-wide.

4. The method of derivation It is rather simple in the case of *AE* and *Dst* indices:

- *AU* and *AL* represent the largest intensity in the eastward ad westward auroral electrojets respectively;
- *Dst* is the axially symmetric part of the equatorial ΔH, and it aims at giving the effect of the magnetospheric ring currents.

In both cases, the indices are estimates of the corresponding quantity as seen from the networks of stations.

In the case of *K*-indices, it is the range of variation which is first measured. The limits of the grids used follow a quasi logarithmic scale in order to allow studies of both quietness and storminess. There exist significant differences between the derivation schemes of *Kp* and *am* indices:

[18] A function based on the eight Kp indices of the day is computed for each UT day of the month. For a given month, the five international Q days are the five days with the lowest values of this function.

- *am* is obtained from a weighted average of amplitude range values, with weight evenly distributed according to the longitude of the stations of the present network. As a whole, the derivation of *aa* follows the same process as that of *am*, except that one has only 2 antipodal observatories from which it has been possible to calculate a more than one hundred long data series;
- *Kp* is the average of codes taken from a quasi-logarithmic scale, with an equal weight given to each station of the initial network.

11.3 THE REMARKABLE MAGNETIC EVENTS

Lists of storm sudden commencement (*ssc*) and solar flare effects (*sfe*) are regularly established and circulated. Their derivation processes can be discussed as in the case of geomagnetic indices.

The measured quantity is a geomagnetic event having particular morphological characteristics. The events are listed in order of occurrence, with information on salient observational and/or morphological features;

The method of derivation relies on visual morphological analysis of magnetograms. The preliminary lists of events are compiled from reports of Rapid Variations prepared by the observatories and sent to the Service of Rapid Variations, at the Observatorio del Ebro. The final lists are compiled at the Service of Rapid Variations from the preliminary lists using magnetograms from a network of selected low latitude stations in the case of ssc's, or reports from all reporting observatories in the case of sfe's.

11.4 DATA ACQUISATION AND PROCESSING

11.4.1 Definitive, provisional, quick look, and estimated values

In the past, data were made available by the observatories as hard copy magnetograms or data sheets. Because many months were necessary to get all the definitive data, provisional values were computed in order to circulate the indices within reasonable delays. They are still computed and circulated by the observatories within a delay of a few weeks, they aim at providing estimates of the definitive values of the indices. The provisional data series have similar statistical properties as the definitive ones.

The possibility of dissemination of data through electronic network opened a new era. The *I.S.G.I. Publication Office* (for *K*-derived planetary indices) and the *WDC-C2 for Geomagnetism* (for *Dst* and *AE* indices) started routinely preparing and circulating quick-look values of geomagnetic indices within delays of the order of a few days. As it is the case for the provisional values, the quick look values aim at providing estimates of the definitive values, and the quick look data series have similar statistical properties as the definitive ones. The confidence interval on each individual estimate is however significantly larger for the quick look values than for the provisional ones.

Institutes which are not part of *I.S.G.I.* may however easily derive and circulate preliminary values of geomagnetic indices, for instance in response to strong requests to have preliminary values of geomagnetic indices available on line within very short delays. This is confusing, and could result in a dramatic loss of quality of geomagnetic indices. During its VIII Scientific Assembly (Uppsala, 1997), the *International Association of Geomagnetism and Aeronomy* adopted a resolution which recommend geomagnetic indices designed to provide quasi-real time estimates of existing *I.A.G.A.* indices to be named by adding *est* to the name of the index (e.g. *Kpest* for *Kp* estimates).

11.4.2 *AE* index

The present derivation scheme of *AE*, *AU*, and *AL* indices is well suited for producing and circulating provisional values within very short delays. The main challenge is then to have digital data routinely available from all the observatories through electronic networks. At the end of the 1980's, the situation ranged from no digital data at all, through poor data, to good data but delayed by weeks or months. Connecting the existing digital observatories to the INTERMAGNET network, and replacing progressively analogical observations by digital ones with automatic data transfer allowed to significantly improve the situation. If not perfect, the situation is now far better: all the 12 *AE* observatories are in principle capable of transferring digital data, but in practice with varying degrees of difficulties in transmitting the data on a reliable routine basis, thanks to the joint efforts of the *WDC-C2 for Geomagnetism* (Kyoto University, Japan) and of the Institutes ruling the observatories

The *AE* index is now being made available in three steps. The index in the first of these three steps is a near real-time *AE* index, or a 'quick-look' *AE* index, which is made available on line (at the WDC-C2 WWW homepage) with a 12 hours delay in summer 1997. The index is derived on an 'available data' basis, and is updated on a daily basis as the missing data are filled. Therefore the derivation of the quick-look *AE* index is an 'evolving' process, and a due caution is required in using this index, which is primarily meant for diagnostic purposes and not for scientific analyses. The quick-look *AE* index is plotted on WWW in colour to indicate the number of observatories that are contributing data to each minute. There is a maximum of 8 observatories that can contribute data for the quick-look *AE* at the present time. It is worth noting that no quality check is made on the data used for the quick-look *AE* index. The *AE* index in the second step is a provisional *AE* index derived (and published in a Prompt Report) often responding to demands by various projects. The *AE* index derived by the third step is the final *AE* index in the form familiar to the scientific community.

11.4.3 *Dst* index

Similarly, the *Equatorial Dst* index (*Dst*) is now prepared and issued in three steps. In the first step, a near real-time *Dst*, or quick-look *Dst*, is derived using data from any number of observatories of the five designated *Dst* observatories (the four observatories shown in Figure 8 plus Alibag), beginning with a 12-hour delay and updated on a daily basis. As in the case of the quick-look *AE* index, no quality check is made on the data used for the quick-look *Dst* index. Therefore it is recommended that the quick-look *Dst* index is used only for diagnostic purposes; it should not be used for scientific analyses. The second stage product is the provisional *Dst* index which is now being made available on a monthly basis with approximately 2 months delay. Beginning January 1997 the provisional *Dst* index is derived using data from 5 observatories including Alibag. The *Dst* index derived by the third step is the final *Dst* index published annually, normally with several months delay. To derive this index, the secular change and a model S_q of the year for each of the observatories are removed. S_q is a function of the local time and season.

11.4.4 *K*-derived planetary indices

The *K*-derived planetary indices (*am*, *an*, *as*, *aa*, and *Kp*) were traditionally computed on a monthly basis with *K*-indices hand scaled on analogical magnetograms and provided as hard copies by the observatories. Provisional values were thus circulated with a delay of a few weeks after the end of the month of observation. Definitive values were computed once definitive *K* values made available by all the observatories.

Provisional and definitive values are still computed with the *K* values provided by the observatories. In summer 1997, provisional values were circulated on a monthly basis with a few

weeks delay for *am*, *an*, and *as*, twice a month with a few weeks delay for *Ap*, and on a weekly basis with a few days delay for *aa*. Reducing these delays down to a few days implied to derive provisional *K* values from digital minute values. Algorithm for computer derivation of S_R, leading to automatic calculation of *K* indices have then been set up and tested by different research groups. Four of them have been acknowledged by *I.A.G.A. (Menvielle, 1995)*. A software which aims at calculating in quasi real time these indices was then developed at the *I.S.G.I. Publication Office*. It gets automatically on a daily basis digital minute values from geomagnetic observatories through electronic data transfer procedures, and computes *K* indices using the *FMI* method *[see e.g., Menvielle (1995) and references therein]*. The quick-look values of planetary indices are then computed and circulated once data availability makes it possible. As it is the case for *AE* and *Dst* indices, the *am* and *Km* quick-look indices are derived on an 'available data' basis, and a due caution is required in using them.

11.5 DATA DISSEMINATION

11.5.1 On-line services

The question of dissemination of geomagnetic indices through electronic network is at present of major concern. There is in fact a strong request from industrial and military communities to have preliminary values of geomagnetic indices available on line within very short delays. Some of them are asking to have them circulated within a one hour delay. The *I.S.G.I. Publication Office*, the *World Data Centre C2 for Geomagnetism* (Kyoto University, Japan), and the *GeoForschungsZentrum (GFZ) Potsdam* (Germany) have therefore developed their WWW homepage for on line dissemination of geomagnetic indices:

- the I.S.G.I. www homepage[19] is developed in the frame of the C.E.T.P. homepage, with mirror link with www homepages of interest in the field of indices. The am and aa data series are available at this www homepage, including the quick look and provisional values; am and aa indices expressed in terms of Kp units (Kpa and Kpm indices) are also provided. The I.S.G.I. www homepage makes also possible to have easily access to descriptions of I.A.G.A. indices, and to all the available data;
- the WDC-C2 for Geomagnetism www homepage[20] makes available the Dst and AE data series, including the quick look values.
- the *GFZ Potsdam* WWW homepage[21] makes available the *Kp* series, as well as the derived indices and the international Q and D[22] days of every month.

11.5.2 Printed Bulletins

In parallel with the development of the on-line facilities described in the previous section, the *I.S.G.I. Publication Office*, the *WDC-C2 for Geomagnetism* and the *GeoForschungZentrum Potsdam* continue to issue printed bulletins[23]:

- the *I.S.G.I. Publication Office* circulates a *monthly bulletin* which contains the provisional values of planetary magnetic indices (*am*, *aa*, *Kp*, and *Dst*) and the list of the quiet magnetic days of the month. It is normally sent six to eight weeks after the end of the current month. It also

[19] http://tango.cetp.ipsl.fr/~isgi/homepag1.htm

[20] http://swdcdb.kugi.kyoto-u.ac.jp/

[21] http://www.gfz-potsdam.de/pub/home/obs/kp-ap/

[22] A function based on the eight *Kp* indices of the day is computed for each UT day of the month. For a given month, the five international D days are the five days with the highest values of this function.

[23] All the printed bulletins are available on request

publishes *the yearly IAGA Bulletin 32 series*, which contains the definitive values of the *I.A.G.A.* indices;

- the *WDC-C2 for Geomagnetism*, Kyoto University, publishes and distributes the provisional *Dst* index on a monthly basis, the provisional *AE* index in Prompt Reports, and the final *AE* index in Data Books;
- the *GeoForschungZentrum Potsdam* circulates *Kp* and *Kp*-related geomagnetic indices on tables edited on a half-monthly basis. The definitive values of these indices are circulated on monthly tables, together with musical diagrams of *Kp*, semi graphic tables of *C9*, and lists of the quietest and most disturbed days of the month.

The provisional values of geomagnetic indices are also published in the *Solar Geophysical Data* NOAA/NGDC reports, and in *Journal of Geophysical Research* (Editor: H. Coffey).